**Contract No:**

This document was prepared in conjunction with work accomplished under Contract No. DE-AC09-08SR22470 with the U.S. Department of Energy (DOE) Office of Environmental Management (EM).

Disclaimer:

This work was prepared under an agreement with and funded by the U.S. Government. Neither the U. S. Government or its employees, nor any of its contractors, subcontractors or their employees, makes any express or implied:

1.) warranty or assumes any legal liability for the accuracy, completeness, or for the use or results of such use of any information, product, or process disclosed; or
2.) representation that such use or results of such use would not infringe privately owned rights; or
3.) endorsement or recommendation of any specifically identified commercial product, process, or service.

Any views and opinions of authors expressed in this work do not necessarily state or reflect those of the United States Government, or its contractors, or subcontractors.
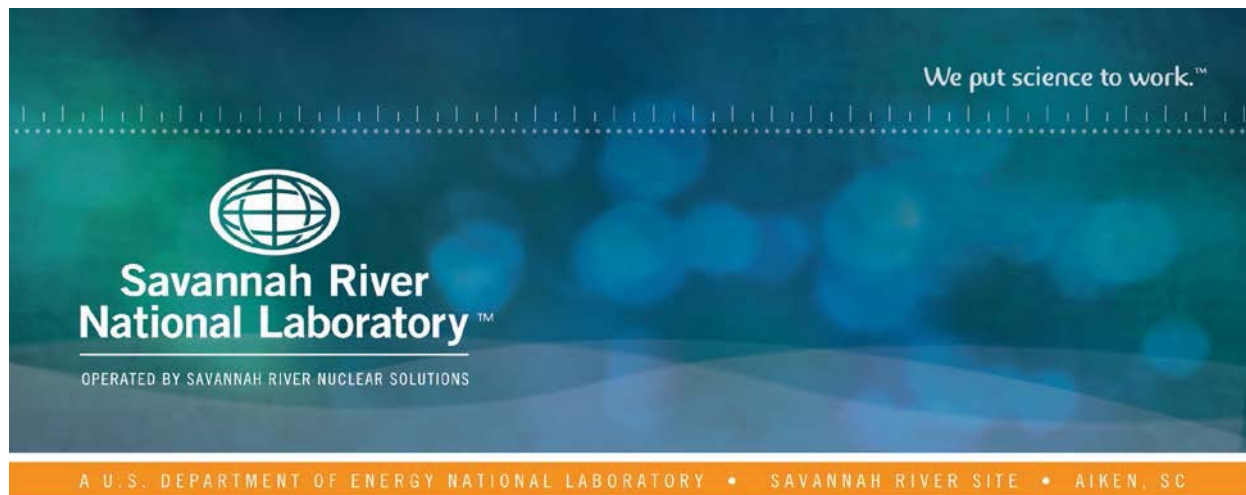
Impact of Glycolate Anion on Aqueous Corrosion in DWPF and Downstream Facilities

J.I. Mickalonis

July 2017

SRNL-STI-2015-00482, Revision 1

DISCLAIMER

Impact of Glycolate Anion on Aqueous Corrosion in DWPF and Downstream Facilities

J.I. Mickalonis

July 2017

Savannah River National Laboratory™

OPERATED BY SAVANNAH RIVER NUCLEAR SOLUTIONS

iii

REVISION LOG

Revision	Sections Affected	Description of Revisions
0	All	Initial issue
1	All	Editorial and format changes
	Executive Summary	Major re-write to summarize the entire multi-year test program, which include a first phase and follow-up testing, and the addition of a summary table highlighting the acceptability of the materials of construction for Savannah River Site waste processing facilities exposed to glycolic acid
	First Phase Results	Major re-write to more fully discuss the first phase test results where localized corrosion was observed and the path forward for resolving results and the addition of a summary table for path forward; section was renamed, *Summary of First Phase Testing Localized Corrosion Occurrences*
	Experimental Procedure	Addition of electrochemical test matrix for evaluation the impact of glycolic and formic acids on the Tank Farm Corrosion Control Program
	Results and Discussion	Re-organization of the section into three sections for each of the three areas that were covered by the follow-up testing: the Defense Waste Processing Facility, High Level Waste Evaporators, and the Tank Farm Corrosion Control Program; data analysis added for testing that supports the current Corrosion Control Program even in the presence of formate and glycolate
	Appendices	Addition of three appendices including the summary table of first-phase testing and follow-up testing path forward, summary table of the Tank Farm Corrosion Control Program, and Non-Destructive Examination reports cited as references in the report

REVIEWS AND APPROVALS

AUTHOR:

_____

J.I. Mickalonis, SRNL/Material Science & Technology   Date

TECHNICAL REVIEW:

_____

K.J. Imrich, SRNL/Material Science & Technology, Reviewed per E7 2.60 Date

APPROVAL:

_____

B.J. Wiersma, Manager   Date
SRNL/Materials Science & Technology/Corrosion & Materials Performance

_____

F. M. Pennebaker, Manager   Date
SRNL/E&CPT Research Programs

_____

K.E. Zeigler, Manager   Date
SRNL/Materials Science & Technology

_____

E. J. Freed, Manager   Date
SRR/Defense Waste Processing Facility & Saltstone Facility Engineering

ACKNOWLEDGEMENTS

EXECUTIVE SUMMARY

Glycolic acid is being evaluated as an alternate reductant in the preparation of high level waste for the Defense Waste Processing Facility (DWPF) at the Savannah River Site (SRS). During processing, the glycolic acid may not be completely consumed with small quantities of the glycolate anion being carried forward to other high level waste (HLW) facilities. The SRS liquid waste contractor requested an assessment of the impact of the glycolate anion on the corrosion of the materials of construction (MoC) throughout the waste processing system since this impact had not been previously evaluated. A literature review revealed that corrosion data were not available for the MoCs in glycolic-bearing solutions applicable to SRS systems. Data on the material compatibility with only glycolic acid or its derivative products were identified; however, data were limited for solutions containing glycolic acid or the glycolate anion. For the proprietary coating systems applied to the DWPF concrete, glycolic acid was deemed compatible since the coatings were resistant to more aggressive chemistries than glycolic acid. Additionally similar coating resins showed acceptable resistance to glycolic acid.

A multi-year test program recommended by the Savannah River National Laboratory was conducted to evaluate the MoCs of vessels, piping and components within DWPF and downstream facilities. The two-phase program consisted of both accelerated tests (electrochemical and hot-wall) with corrosion coupons in laboratory vessels, prototypical tests with coupons immersed in scale-up and mock-up test systems, and a six-month coupon immersion test with periodic removal of multiple coupons.

The first phase for aqueous corrosion testing consisted of electrochemical tests, hot-wall tests, and a coupon exposure test performed as part of the intermediary (22 L) scale-up testing for the chemical process cell (CPC) flowsheet development.[1] Test conditions simulated the service conditions for DWPF and downstream facilities. The MoCs for most vessels, components and piping were not impacted by the presence of the glycolate anion or the impact was not expected to affect the service life (see shaded rows in summary table below). The performance of some MoCs within the DWPF CPC and feed tanks required additional testing due to the susceptibility to localized corrosion (pitting, crevice and underdeposit corrosion) identified during the accelerated electrochemical and hot-wall testing. In other hot-wall tests, localized corrosion was also observed for the MoCs of heat transfer surfaces in downstream facilities.

Follow-up testing was recommended to better identify waste chemistries with acceptable performance of the MoCs, especially for susceptibility to localized corrosion in the presence of the glycolate anion and to verify performance over an extended time period. The testing included a series of electrochemical and hot-wall tests, and a six-month coupon immersion test. The electrochemical tests were targeted towards three areas of the DWPF: glycolic acid feed tanks, CPC components, and the remote equipment decontamination cell (REDC) components. Hot-wall tests were conducted to further clarify the observed localized corrosion during the first phase of testing for the heat transfer surfaces in the CPC and downstream facilities (2H Evaporator and evaporator heater of the Effluent Treatment Facility (ETF). A six-month coupon immersion test was conducted to determine if the accelerated electrochemical results were also observed in the more representative extended exposure testing. Revision 0 of this report included the results of these follow-up tests.

Additionally, the first-phase testing was limited to assessing MoCs for tanks directly impacted by DWPF waste streams. This testing was required to assess the impact in other waste tanks because glycolate could ultimately be distributed more broadly in the Tank Farm depending on waste management objectives. The Corrosion Control Program (CCP) for the waste tanks ensures corrosion mechanisms

---

[1] J. I. Mickalonis, K. J. Imrich, C. M. Jantzen, T. H. Murphy, and J. E. Wilderman "Corrosion Impact of Alternate Reductant on DWPF and Downstream Facilities," SRNL-STI-2014-00281, Revision 0, December 2014

have minimal impact on tank integrity, so these control schemes were used to establish representative electrochemical corrosion test solution conditions (chemistry and temperature) for verifying that glycolic acid does not impact tank integrity. During this phase of testing, the impact of formic acid, the current DWPF reductant, on these control schemes was evaluated for comparative data. Revision 1 of this report includes the results of this testing as well as additional discussion on the suitability of all MoCs.

The results of the DWPF follow-up testing showed that for C276 under the CPC conditions localized corrosion were found to occur at chloride and sulfate concentrations (the primary aggressive anions) as low as those processed in previous sludge batches. Surface deposits or layers occurred and may have contributed to the observed corrosion. These results were seen with similar severity for both glycolic- and formic-based solutions. The observed corrosion was not deep (less than 20 μm) and did not progress with time for a period up to six months. General corrosion rates in both glycolic- and formic-based solutions were found to be approximately 1 mil per year as specified in the DWPF Structural Integrity Program. Although mercury can contribute to localized corrosion, in these glycolic-based solutions mercury was found to impact the general corrosion rate but not the occurrence of localized corrosion.

Test results (i.e. six-month coupon immersion) under CPC conditions from the follow-up testing were more limited for Ultimet® alloy and Stellite™ 6B alloy, which are wear resistant cobalt-chromium alloys. The corrosion of these materials in both glycolic- and formic-based solutions was similar. The localized corrosion, which again was associated with the formation of surface deposits and layers showed a slight progression with time during the six-month coupon immersion test. The impact of this corrosion on the erosion characteristics was not studied. Performance of these materials with the nitric-glycolic flowsheet is expected to be similar to the performance with the current nitric-formic flowsheet.

For other DWPF process areas, the glycolic acid feed tanks and the REDC, the impact of the glycolate anion differed. For the feed tank and associated components made of 304L stainless steel (304L), the material was found to be susceptible to pitting in 70 wt% glycolic acid at temperatures from room temperature up to 50 °C. If 304L components are to handle the 70 wt% glycolic acid, an inspection program was recommended to determine if this occurs in the DWPF tanks or piping. Alternatively, tanks fabricated from 316L stainless steel should be used for 70 wt% glycolic acid exposure. Dilution of the glycolic acid was not investigated. For the REDC, the presence of glycolate in the cleaning solution will not impact MoC performance.

The electrochemical corrosion test results demonstrated that the presence of either the glycolate or formate anion or both together do not alter the requirements of the CCP. Testing was conducted in eight representative chemistries for the various current and expected waste compositions within the Tank Farm with a bounding concentration for each glycolate and formate of 10,000 g/L. Although small differences were seen in the electrochemical response, these differences were not sufficient to impact the corrosion mechanism and ultimately the integrity of the waste tanks.

For the nickel-chromium-iron alloys G-30® and G-3, the MoCs used in the 2H and ETF (as well as 3H) Evaporators, the results of both phases of testing showed that localized corrosion was observed in the hot-wall tests regardless of the presence of the glycolate anion. Pit depths were found to be approximately 1 mil and associated with deposits whether the glycolate anion was present or not. The current operation of desalting or descaling in these facilities minimizes the formation of these deposits and would be expected to work similarly with deposits from glycolate-containing waste.

Although 3H Evaporator conditions were not part of this testing, the current test results to evaluate the impact of glycolic acid along with the results of validation testing performed previously for G-3 provide data that glycolate will not impact the corrosion resistance for the 3H evaporator. The results showed that operating at up to 428 °F, G-3 showed either salt deposits with slight staining or no deposits (at 45 wt%

NaOH only). Both G30® and G-3 in the current hot-wall testing also showed deposits both with and without glycolate present in the solution. For all the MoCs tested in a range of waste compositions, the glycolate anion was not found to significantly alter the corrosion behavior of the MoC. G-3 under high hydroxide concentrations in the presence of glycolate, therefore, is not expected to impact the corrosion resistance for the 3H Evaporator.

Localized corrosion was found to occur in solutions with the glycolate anion at boiling, which simulated the conditions for CPC vessels, and in 70 wt% glycolic acid at ambient temperature, which simulated the DWPF feed tanks and piping. This corrosion was not severe and may not impact service life. However, if components are removed from service within the CPC or a failure occurs, a failure or metallurgical analysis is recommended of the failure area or probable areas of corrosion. These data would be used to substantiate laboratory results and assess if localized corrosion would cause a leak. For the feed tanks and components which are housed outside of the CPC and are more accessible, ultrasonic thickness inspections configured to establish localized corrosion occurrence are recommended at the start of glycolic acid service, especially for components fabricated of 304L stainless steel. These inspections provide a baseline for determining the state of corrosion from future inspection data. DWPF has conducted the baseline non-destructive examination of the spool piece which only had seen formic acid service. The examination showed no localized corrosion and minimal loss of wall thickness. Subsequent inspections are planned at six months after the start of glycolic acid service.

In the accompanying table, the assessed impact of glycolic acid on the MoCs throughout the SRS waste management system is summarized.

Summary of Test Program for Glycolic Acid Impact on Performance of MoC in the DWPF and Downstream Facilities

Process Stream	[Glycolate] (g/L)	Temperature (°C)	Material	Material Performance
Glycolic Acid	700	50	316L	Acceptable – insignificant corrosion expected for service
		50	304L	Possible susceptibility to localized corrosion – representative components inspected and added to the DWPF structural integrity program
SRAT/SME* Supernate	63	95-100	C276	Acceptable – insignificant corrosion expected for service
		50	C276	Acceptable – insignificant corrosion expected for service
		90-100	Ultimet®	Possible susceptibility to localized corrosion – not expected to impact material integrity
		100	Stellite™	Possible susceptibility to localized corrosion – not expected to impact material integrity
		50	304L	Acceptable – insignificant corrosion expected for service
SRAT/SME* Condensate	0.18	50	316L	Acceptable – insignificant corrosion expected for service

Process Stream	[Glycolate] (g/L)	Temperature (°C)	Material	Material Performance
	6	50	304L	Acceptable – insignificant corrosion expected for service
DWPF Acidic Recycle	10	100	AllCorr®	Susceptible to localized corrosion, especially at neutral pH, corrosion at service (acidic) conditions acceptable
		30	AllCorr®	Acceptable – insignificant corrosion expected for service
		100/50	C276	Acceptable – insignificant corrosion expected for service
		30	304L	Acceptable – insignificant corrosion expected for service
		50	A285	Acceptable – insignificant corrosion expected for service
Basic Recycle	10	100	G30®	Possible susceptibility to localized corrosion due to deposit formation which is not exclusively associated with glycolate – 2H Evaporator uses cleaning to minimize deposit formation
		40		Acceptable – insignificant corrosion expected for service
		100/30	316L	Acceptable – insignificant corrosion expected for service
		100/30	304L	Acceptable – insignificant corrosion expected for service
		30	304L	Acceptable – insignificant corrosion expected for service
		100	A537	Acceptable – insignificant corrosion expected for service
		30	A537	Acceptable – insignificant corrosion expected for service
Salt Processing	10	50	Astralloy®	Acceptable – insignificant corrosion expected for service
			316L	Acceptable – insignificant corrosion expected for service
			304L	Acceptable – insignificant corrosion expected for service
			A537	Acceptable – insignificant corrosion expected for service
Boric Acid	10	50	316L	Acceptable – insignificant corrosion expected for service

Process Stream	[Glycolate] (g/L)	Temperature (°C)	Material	Material Performance
Dilute Waste	0.033	107	G-3	Possible susceptibility to localized corrosion due to deposit formation which is not exclusively associated with glycolate – ETF evaporator controls process and flushes to minimize deposit formation – 3H Evaporator has extended service life indicating minimal effect of deposit formation
		95	304L	Acceptable – insignificant corrosion expected for service
		30	304L	Acceptable – insignificant corrosion expected for service
		95	A537	Acceptable – insignificant corrosion expected for service
		30	A537	Acceptable – insignificant corrosion expected for service
Molten Glass			Inconel® 690	Acceptable – insignificant corrosion expected for service
			Monofrax™ K-3	Corrosion mechanism is the same for nitric-glycolic and nitric-formic flowsheets (NG, NF). The steady-state corrosion rate with NG is lower than NF, but is initially higher. Fe^0 depletion results when higher nitrate concentration on NG although iron is incorporated into passivating spinel layer that lowers K-3 corrosion rate in a minimally agitated melt pool.[2]
DWPF			Vinyl esters, polyurethanes, and epoxy coating systems	Acceptable - from literature review, the proprietary coating systems applied to DWPF concrete were found to be resistant to more aggressive chemistries than glycolic acid and limited data showed similar resins with acceptable resistance to glycolic acid.[3]

*SRAT – Sludge Receipt and Adjustment Tank, SME – Slurry Mix Evaporator

---

[2] M. S. Willams et al, "Corrosion Testing of Monofrax™ K-3 Refractory in Defense Waste Processing Facility (DWPF) Alternate Reductant Feeds," SRNL-STI-2016-00030, April 6, 2016

[3] J. I. Mickalonis and T. E. Skidmore, "Material Compatibility Evaluation for DWPF Nitric-Glycolic Acid – Literature Review," SRNL-STI-2013-00281, Revision 0, June 2013

TABLE OF CONTENTS

LIST OF TABLES

LIST OF FIGURES

LIST OF ABBREVIATIONS

304L	Type 304L Stainless Steel
316L	Type 316L Stainless Steel
G30	G-30® Alloy
Stellite	Stellite™ 6B
Ultimet	Ultimet® Alloy
AARTC	Association of American Railroads – Tank Car Specification
ASTM	ASTM International
CCP	Corrosion Control Program
CI	Coupon Immersion
CPC	Chemical Processing Cell
CPP	Cyclic Potentiodynamic Polarization
CR	Corrosion Rate
DWPF	Defense Waste Processing Facility
E_{corr}	Corrosion Potential (V, SCE)
E_{rp}	Pit Repassivation Potential (V, SCE)
EDS	Energy Dispersive Spectroscopy
ETF	Effluent Treatment Facility
EW	Equivalent Weight
GA	Glycolic Acid
HLW	High Level Waste
HW	Hot-Wall
i_{pass}	Passive current density (A/cm^2)
IGA	Intergranular Attack
LCM	Laser Confocal Microscope
LPR	Linear Polarization Resistance
MCU	Modular Caustic-side Solvent Extraction Unit
MFT	Melter Feed Tank
mo (mos)	Month(s)
MoC	Material of Construction
mpy	Mils per year
ND	No Data
NDE	Non-Destructive Examination
OCP	Open Circuit Potential
ppm	parts per million
REDC	Remote Equipment Decontamination Cell
REDOX	Reduction/Oxidation Reaction
SA	Surface Area
SCC	Stress Corrosion Cracking
SCE	Saturated Calomel Electrode
SEM	Scanning Electron Microscope
SME	Slurry Mix Evaporator

SMECT   Slurry Mix Evaporator Condensate Tank
SRAT   Slurry Receipt Adjustment Tank
SRNL   Savannah River National Laboratory
SRS   Savannah River Site
UT   Ultrasonic Thickness
WAC   Waste Acceptance Criteria

1.0 Introduction

The Savannah River Site (SRS) is preparing for a new alternate reductant flowsheet for the Defense Waste Processing Facility (DWPF), specifically a nitric acid-glycolic acid flowsheet. DWPF requested a corrosion assessment from the Savannah River National Laboratory (SRNL) for the components of the DWPF facility and the other high level waste (HLW) and low level waste processing facilities that would be exposed to glycolic acid or the glycolate anion [1]. Testing was conducted for both aqueous and glass environments [2]. Follow-up testing was required to further investigate several results where the corrosion behavior could not be definitely determined. Additional follow-up testing was requested to evaluate the impact of glycolic acid for all the different waste compositions covered by the Tank Farm Corrosion Control Program (CCP) [22]. This report presents and discusses the electrochemical, hot-wall, and coupon immersion test results that were performed to further clarify the corrosion in aqueous waste environments with the glycolate anion present. The approved report meets deliverable #3 of HLW-DWPF-TTR-2013-0004 and deliverable #4 of X-TTR-S-0006 [1, 22]. The follow-up testing for the melter refractory material is covered in a separate report [23].

A literature review was conducted prior to any testing and showed that there was insufficient corrosion data available to assess the impact of glycolic acid on the DWPF and downstream waste processing facilities [3]. Data on the material compatibility with just glycolic acid or its derivative products was identified; however, data were limited for solutions containing glycolic acid and other species that would be present in the DWPF, Tank Farm, and Modular Caustic-Side Solvent Extraction Unit (MCU) facilities. Corrosion testing was necessary to provide data to evaluate the corrosion compatibility for the specific materials of construction (MoC) and expected service conditions. For the proprietary coating systems applied to the DWPF concrete, glycolic acid was deemed compatible since the coatings were resistant to more aggressive chemistries than glycolic acid. Additionally similar coating resins showed acceptable resistance to glycolic acid.

The first phase for aqueous corrosion testing consisted of electrochemical tests, hot-wall tests, and a coupon exposure test performed in conjunction with the intermediary (22 L) scale-up testing for the chemical process cell (CPC) flowsheet development [2]. The test conditions simulated the service conditions for DWPF and downstream facilities. For the MoCs within the DWPF CPC and cold-feed tanks, localized corrosion was identified during this testing. Since the glycolate anion concentration is at the highest in the CPC for the whole HLW processing system, determining operating conditions where localized corrosion is a concern was stressed. Localized corrosion was also observed at HLW compositions for carbon steel and for the MoCs of heat transfer surfaces in downstream facilities.

The follow-up testing included a series of accelerated electrochemical and hot-wall tests, and a six-month coupon immersion test. These tests were recommended to better identify the waste chemistries for acceptable performance of the MoCs found to be susceptible to localized corrosion. Electrochemical tests were targeted towards three areas of the DWPF (glycolic acid feed tanks, CPC components, and the remote equipment decontamination cell (REDC) components) as well as the SRS Tank Farm waste tanks. Hot-wall tests were conducted to further clarify the observed localized corrosion during the first phase of testing for the heat transfer surfaces in the CPC and downstream facilities (2H Evaporator and evaporator heater of the Effluent Treatment Facility (ETF). A six-month coupon immersion test was conducted to verify that the accelerated results of the electrochemical test were substantiated for an extended exposure for CPC tanks and components.

2.0 Summary of First Phase Testing Localized Corrosion Occurrences

The first phase test results showed that for most MoCs the presence of the glycolate anion in the waste stream did not impact their corrosion resistance [2]. There were several waste streams where the impact

on the MoC corrosion resistance was inconclusive or insufficient and additional testing as presented in this report revision was required. These waste streams pertain to three facilities: the DWPF, especially the CPC; the HLW evaporators (2H, 3H, and ETF); and the Tank Farm. The table in Appendix A presents a summary of the first phase test conditions and results, and the follow-up testing needed to assess the impact of glycolic acid on these MoCs (In the table different shading indicates the different facilities).

During the first phase of testing, localized corrosion was identified for a few solutions tested in electrochemical and hot-wall tests. The observed localized corrosion was pitting, crevice and underdeposit corrosion. Pitting occurred during electrochemical tests with 304L stainless steel (304L) in 70 wt% glycolic acid at 50 °C (Appendix A, Row 1) and with C276, Stellite™ 6B (Stellite), and Ultimet® cobalt-chromium alloy (Ultimet) in CPC simulants at 95-100 °C (Appendix A, Rows 2-4). The CPC test solutions were based on simulants from experiments conducted during the trials on the efficacy of glycolic acid as an alternate reductant and were composed of a range of aggressive species (chloride, sulfate, and mercury) [4]. For both the 70 wt% glycolic acid and the CPC solutions, pitting was not observed on all samples during duplicate runs.

Follow-up testing was needed to determine the waste chemistries, specifically the chloride and sulfate concentrations, where localized corrosion was not observed when the glycolate anion was present. Electrochemical tests were performed first to identify possible concentration limits of aggressive species where localized corrosion was not observed, as well as, to determine baseline data for current DWPF operations in formic acid based solutions for comparative purposes. A coupon immersion test followed at bounding conditions to evaluate the change over an extended period (3 to 6 months).

In solutions based on the slurry mix evaporator condensate tank (SMECT), indications of pitting were identified during the first phase of electrochemical testing for both AllCorr® (primary quencher[4] MoC) and Type 304L stainless steel (304L, used as a conservative indicator for 316L, MoC of condensate tank components) at a near neutral pH (Appendix A, Rows 5 and 6). The electrochemical data for both MoCs had a repassivation potential (E_r) greater than 200 mV from the corrosion potential (E_{corr}), so pitting is not expected in service. This potential difference between E_{rp} and E_{corr} is a corrosion industry value used to indicate if pitting would be expected and a value greater than 100-200 mV indicates pitting would not be expected [12]. Additional testing therefore was not performed and the performance of the materials is expected to be acceptable.

Pitting, crevice, and underdeposit corrosion were all observed during hot-wall tests for C276, Stellite, and Ultimet in a CPC solution, for G-30® (G30) in a basic recycle simulant, and for G-3 in a dilute waste simulant. Hot-wall tests are conducted at boiling conditions with heat transfer through the test sample (Appendix A, Rows 2, 3, 4, 7, and 8). The occurrence of this corrosion might have been due to the change in solution, which may not be representative of process conditions. The solution volume was 500 ml and due to the high heat input quickly boiled down, requiring frequent replenishment. This fast volume change lead to a large amount of precipitates and surface deposits. Previous results by Chandler et al [5] also noted deposits during the hot-wall testing performed with a 2-3 L test volume. Although no localized corrosion was found, sample staining and some deposits were noted.   Testing in formic-based solutions was needed to establish baseline data for current DWPF operations and comparison to data from glycolic-based solutions, similar to the approach taken for the follow-up electrochemical testing.

For the HLW tanks, the first phase of testing (Appendix A, Rows 9-11) was performed in simulants representative of several waste types that would receive the DWPF recycle stream, including the inhibited

---

[4] Backup quencher is fabricated from C276; C276 showed no localized corrosion in the first phase testing with glycolic acid in solution.

acidic recycle stream, a dilute waste from evaporator overheads, and a feed for the Saltstone Facility. In one case, the test conditions, i.e. inhibitor levels and temperature met the requirements of the Corrosion Control Program (CCP) [25] for the waste tanks; the other tests violated either the maximum temperature or required nitrite concentration. In a neutralized acidic melter off gas stream (Appendix A, Row 9) which fell within the waste tank CCP, carbon steel was passive with very low corrosion rates (<0.1 mpy) both with and without the glycolate anion. For the other two waste compositions which did not meet the requirements of the CCP, the observed localized corrosion was independent of the presence of the glycolate anion.

The current waste tank CCP was based on extensive testing over a range of conditions, i.e. waste compositions and operating or storage temperatures. There is high confidence that if conditions are kept within the current control program constraints, the MOC behavior will be acceptable with the glycolate anion present. The control schemes of the current program were used to establish representative electrochemical corrosion test solution conditions (chemistry and temperature) for verifying that glycolic acid does not impact tank integrity. During this follow-up testing, the impact of formic acid, the current DWPF reductant, on these control schemes also was evaluated for comparative data.

3.0 Experimental Procedure

The follow-up testing consisted of three primary test types: electrochemical, which included a series of techniques, hot-wall, and coupon immersion. Additionally, the vessel and coils that were used for the large scale (1/200th scale) testing for the CPC flowsheet development were also examined using non-destructive examination (NDE). The test techniques/protocols, solutions, and materials used for these tests are discussed.

3.1 Electrochemical Testing

The electrochemical testing was chosen as an accelerated method to determine if the glycolic acid would impact the localized corrosion resistance of the MoCs as well as to measure a general corrosion rate. The electrochemical testing followed the guidelines given in applicable ASTM International standards [6-10]. The electrochemical testing consisted of a series of individual tests including open-circuit potential measurement, linear polarization resistance and cyclic potentiodynamic polarization.

Open-circuit potential (OCP) monitoring was used to follow the equilibration of the sample in the test solution and varied from one hour up to a maximum of three hours. In some cases the sample had not completely stabilized within the three-hour period (i.e. continue to slightly become more noble). Immediately at the end of the OCP monitoring, linear polarization resistance (LPR) was performed to determine a general corrosion rate. This test involves application of a scanning potential ramp (0.2 mV/sec) over a potential range of +/- 15 mV around the OCP. From the plot of the potential and resulting current, a polarization resistance value (R_p) is determined and Equation 1 is used to calculate a general corrosion rate (CR) for the material.

$$CR = 3.27 \ 10^3 \times B \times EW / (R_p \times \rho \times SA) \qquad \text{\{Equation 1\}}$$

where B is a constant related to the electrochemical behavior of the material in the environment, 0.026 for this testing; EW is the equivalent weight (g) of the material; ρ is the material density (g/cm^3); and SA is the surface area of the sample (cm^2). The material values are given in Table 3-1 for those materials used in the follow-up testing only. AARTC128 rail car steel was used as representative material for the waste tank MoCs (A537 and A516 (Type III), A285 (Type I, II, and IV tanks), and A106 (cooling coils)) since the compositions are similar. Additionally, the material is representative of the time period during which the HLW tanks were fabricated [25].

Table 3-1. Material Values for Determining Corrosion Rate from Electrochemical Data

Material	Surface Area* (cm^2)	Density (g/cm^3)	Equivalent Weight
304L	3	7.96	25.12
C276	2	8.8	27.09
AARTC128	5	7.86	27.9

* Approximate values

At the conclusion of the LPR, a cyclic potentiodynamic polarization (CPP) was performed to assess the susceptibility to localized corrosion. In this technique, a potential ramp (0.2 mV/sec) is applied towards more electropositive potentials reaching a defined vertex potential where the potential scan direction is reversed back to the OCP. The potential/responding current plot provides data on the passivity and susceptibility to pitting, crevice corrosion and stress corrosion cracking. An indication of pitting susceptibility is a positive hysteresis which occurs when the reverse scan is at larger currents than those of the forward scan[5]. A pit repassivation potential (E_{rp}) is defined where the reverse scan for a plot that exhibits positive hysteresis crosses the forward scan.

Potentiostatic testing was performed for some solution chemistries to investigate the occurrence of pitting. During the test a constant potential is applied to a sample for a desired time and the responding current is measured. The potential was chosen within the positive hysteresis loop observed in a CPP scan. The current-time behavior in conjunction with the sample's physical condition indicates the growth of stable pits. These tests were conducted for one hour, which is longer than the 1-2 minutes a sample is at potentials within the positive hysteresis loop during a CPP scan.

For most of the electrochemical tests, Ametek PAR Model 273A potentiostat/galvanostats were used in conjunction with a laptop computer and Scribner Associates Inc. CorrWare® software. For testing that supported the CCP, Gamry Reference 600 potentiostat/galvanostats and software were used. The test cell consisted of borosilicate glass five-port flasks with a standard three-electrode set up: a reference, counter and working electrodes. The counter electrode was 0.25-inch diameter graphite rods, while the reference electrode was a saturated calomel electrode (SCE, +0.243 V vs Normal Hydrogen Electrode). All potentials in this report are given in reference to the SCE potential. Prior to each test, the reference electrode potential was verified against that of an unused reference maintained in a saturated potassium chloride solution. After the potential check, the reference electrode was placed in a salt bridge containing 0.1 M sodium nitrate solution. In tests greater than 50 °C, water-cooled salt bridges were used in most cases to maintain the reference electrode at a constant value.

The potentiostat performance was verified following the test guidelines given in ASTM International G5 standard test method [6]. The data shown in Figure 3-1 for one of the potentiostats demonstrates that for a standardized test condition (430 stainless steel in de-aerated 1N sulfuric acid at 30 °C) the measured currents are within the acceptable minimum and maximum ranges both prior to and at the conclusion of testing. The other potentiostats had similar acceptable behavior.

The working electrode was one of the candidate materials of construction. The C276 and 304L samples had a Teflon®-coated copper wire attached to the back with a conductive silver epoxy. The sample with attached wire was placed in a metallurgical mount with fast-set epoxy. The mount exposed one surface of the sample for testing and facilitated surface preparation with 600-grit silicon carbide paper prior to testing. The carbon steel sample used for the CCP testing were bullet shaped (0.25 in diameter by 1.25 in

---

[5] A negative hysteresis occurs when the reverse scan is at lower currents than the forward scan.

long). Samples were used multiple times and prepared prior to the start of each test by grinding on 600-grit paper and rinsing with the following sequence –distilled water, acetone, distilled water – then blowing dry. At the conclusion of the test, the samples were examined for corrosion. Pictures were taken on a laser confocal microscope (LCM) along with scans for characterizing any observed pitting (pit depths). The LCM brings a higher level of examination for identifying surface features and measuring a depth.
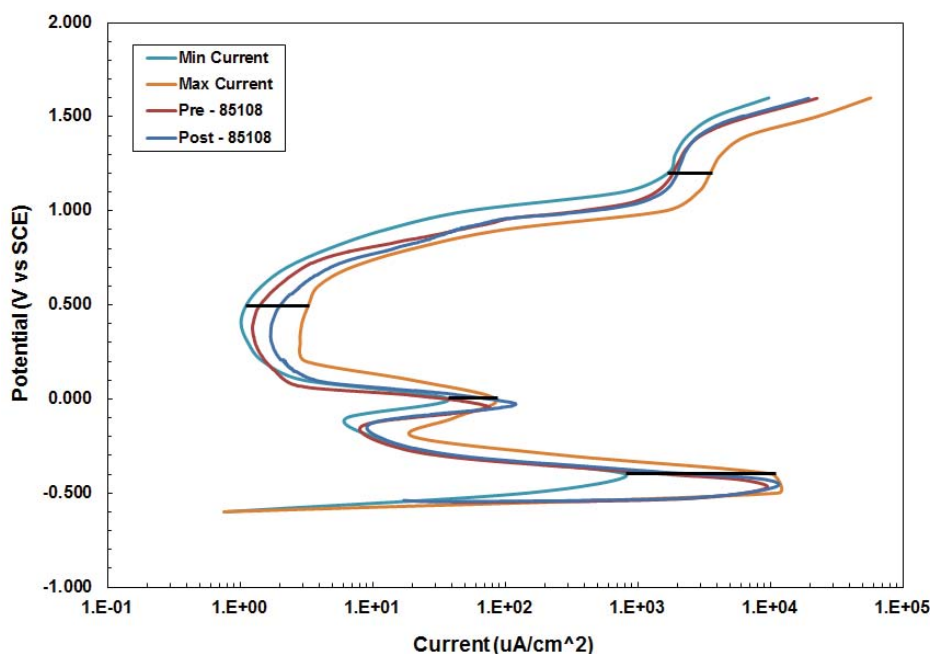
Figure 3-1. Polarization results from ASTM G5 standardized tests performed with potentiostat SN 85108 that was used during the alternate reductant testing

Test solutions were prepared up to one day prior to performing the test and prepared in 1 to- 2L batches. Test solutions are discussed in a following section. The solution volume ranged between 600 to 900 ml. Each test condition, i.e. temperature, solution chemistry, material, was performed in duplicate. All duplicate tests were not performed with the same batch of solution, which contributed to some of the data variability. At the conclusion of testing, some deposits or precipitates were generally seen in the bottom of the test cell. Measurement of the solution pH was made before and after each test, although pH measurements were not made for the high hydroxide (>1M) solutions. Tests were performed without bubbling of air. The natural convection of solutions due to heating from the bottom provided for solution mixing, especially at boiling conditions.

3.2 Hot-Wall Testing

Hot-wall tests are performed to determine corrosion rates for materials exposed to solutions under heat transfer conditions. The hot-wall test was discussed in greater detail in Reference 5. The hot-wall apparatus is shown in Figure 3-2. The sample is clamped in position with the heater block on one side and the glass vessel, which contains the solution, on the other. A gasket made of ethylene propylene diene terapolymer is used to form the seal between the sample and the glass vessel. Solution volume was approximately 2.5 L. Solution levels dropped during testing due to evaporation and were replenished on an alternating schedule between fresh solution and distilled water so as not to concentrate constituents.

The heater blocks were operated at full power to generate a maximum temperature on the sample surface. A thermocouple was placed through a port on the glass vessel so as to just touch the sample surface.

Thermocouples, which plugged into the heater block, were used to control the operation of the heater. Once at temperature, the tests were conducted for approximately 1 month.

Testing was performed on MoCs for the heating coils in the CPC vessels (C276), the tube bundle and warming coils for the 2H Evaporator (G30) and the heater for the ETF Evaporator (G-3). Samples, which were procured from Metal Samples (Munford, AL), had surfaces prepared with a 600-grit silicon carbide paper. Samples were 3-inch diameter and had a thickness of 1/8 to 1/16 inch. The solutions used to clean the samples after testing were nitric acid solutions from 0.1 M up to 2.0 M. The sample tested in the formic-based solution had a tenacious coating on the exposed surface at the conclusion of the test. Other cleaners, including sodium hydroxide (pH 14) solutions and glycolic acid, were tried but were ineffective. At the conclusion of the hot-wall test and after cleaning, the samples were examined for corrosion using a LCM. Laser scans were taken to characterize any localized corrosion and the condition of untested material surfaces.
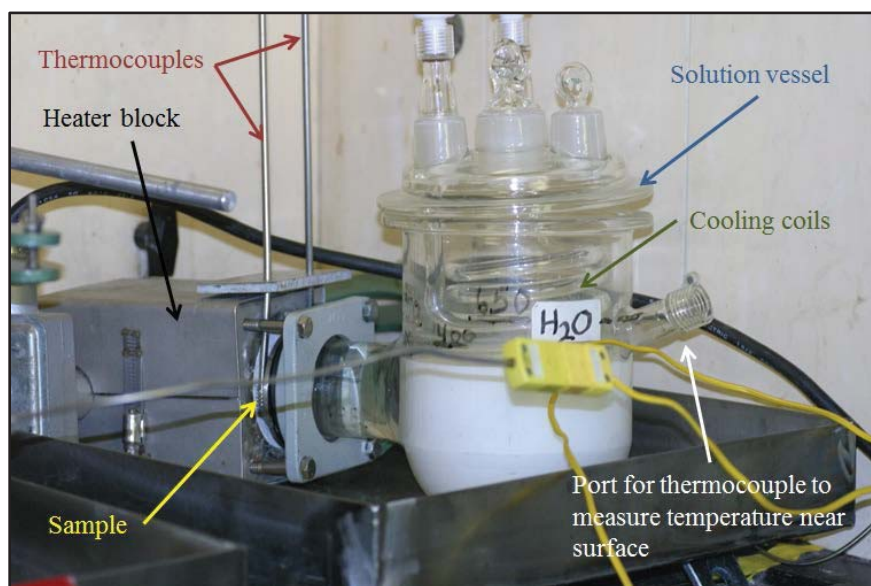
Figure 3-2. Hot-wall test apparatus for corrosion testing under heat transfer conditions

3.3 Coupon Immersion Tests

Laboratory coupon immersion tests are used to assess the corrosion performance of materials and to understand the influencing factors under controlled but simulated industrial environments. The SRNL coupon immersion testing followed the guidelines given in ASTM International standard G31 [10]. The coupon immersion tests were performed to evaluate the corrosion in the CPC vessels over an extended period (up to 6 months) with simulated CPC supernates and typical operating temperatures (i.e. boiling). The tests were conducted in borosilicate glass containers using laboratory digital hot-plates for temperature control. Figure 3-3 shows the laboratory set up where four different solutions were tested. Each container had a condenser to minimize evaporative losses.

The test solutions were based on the results from the electrochemical testing and were chosen to bracket a range of sulfate concentrations since it was shown to be the dominant aggressive species for localized corrosion. The chloride concentration has typically been below 100 ppm (mg/L) for the DWPF sludge batches and HLW processing at the SRS is not expected to introduce additional chloride species that would increase the concentration in the waste. Three glycolic-based compositions and one formic-based composition were chosen. Besides the reductant, the sulfate, nitrate, chloride, and mercury concentrations were also variables. The solution chemistries are discussed further in Test Solutions.

Figure 3-3. Coupon immersion test setup

The materials tested were those that are the MoCs within the CPC and at high temperatures, i.e. C276, Ultimet, and Stellite. C276 is used for the vessels and most components exposed to the waste at elevated temperatures. Ultimet cover plates are used on the heating coils adjacent to the supports to minimize wear in the slurry mix evaporator (SME). Stellite is used around the cooling coil guides in the SME, sludge receipt and adjustment tank (SRAT) and the melter feed tank. Coupons were procured from Metal Samples (Munford, AL) and had surfaces prepared with a 600-grit silicon carbide paper. A welded C276 sample was also included for this testing. Coupon dimensions are shown in Table 3-2.

Coupons were exposed on borosilicate supports that were hung from the container lid. Sets of coupons were exposed for 1, 3, 4, 5, and 6 months. Coupons were cleaned with a mild alkaline cleaner, thoroughly rinsed with water, rinsed with ethyl alcohol and blown dry before testing. After exposure, the coupons were cleaned using nitric acid solutions (0.1 M). Coupons were weighed before and after testing to calculate corrosion rates through mass loss according to Equation 2.

$$CR = (K \times W) / (SA \times T \times \rho) \hspace{3cm} \{Equation\ 2\}$$

Where K is a constant (3.45×10^6 for CR units of mils per year (mpy)), W is mass loss (grams (g)), SA is the surface area of the coupon (cm^2), T is exposure time (hours (hr)), and ρ is the material density (g/cm^3). The values for the materials used in this testing are shown in Table 3-2.

Table 3-2. Material Parameters for Calculating Corrosion Rate from Mass Loss

Material	Dimensions (cm)	Surface Area (cm^2)	Density (g/cm^3)
C276	5.08×2.54×0.32	31.22	8.8
C276W	5.08×2.54×0.32	31.22	8.8
Stellite	5.08×2.54×0.15	28.34	8.52
Ultimet	5.08×2.54×0.15 5.08×1.27×0.15	28.34 15.06	8.47

3.4 <u>NDE – Large Scale Testing</u>

The vessel and coils for the large scale testing during the CPC flowsheet development were used as large coupons. Ultrasonic Thickness (UT) measurements were made to evaluate the erosion/corrosion loss during this two-week test [11]. Measurement locations are shown in Figure 3-4 for both the vessel and coils. The MoC is 14 gage 304L stainless steel. Baseline measurements were made prior to testing at

several locations including in areas where corrosion or erosion might be more probable. The UT reports are in Appendix E. For the coils, 249 measurements were made around the circumference of approximately four rings and on inlets and outlets that were above the liquid level [17]. Near the outer radius, thickness measurements were typically 0.033 inch and at the inner radius 0.035 inch. The thinnest reading was 0.03 inch. Thickness values at 7 circumferential welds were also obtained ranging from 0.022 to 0.035 inch (lowest values may be associated with less than full penetration welds). The twenty-four baseline vessel thickness measurements ranged from 0.049 to 0.073 inch [18].

| (A) | (B) | (C) | (D) |
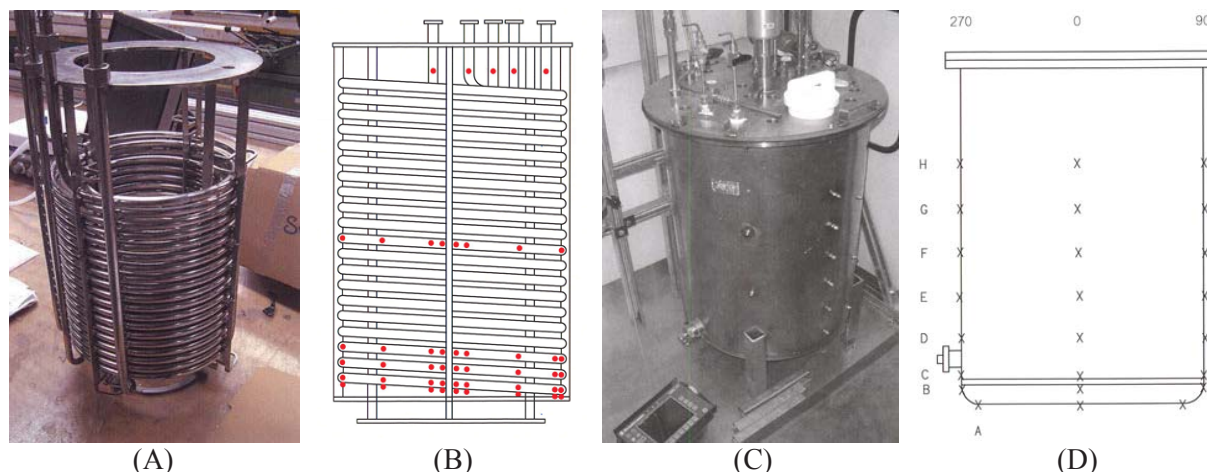
Figure 3-4. Large scale test vessel and heating coils: (A) coil photograph, (B) coil UT locations, (C) vessel photograph, and (D) vessel UT locations

3.5 Test Solutions[6]

The test solutions were similar to those used for the first phase testing including 70 wt% glycolic acid, multi-component CPC solutions, HLW evaporator feeds and Tank Farm waste simulants. The glycolic acid was used as provided by the supplier (stock bottle, reagent grade) and is the expected starting concentration for use in DWPF.

The baseline CPC simulant composition from the flowsheet development is shown in Appendix B, Table B-1. The primary component concentrations that were altered for this testing were the corrosive species, chloride, sulfate, nitrate and mercury, since these species affect the corrosion of the MoCs. Mercury was not in the baseline compositions since this composition was based on a SME supernate after mercury reduction. Mercury, however, will be present in sludge batches that are fed to the DWPF and be present in the process solution during reduction carried on in the SRAT. Test solutions were made with standard reagent grade chemicals and distilled water. Chemicals were added in the order given in Appendix B, Table B-2 for a glycolate-based solution, allowing a chemical to completely dissolve prior to adding the next chemical. Formate-based solutions were similar although nitrate species concentrations differed slightly. The highest used mercury addition was near the solubility limit of the solution, i.e. an additional quantity would not dissolve (~ 7 grams), although most quantities were far less (~300 mg). Most solutions were made one day ahead of use.

---

[6] The concentration units used in this document are either ppm as based on a mg/L calculation or analytical result or M (moles/liter). In general, concentration units associated with the Tank Farm testing is in M, while for the other tests the unit is ppm.

For the electrochemical tests, a range of the corrosive species was tested to determine limits for the occurrence of localized corrosion in glycolic-based solutions as well as obtain baseline data for formic-based solutions. The concentration ranges for these species are shown in Table 3-3.

Table 3-3. Concentrations for Corrosive Species in Electrochemical Test Solutions

Species	Range (ppm)
Chloride	100 – 823
Sulfate	1300 – 5200
Nitrate	27500 - 92700
Mercury	0 – 300

The test solutions for the hot-wall and coupon immersion tests were based on the results from the electrochemical tests. The concentrations (ppm) of corrosive species for these solutions are shown in Table 3-4. For the hot-wall tests, a single composition was used for both glycolic-based and formic-based solutions, which were the same compositions also used as part of the coupon immersion test. For the coupon immersion, three different compositions were used for the glycolic-based solutions and one for the formic-based solution. Initially, mercury was present in only one solution (Glycolic #1), however, after three months of testing mercury was added to the remaining solutions to assess the impact of mercury on the corrosion of the CPC MoCs.

Table 3-4. Concentrations (ppm) for Corrosive Species in Hot-Wall (HW) and Coupon Immersion (CI) Tests Solutions

Species	HW and CI Solutions		CI Solutions	
	Glycolic #1	*Formic #1*	*Glycolic #2*	*Glycolic #3*
Chloride	97	50	50	97
Sulfate	5570	2000	2000	2635
Nitrate	98347	42000	43350	98347
Mercury	~300	*	*	*

  * After three months of testing in the CI test, ~300 ppm was added to these solutions

Two other test solutions used for the hot-wall tests were a dilute waste chemistry and basic concentrated recycle, which were representative of feed solutions for the ETF Evaporator and the 2H Evaporator, respectively. In the first phase of testing these solutions with the glycolate anion present resulted in localized corrosion for the MoCs of these components. The occurrence of the corrosion was hypothesized to have resulted from the significant change in the solution due to the small volume of test solution used (500 ml versus the standard 2-2.5 L). These changes lead to numerous deposits. Two hot-wall tests were performed for each MoC with and without the glycolate anion present. The compositions of these solutions are shown in Appendix B, Table B-3 and Table B-4.

Through a review of the Tank Farm CCP and previous laboratory testing results, waste chemistries were identified where testing with glycolate was needed to demonstrate the impact on the CCP. The CCP identifies inhibitor and temperature requirements to minimize the occurrence of general and localized corrosion, including pitting, crevice corrosion and stress corrosion cracking (SCC). These chemistries and the requirements of the CCP are shown in Appendix C, where italicized portions of the CCP requirements identify experimental gaps. Three waste chemistries were covered by previous testing, which showed no impact of glycolate or a slight inhibitive effect. A test matrix was developed to address corrosion impacts of glycolate and formate over the remaining portions of the CCP. The test matrix is shown in Table 3-5 where bounding concentrations are used for glycolate and formate. For the identified gaps, the following conditions were used: (1) 10,000 mg/L formate; (2) 10,000 mg/L glycolate; and (3) 10,000 mg/L formate and 10,000 mg/L glycolate combined.

Table 3-5. Experimental Test Matrix To Determine Impacts of Glycolate and Formate on the CCP

Test #	Regions (M)	Corrosion	Inhibitor Requirements	Max T (°C)	Test Solution Chemistry (M)					Testing T (°C)
					NO_3	NO_2	OH	HCO_2	$C_2H_4O_3$	
1	OH≥8	OH-SCC	NO_2≥0.3 and T≤10	115	0.75	1.0	10	0.07	0	115
2								0	0.13	
3								0.07	0.13	
4	NO_3<1 and OH>8	OH-SCC	OH>1	60	0.75	1.0	10	0.07	0	75
5								0	0.13	
6								0.07	0.13	
7	5.5<NO_3≤8.5	NO_3-SCC	OH≥0.6, NO_2+OH≥1.1	70 (R<2)	7	0.5	0.6	0.07	0	70
8								0	0.13	
9								0.07	0.13	
10	2.75<NO_3≤5.5	NO_3-SCC	OH≥0.3, NO_2+OH≥1.1	112 (R>2)	3	2.5	4	0.07	0	112
11								0	0.13	
12								0.07	0.13	
13	2.75<NO_3≤5.5	NO_3-SCC	OH≥0.3, NO_2+OH≥1.1	105 (R<2)	4	2	0.3	0.07	0	105
14								0	0.13	
15								0.07	0.13	
16	1≤NO_3≤2.75	NO_3-SCC	OH≥0.1[NO_3], NO_2+OH≥0.4[NO_3]	105 (R>2)	1.1	2	2.5	0.07	0	105
17								0	0.13	
18								0.07	0.13	
19	1≤NO_3≤2.75	NO_3-SCC	OH≥0.1[NO_3], NO_2+OH≥0.4[NO_3]	70 (R≤2)	1.1	1.6	0.45	0.07	0	70
20								0	0.13	
21								0.07	0.13	
22	0.02<NO_3<1 and 1<OH≤8	Pitting	OH>1	100	0.75	1.0	2.5	0.07	0	100
23								0	0.13	
24								0.07	0.13	
25	NO_3≤0.02 and OH<1	Pitting	pH>10.3, [NO_2]=f{NO_3, Cl, and SO_4}	40	0.075	0.2	0.15	0.07	0	40
26								0	0.13	
27								0.07	0.13	

3.6 Materials

The materials for testing were the MoCs for the DWPF feed tanks and piping, CPC vessels and components, the REDC soak tank, the HLW Evaporators. Samples were machined at Metal Samples, Inc. (Munford, AL). The material compositions (wt%) for the electrochemical samples were verified through x-ray fluorescence and are shown in Table 3-6. All samples were prepared with a final surface finish from 600-grit silicon carbide grinding paper and cleaned with a mild detergent and ethyl alcohol prior to use.

Table 3-6 Material Compositions for Test Samples (wt%)

Material	Cr	Ni	Fe	Mn	Mo	Si	W	Co	Other
C276	15.5	57.8	6.3	0.5	14.2	0.3	3.3	1.8	
304L	18.5	8.8	69.7	1.8	0.2	0.5	-	-	0.3 Cu
Stellite	30.4	2.3	2.1	1.6	0.8	0.5	4	57.2	
Ultimet	25.2	9.2	3.2	0.8	5.1	0.4	2	53.9	
G30	28.8	40.4	14.9	1.1	5	0.3	3.1	3.6	1.9 Cu, 0.7 Nb, 0.2 Al
G-3	22.3	44	19.8	0.8	7.6	0.5	0.9	1.9	2 Cu
Alloy 20	20	35	Bal	2	1.5	1	-	-	3.5 Cu, 1 Cb+Ta
AARTC128	0.13	-	Bal	1.27	0.05	0.29	-	-	0.225 C, 0.22 Cu

4.0 Results and Discussion - DWPF

The experimental work during this follow-up testing centered on the DWPF vessels and components and included electrochemical, hot-wall and coupon immersion testing. NDE also was performed on the 1/200th scale vessel and heating coils used with the scale up testing for the flowsheet development. These measurements were made to assess the erosion/corrosion potential of the glycolic-based simulants.

4.1 Electrochemical Test Results

Electrochemical tests were performed to better understand the occurrence of localized corrosion with a glycolic-based solution and to generate baseline data in formic-based solutions for comparison. These data were used to establish the solution compositions for the hot-wall and coupon immersion testing, which were performed to evaluate corrosion over time. The electrochemical tests were focused on C276, the primary MoC of the DWPF CPC. Additionally, electrochemical testing was also performed for the MoC of some feed tanks (304L) with 70 wt% glycolic acid and of the decontamination cell soak tank (Alloy 20) located in the REDC which uses a 12 wt% nitric acid solution.

4.1.1 CPC Simulants from Flowsheet Development Testing

During the follow-up testing, two CPC simulants from flowsheet development testing[7] were evaluated to create baseline data for C276 from these processed simulants for comparison to data from solutions prepared from stock chemicals [2]. One simulant came from processing of a simulated Sludge Batch #7 waste using the nitric-glycolic acid flowsheet, while the other simulant was produced using the current nitric-formic acid flowsheet and a Sludge Batch #8 feed. Both simulants were made with higher acid stoichiometry, 110 wt% and 140 wt% for Sludge Batches #7 and #8, respectively. The analyzed chemistries for the simulants are shown in Appendix B, Table B-1. A mercury concentration was not available, but since the experimental processing included SME processing, soluble mercury was believed to be minimal.

The chemistries for the two CPC simulants were similar for most elements and compounds. Besides the expected differences in glycolate and formate concentrations, differences were noted for potassium, sodium, copper, manganese, nickel, chloride, nitrate, and carbonate. These differences are attributed to differences or variations in sludge batch compositions, processing conditions, and experimental feed chemistries. Chloride, sulfate and nitrate are the species primarily involved in the corrosion of the MoCs. Sulfate was at a similar concentration for both simulants while chloride and nitrate were higher in the glycolic-based simulant.

The CPP scans for C276 in both CPC simulants are shown in Figure 4-1; pitting was noted on samples for both simulants after the test. A quasi-passive behavior was noted for both simulants with the glycolic-based simulant (Figure 4-1 (A)) results shifted to higher current densities than those for the formic-based simulants (Figure 4-1 (B)). The scans both have a small positive hysteresis, which indicates possible pitting susceptibility. Average values for the corrosion potential (E_{corr}), general corrosion rate (CR)[8], passive current density [9] (i_{pass}), and pit repassivation potential (E_{rp}) are given in Table 4-1. From these results the glycolic-based simulant appeared to be slightly more corrosive with a slightly higher general corrosion rate and i_{pass}. Both these factors may be associated with the higher concentrations of chlorides and nitrates in solution. The effect of nitrate on the CPP scan will be discussed more fully below. The actual difference in corrosion rates between the glycolic-based and formic-based simulants is small. The general corrosion rates are considered excellent at approximately 1 mpy or less. The E_{rp} value defines the

---

[7] CPC simulants were from the 22L scale up testing for the nitric-glycolic acid flowsheet development and from Sludge Batch #8 qualification testing using the nitric-formic acid flowsheet.
[8] General corrosion rates are calculated from the results of the LPR testing.
[9] The passive current density value is taken at a potential 200mV more electropositive than the corrosion potential.

potential below which pits are not expected to initiate and grow. For both simulants this value is greater than 200 mV from E_{corr}, which is an indication that pitting would not be expected during service [12].
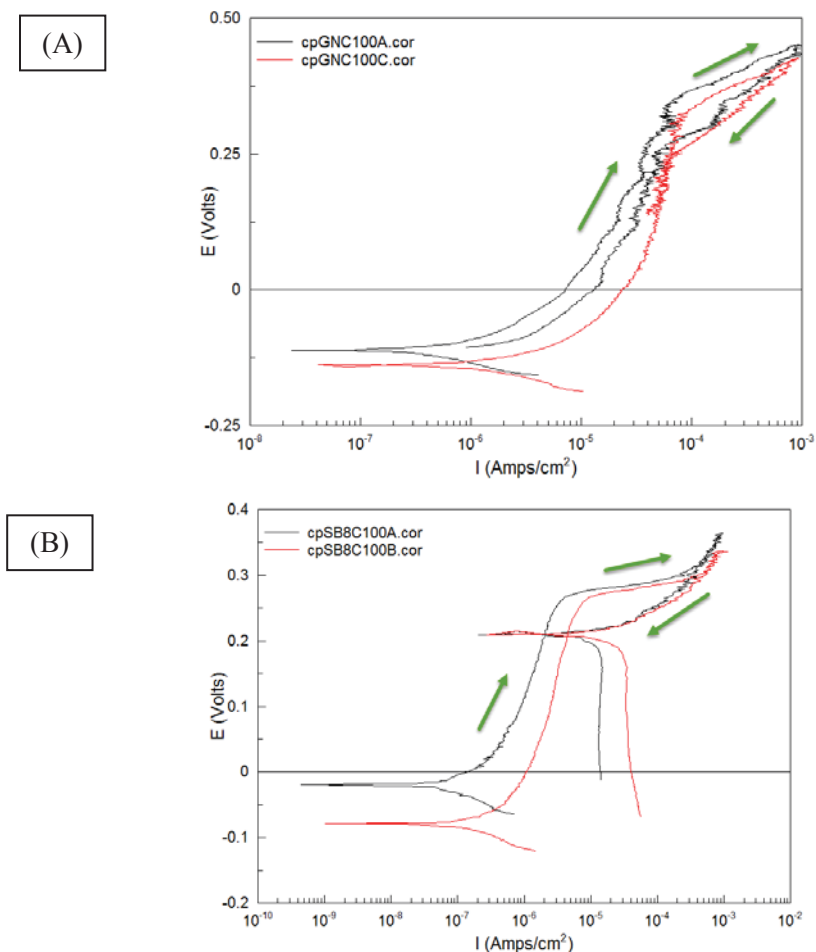
Figure 4-1. CPP scans for C276 in CPC simulants produced using: (A) a nitric-glycolic acid flowsheet (cpGNC100A and C) and (B) a nitric-formic acid flowsheet (cpSB8C100A and B)

Table 4-1. Average Electrochemical Parameters for CPC Simulants

Simulant	E_{corr} (V, SCE)	CR (mpy)	i_{pass} (A/cm^2)	E_{pp} (V, SCE)
Glycolic-based	-0.113	1.2	3.2E-5	0.336
Formic-based	-0.035	0.2	0.2E-5	0.206

(A)

(B)
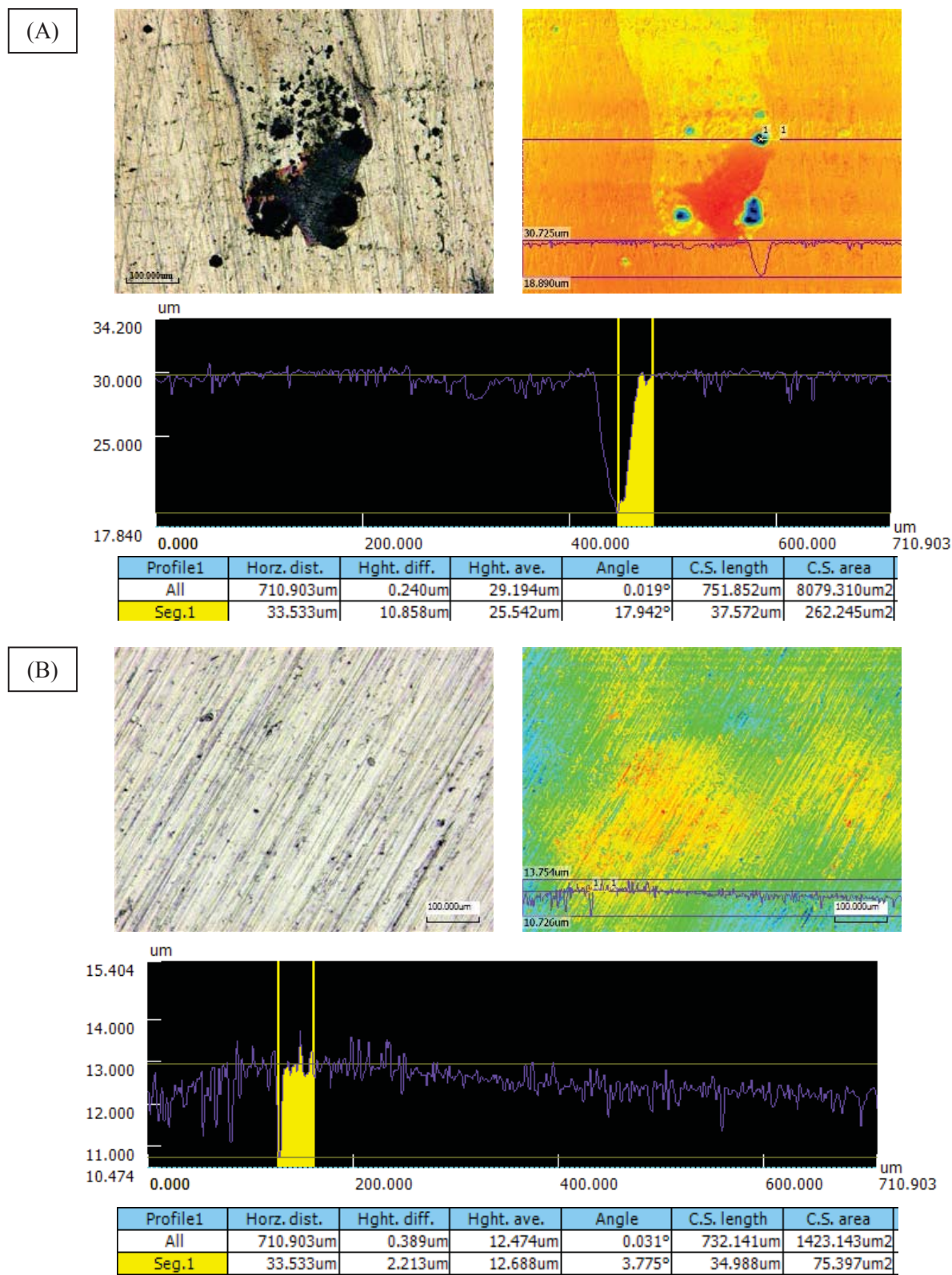
Figure 4-2. Pitting of C276 in glycolic-based (A) and formic-based (B) CPC simulants which were produced during flowsheet development (for each simulant a micrograph and corresponding height scan, line profile, and measurement table are given)

The number of pits that occurred during the CPP scans was small. For the glycolic-based simulant, only one C276 sample had pits ranging from 4 to 11 μm.[10] Only small pits (on the order of 1-3 μm) were found for samples tested in the formic-based simulant. LCM height scans are given in Figure 4-2 and show the pit depth measurements (Hght. diff. for Seg.1 in tables). Both simulants, however, have chloride concentrations that exceed those seen in the DWPF (approximately one order of magnitude) [13].

The C276 samples tested in the formic-based simulant developed an adherent coating, which needed to be removed prior to examination for pits. The coating was 1.5-3 μm thick. Based on x-ray fluorescence data, the coating had a significant manganese peak. This coating had pores and openings as shown in the photograph in Figure 4-3 (A). The determination of openings and pores was made through laser confocal height scans near edges and scratches made in the coating as shown in Figure 4-3 (B). These openings may have allowed crevice-type conditions to occur that led to the observed pitting.
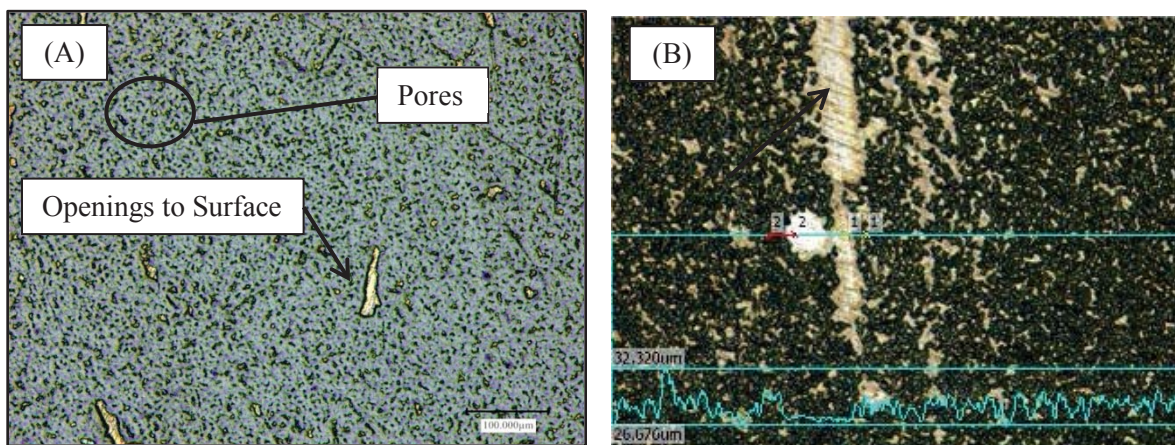
Figure 4-3. Mn-rich coating that formed on C276 sample during CPP scan in formic-based CPC simulant: (A) center of coating and (B) near scratch made through coating

4.1.2 Glycolic-Based Solutions

After analyzing the chemistry of the glycolic-based CPC simulant, the occurrence of pitting could be attributed to the simultaneous high levels of chloride (874 ppm) and sulfate (2636 ppm). These levels were greater than those measured for previous DWPF Sludge Batches. Chloride and sulfate concentrations from previous Sludge Batches are shown in Table 4-2 [13]. In many cases, the chloride concentration was below the detection level of the instrument. Sulfate concentrations were consistently below 2000 ppm and much lower than the Waste Acceptance Criteria (WAC) level of 0.058M (~5600 ppm) [14]. The current processing protocol that requires sulfate be washed below the glass solubility limit also reduces the chloride concentration and resulted in extended lifetimes for most components in the CPC.

A series of electrochemical tests were performed which varied the concentration of chloride and sulfate as well as nitrate and mercury, which are also known to affect corrosion. A list of these tests, the calculated concentrations of the corrosive species (based on added quantities of chemicals) and average electrochemical parameters (E_{corr}, i_{pass}, and CR) are shown in Table 4-3. The corrosion rates come from the results of the LPR test, while E_{corr} and i_{pass} were taken from the CPP scans. As can be seen from an initial review of the data presented in Table 4-3, there were only a few instances in which pitting was found in these electrochemical tests. That is, pitting is avoided by lowering either the chloride or sulfate concentration to historic DWPF operating values.

---

[10] Note that 25.4 μm is equivalent to 1 mil or 0.001 inch so a 5 μm pit is equivalent to 0.2 mil or 0.0002 inch.

Table 4-2. DWPF Sludge Batch Concentrations for Chloride and Sulfate*

Sludge Batch	Chloride (mg/Kg)	Sulfate (mg/Kg)
1B	12	665
2	7.4	849
3	<27	1790
4	<52	1173
5	<310	790
6	46	834
7a	ND	1466
7b	<268	1460
8	<96	1260

*The data in this table are the actual analytical results from DWPF which were determined in the mg/Kg also equivalent to ppm.

Table 4-3. Solution Compositions and Electrochemical Results for C276 in Glycolate-based Solutions at 100 °C[α]

Test	Calculated concentrations (ppm)				Pitting	Average Electrochemical Data		
	Chloride	Sulfate	Nitrate	Mercury[β]		E_{corr} (V)	CR (mpy)	i_{pass} (A/cm^2)
CPC[γ]	874	2635	92700	0	Y[£]	-0.113	1.17	3.20E-05
1	100	5572	57463	0	N	-0.212	0.85	3.90E-05
1-Hg	100	5572	57463	~300	N	-0.229	1.41	4.20E-05
2	<1	5571	57463	0	N	-0.205	0.77	1.60E-05
2-Hg[δ]	<1	5571	57463	59 to 21	N	-0.26	0.5	1.80E-05
3	50	2000	57251	0	N	-0.236	0.83	2.60E-05
3-Hg	50	2000	57251	~300	N	0.294	34	6.00E-05
4	0	1921	57251	0	N	-0.154	0.75	5.80E-06
4-Hg[δ]	0	1921	57251	323	N	0.299	24.4	1.08E-05
5	35	507	57463	0	N[£]	-0.158	0.99	8.80E-06
6	100	5572	98558	0	N	-0.215	0.83	2.20E-05
6-Hg	100	5572	98558	~300	N	-0.273	0.76	2.10E-05
7	86	2636	98347	0	N	-0.173	1	1.60E-05
7-Hg	86	2636	98347	~300	N	-0.26	1	2.70E-05
8	35	1921	34237	0	Y[£]	-0.045	0.46	4.30E-06
9	36	1128	34025	0	Y[£]	-0.163	1.38	3.70E-05
10	821	423	57463	0	N	-0.218	0.76	1.4E-05

α Shading indicates solutions that are paired, such that one contains mercury and the other is mercury free.
β Estimated mercury concentrations are denoted by the symbol ~. Estimated values are based on the correlation of added gram quantities and measured values performed previously.
γ This test was the CPC simulant produced during flowsheet development.
δ Measured values of mercury
£ Samples had deposits at end of testing

Although mercury did not adversely impact the localized corrosion susceptibility in these solutions, mercury did increase the general corrosion rate and alter the electrochemical response. The results were at first confusing since comparable additions of mercury nitrate to different batches of the same solution chemistry did not yield the same electrochemical results. This problem resulted from the source of mercury used. Mercury was added from an in-stock bottle of mercury nitrate salt ($Hg(NO_3)_2$), which had absorbed water over time, so concentrations were lower than expected. Verification of mercury concentration was only performed for two tests (Tests #2 and #4 in Table 4-3).

The results of Tests #3 through #4-Hg in Table 4-3 clearly show that the presence of a large concentration of mercury does not lead to an increased susceptibility to localized corrosion. Pitting of the C276 coupon was not observed after testing in the mercury-containing solutions and the CPP scans showed negative hystereses. The general corrosion rate, however, is definitely impacted with greater than an order of magnitude increase from less than >1 mpy to 25-35 mpy.

When mercury is present in a sufficiently high concentration, the OCP, E_{corr} and the entire CPP scan are shifted to more electropositive potentials. In Figure 4-4, the OCP measurements prior to CPP scans are shown for three different mercury concentrations (Tests #2 (0 ppm Hg), #2-Hg (59 ppm Hg), and #4-Hg (323 ppm Hg) in Table 4-3). For Test #2-Hg, the initial mercury concentration was 59 ppm and after electrochemical testing was 21 ppm. When sufficient mercury is present the OCP is maintained at values greater than 0.0 V. When no mercury is present the OCP values always stayed below 0.0 V. At intermediate concentrations, the OCP values transition from greater than 0.0 V to less than 0.0 V. The interpretation of this data is that the soluble Hg^{+2} is reduced with time. The mercury decrease may be from the formation of mercuric chloride ($HgCl_2$), although these particular solutions had low to no chloride.
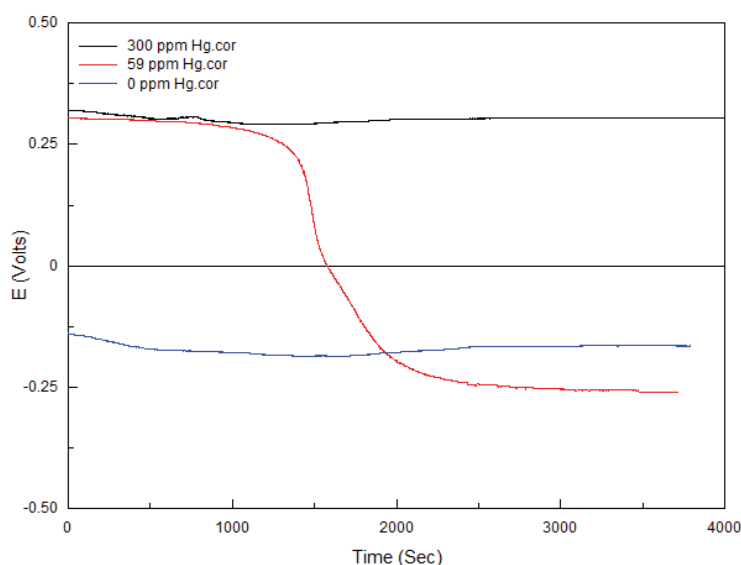
Figure 4-4. Open-circuit potential measurements over time in glycolic-based solutions showing the impact of mercury concentration

Cathodic polarization scans shown in Figure 4-5 were performed to investigate the difference in cathodic reactions that might be occurring under these different conditions. The same solutions that were used for the CPP scans were used for these tests. The after test concentration of mercury was not measured for Test #4 so the initial is given in the figure. The two batches of solution for Test #4 (300 ppm Hg initial A and B), however, appear to have slightly different mercury concentrations as indicated by the lower starting potential for A than B. The polarization scans show at the high mercury concentration the cathodic reduction reaction is at a limiting current density, indicating a diffusion controlled reaction and a a concentration limit had been reached for the reductant. This reaction dominates the cathodic reactions until more electropositive potentials are reached where other reactions such as hydrogen reduction can occur. Mercury reduction would be expected at the electropositive potentials with 300 ppm Hg present. However, on examination after testing mercury was not seen visually or analytically with energy dispersive spectroscopy of the samples surfaces. The reaction associated with high limiting current density in the presence of mercury contributed to the higher general corrosion rates observed in these

solutions as shown in Table 4-3. This increase in corrosion rate, however, is dependent on other constituents in solution. At high sulfate or nitrate concentration there is not an increase in corrosion rate. More study will be needed to delineate the impact of mercury in these solution chemistries.
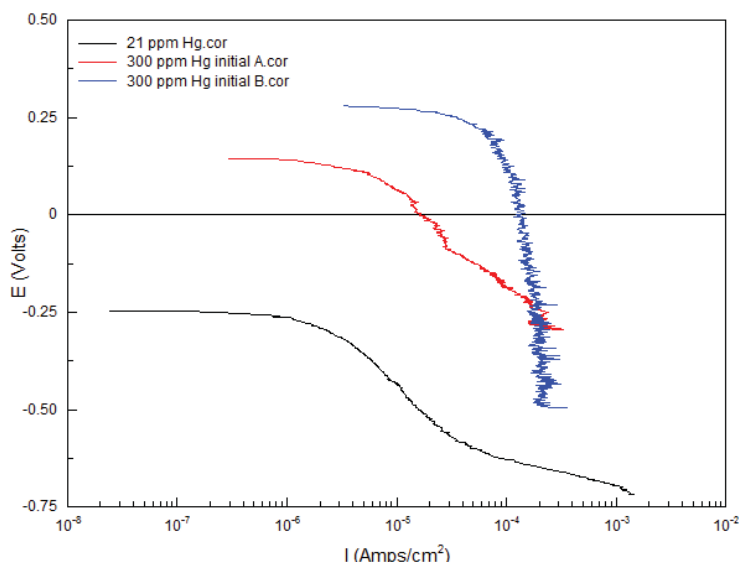
Figure 4-5. Cathodic polarization curves at high and low mercury concentrations

A review of Table 4-3 shows that once the chloride concentration was dropped to 100 ppm or below pitting was nearly eliminated. There were two exceptions (Tests #8 and #9) and these will be discussed below. One test (Test #10) was performed while maintaining a high chloride concentration but greatly reducing the sulfate concentration to investigate if any synergy existed between these two species. This condition is not likely to occur for the SRS sludges to be processed through the DWPF. Although these data are minimal, the results from Test #10 showed that pitting was not observed along with low general corrosion rates when a high chloride (821 ppm) concentration was maintained with a very low sulfate concentration (423 ppm), indicating some type of synergy between these species to drive pitting corrosion.

For the low chloride solutions where pitting was observed (Tests #8 and #9 in Table 4-3), deposits formed during the test. These solutions had low nitrate concentrations. In making these low nitrate solutions, the glycolate concentration was also reduced by molar equivalents, which appeared to have reduced the complexing capability of the solution and led to the formation of deposits on the surface. With chlorides and a crevice present from deposits, pitting or localized breakdown occurred during the polarization test. The pits ranged from 5 to 20 μm on these samples.

As can be seen from the corrosion rates for the low nitrate solutions, which do not contain mercury, the average corrosion rates (0.46 and 1.38 mpy) bracket the rates for the higher nitrate solutions (0.75 to 1 mpy). While not affecting the corrosion rate, the reduced nitrate concentration on average shifted CPP scans to lower current densities in these glycolic-based solutions as shown in Figure 4-6 for C276, although the range of i_{pass} values overlapped for different nitrate concentrations (see Table 4-3).

Although the chloride and sulfate concentrations had a significant impact on the occurrence of pitting if their concentrations were sufficiently high, there were no measurable, correlated changes in the electrochemical response of C276 to variations in their concentrations. Figure 4-7 and Figure 4-8 show CPP scans for solutions containing different concentrations of sulfates and chlorides, respectively. These scans do not show consistent changes in E_{corr} or i_{pass} with respect to the concentration changes. The effect may be obfuscated by changes in the concentration of other constituents.

17

The CPP scans shown in Figure 4-6 through Figure 4-8 for glycolic-based solutions have positive hystereses similar to that observed for the CPC glycolic-based simulant from the 22-L scale up testing (Figure 4-3). The potentials at which reverse scan currents are greater than the forward scan currents are close to the vertex potential (potential at which the scan reverses direction) and not E_{corr}, i.e. E_{rp} is greater than 200 mV from E_{corr}. Therefore, pitting would not be expected during service in these type solutions [12].
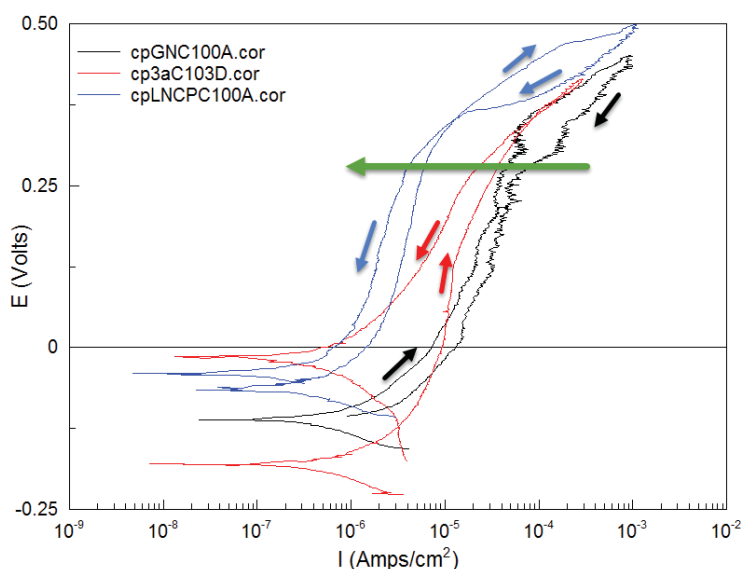
Figure 4-6. **Effect of nitrate concentration on the CPP scans for C276 in glycolic-based solutions at boiling (arrow indicates decreasing nitrate concentration from 92,700 to 34,237 ppm)**
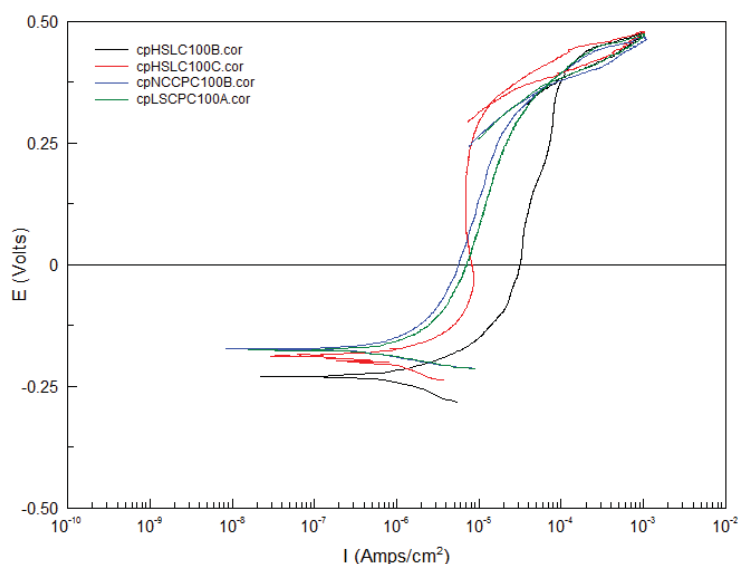
Figure 4-7. **CPP scans for C276 in boiling glycolic-based solutions with different sulfate concentrations, ranging from 507 to 5571 ppm (chloride concentration ranged from 0 to 35 ppm)**
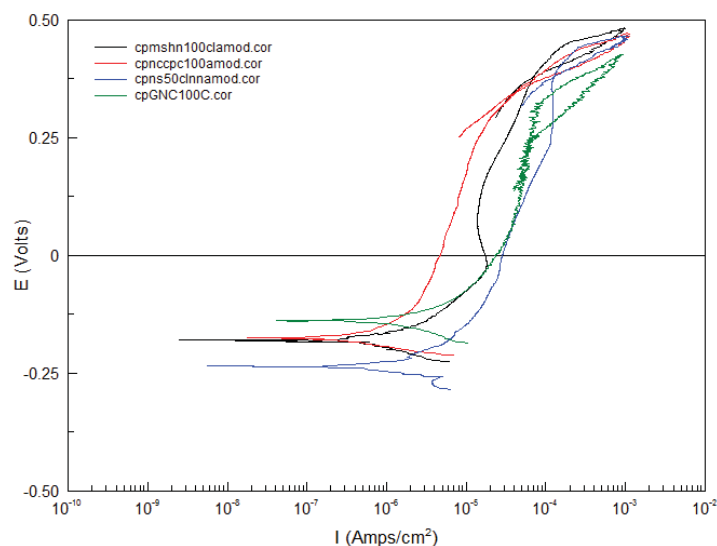
Figure 4-8. CPP scans for C276 in boiling glycolic-based solutions with different chloride concentrations, ranging from 0 to 874 ppm (sulfate concentration ranged from 2000 to 2635 ppm)

A series of potentiostatic test was conducted at applied potentials within a positive hysteresis loop (greater than the E_{rp}) to determine if pitting was found to occur at times longer than during a CPP scan (60 minutes versus 1-2 minutes to pass through the potential range of the loop). The test solutions contained approximately 57500 ppm nitrate, 5600 ppm sulfate, and 100 ppm chloride, and were with and without mercury (Solutions from Tests #1 and #1-Hg in Table 4-3). Figure 4-9 shows the chrono-current traces, which in general started at the highest current value for the trace and quickly dropped to a lower constant value. This type of trace is consistent with a material undergoing general corrosion. A chrono-current trace for pitting would be increasing because as pits develop more current is generated at the expanding surface area.
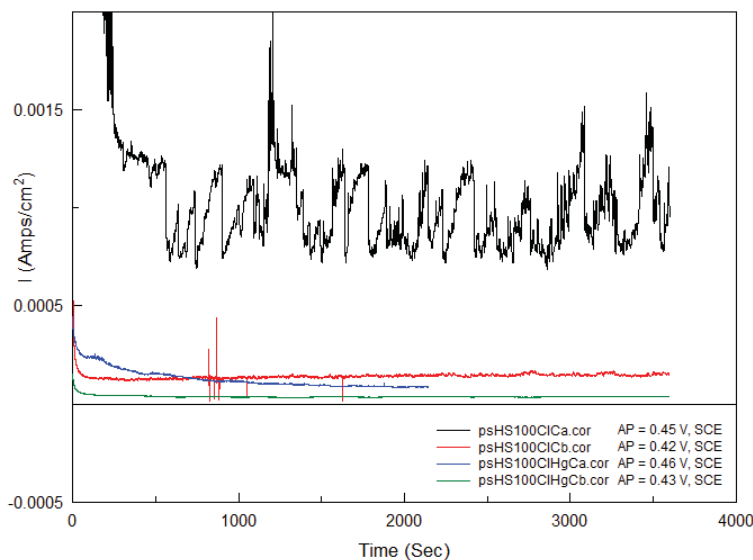
Figure 4-9. Chrono-current traces for potentiostatic tests at potentials within the positive hysteresis loop for boiling glycolic-based solutions with and without mercury

19

The chrono-current trace in the mercury-free solution at an applied potential of 0.45 V differed slightly from the others in that large current transients were observed. The source of these transients is not known, however, pitting transients have similar characteristics. The current is on the order of 1 mA which suggests these transient could be indications of pitting. Meta-stable pitting transients or passivating pits have transients that are 1-2 orders of magnitude lower than those observed [6]. However, pitting was not observed on the sample. Other sources for these transients may be reactions of solutions species on the sample surface.

4.1.3 Formic-Based Solutions

Several tests were performed for C276 in formic-based solutions to assist in selection of chemistries for hot-wall and coupon immersion tests. The results are summarized in Table 4-4. The mercury source was similar to that used for the glycolic-based solutions so the actual mercury concentration is probably lower than 300 ppm for Test #1-Hg. The electrochemical responses also did not indicate a shift in potentials to more noble values. Test #1 is actually the one used for the coupon immersion test and pitting was observed on those samples. The CPP scans for these were all similar in appearance to that shown in Figure 4-1 (B) for the formic-based CPC simulant, which had a slight positive hysteresis.

Table 4-4. Solution Compositions and Electrochemical Results for C276 in Formate-based Solutions at 100 °C$^\alpha$

Test	Calculated concentrations (ppm)				Pitting	Average Electrochemical Data		
	Chloride	Sulfate	Nitrate	Mercury$^\beta$		E_{corr} (V)	CR (mpy)	i_{pass} (A/cm2)
CPC$^\gamma$	247	2550	27500	0	Y$^£$	-0.035	0.2	0.2E-5
1	50	2000	43590	0	N	-0.399	0.27	1.6E-5
1-Hg	50	2000	43590	~300	N	-0.406	0.28	7.1E-5
3	100	5571	43560	0	N$^\delta$	-0.303	0.6	1.1E-4
3'	100	5571	43560	0	Y$^£$	-0.403	0.46	3E-5

α Shading indicates solutions that are paired, such that one contains mercury and the other is mercury free.
β Estimated mercury concentrations are denoted by the symbol ~. Estimated values are based on the correlation of added gram quantities and measured values performed previously for glycolic-based solutions.
γ This test was the CPC simulant produced during flowsheet development.
δ Sample bronzed over
£ Samples had deposits at end of testing

For Tests #3 and #3' in Table 4-4, which were similar test conditions, pitting was observed in one test but not the other. The pits (2-5 μm) were associated with small deposits that formed on the Test #3' sample. The sample from the Test #3 bronzed over, but did not have any pits. The electrochemical data are similar although not identical with Test #3 having results of a higher i_{pass} and a more noble E_{corr} than the results from Test #3'. This chemistry with a high sulfate concentration (WAC limit) appears to have surface reactions with C276 which may or may not make it susceptible to pitting. The deposits were not analyzed further to determine their composition.

4.1.4 70 wt% Glycolic Acid

From the literature review [3], the corrosion of 304L in 70 wt% glycolic acid was reported to be acceptable at temperatures of 50 °C or below [3]. During the first phase of testing, however, 304L was shown to pit at 50 °C as well as to have a variable electrochemical response [2]. The OCP stabilized at two different values (0.2 and -0.28 V) which also had different corrosion rates (0.2 and 6 mpy, respectively). Although CPP scans for these different OCPs had different characteristics, both showed passive behavior and negative hysteresis with samples pitting during the test. During this follow-up testing, tests were performed at 35 °C and room temperature. At 35 °C, two OCPs were also found to occur, while at room temperature only the more noble potential occurred as shown in Figure 4-10. The

different OCPs again were associated with different LPR corrosion rates, 0.05 mpy at 0.2V and 0.42 mpy at -0.123V. At room temperature the average LPR corrosion rate was 0.08 mpy.
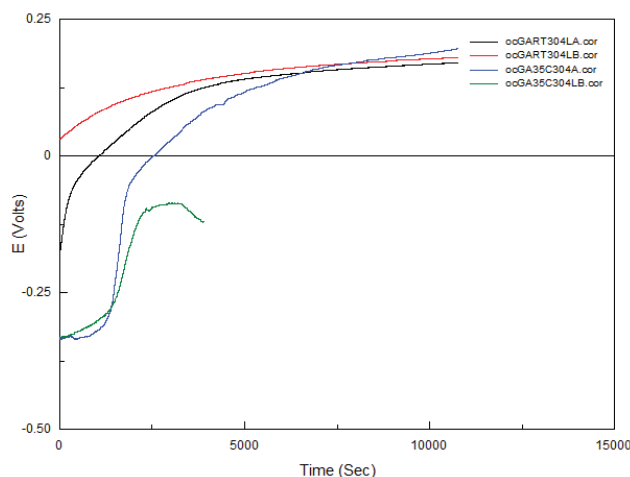
Figure 4-10. Open-circuit potentials of 304L stainless steel in 70 wt% glycolic acid at room temperature and 35° C

The CPP scans also depended on the initial OCP value as shown by the data in Figure 4-11. The more active OCP value (< 0.0 V, cpGA35C304LB.cor) has a CPP scan with a greater i_P value as well as a possible transition in state of the surface oxide or cathodic reaction occurring at the surface. The CPP scan with a passive OCP (> 0.0 V, cpGART304LA.cor) was independent of temperature and all showed simple passive polarization curves.
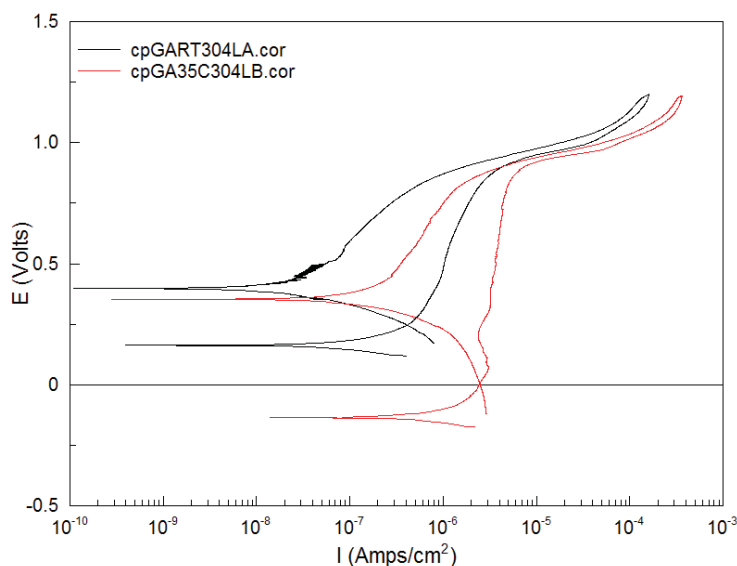
Figure 4-11. CPP scans for 304L in 70 wt% glycolic acid at room temperature and 35° C

Independent of temperature, small pits (< 5 μm) were located on all samples. The pits formed on the room temperature samples appeared to be associated with inclusions since they formed in a linear array, as shown in Figure 4-12 (A), such as might results from inclusions preferentially oriented with the rolling direction. Inclusions, specifically manganese sulfides, are locations of pit initiation in austenitic stainless steels. At 35 °C, the samples appeared free of pits; however, on examination at higher magnification a few pit-like features were located as shown by the micrograph in Figure 4-12 (B). Their depth (~ 5 μm)

was difficult to differentiate from variability in the surface morphology as shown by the laser height scan in Figure 4-13. With a negative hysteresis in the CPP scans, these pits are most likely metastable pits that initiated and passivated. Pit growth; however, is not determined from these types of electrochemical tests.
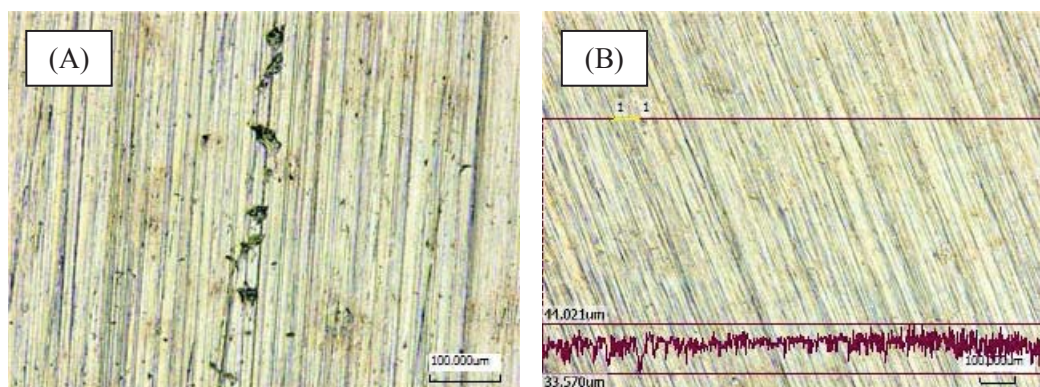
Figure 4-12. Micrographs of 304L stainless steel after electrochemical testing in 70 wt% glycolic acid at (A) room temperature and (B) 35 °C
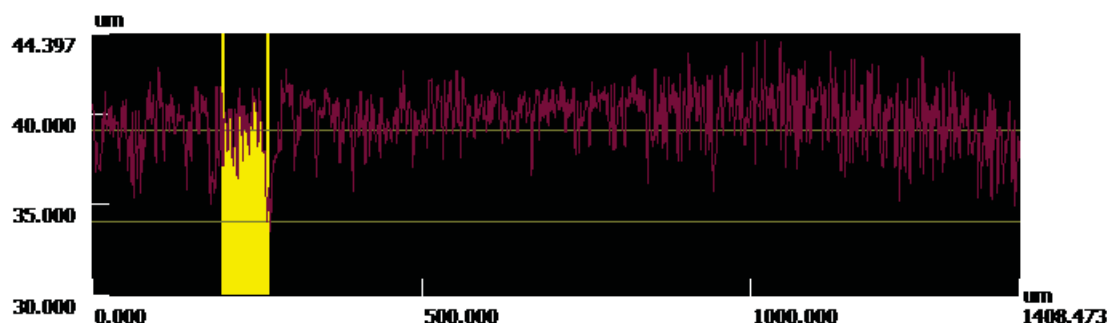
Figure 4-13. Laser-height scan for 304L stainless steel after electrochemical testing in 70 wt% glycolic acid at 35 °C (for micrograph in Figure 4-12 (B))

4.1.5 REDC Decontamination Solution – 12.5 wt% Nitric Acid

In the REDC, equipment is decontaminated using a 12.5 wt% nitric acid solution. As equipment is cleaned the soak solution is expected to build up in glycolic acid at some unknown rate from residual glycolate on equipment. For testing purposes, that concentration was taken at slightly greater than the initial estimated maximum concentration that would be carried over in the off gas components of the CPC (10 g/L). Alloy 20 is the principal MoC since it is the material for the soak tank. The test solution was boiled since future requirements may include a hot solution, which would be accomplished by using a steam lance. Electrochemical tests both with and without added sodium glycolate to the boiling 12.5 wt% nitric acid solution showed passive behavior with no pitting observed on the sample after testing. General corrosion rates were also similar with average rates of 3.1 mpy and 3.3 mpy for the solutions with and without added sodium glycolate, respectively. Figure 4-14 shows the CPP curves for both sets of samples and a micrograph of a sample surface tested in the glycolate-bearing nitric acid solution, demonstrating the absence of localized corrosion. If additional contaminants and aggressive species (chloride and sulfate) are expected to increase with continual re-use of solutions, additional testing should be considered.
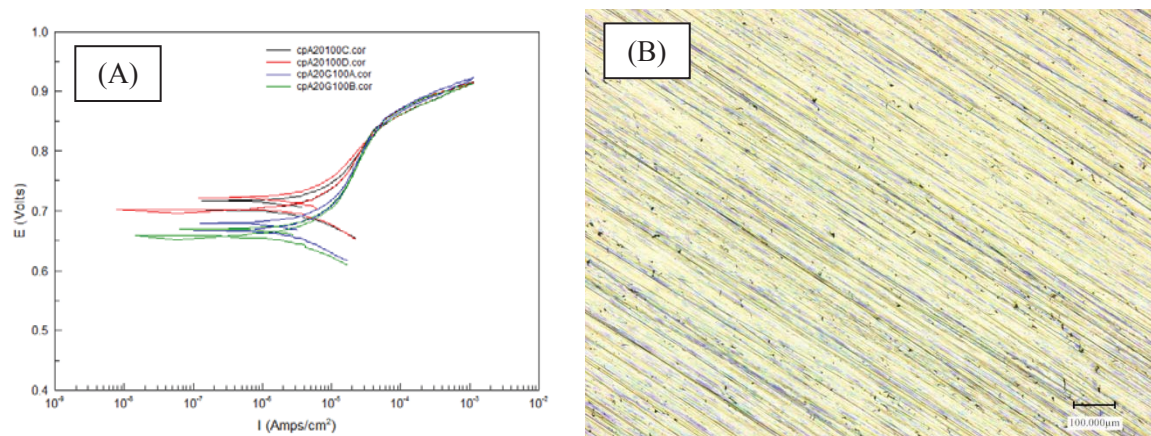
Figure 4-14. Alloy 20 in a boiling 12.5 wt% nitric acid solution: (A) CPP scan for solutions with and without the glycolate anion and (B) micrograph of sample surface tested in solution containing the glycolate anion

4.2 Hot-Wall Test Results

The hot-wall test is used to evaluate corrosion under heat transfer conditions that would be experienced during a heating cycle. For both the first phase and follow-up testing, C276 (SRAT and SME heating coils) and Ultimet (SME heating coils clam shells adjacent to support guards) were found to have degraded from pitting and crevice corrosion within a period of 22 to 34 days. The location, type and depth of corrosion are summarized in Table 3-5 for both sets of tests.

Table 4-5. Depth Measurements of Pit-Like Features from Hot-Wall Tests for DWPF Solutions

Testing	Material	Solution	Duration (days)	Type	Location	Depth* (µm)
First Phase	C276	Glycolic-based SRAT/SME Supernate	22	Pitting	Center	7
				Crevice	Gasket	8
	Ultimet	Glycolic-based SRAT/SME Supernate	34	Pitting	Center	20
				Crevice	Gasket	42
Follow-up	C276	Glycolic-based SRAT/SME Supernate	28	Crevice	Deposits	3-5
	C276	Formic-based SRAT/SME Supernate	29	Pitting/ Crevice	Deposits	19

* Deepest measured pit

These first phase test results showed that pitting and crevice corrosion occurred in the presence of glycolic acid under heat transfer conditions. Several aspects of the testing, however, made application of the test results to the current facilities difficult. The solution volume was maintained low to minimize the generation of hazardous waste, but this small volume lead to significant changes in the solution structure with deposits forming both in the solution and on the test sample and probable changes in solution chemistry. For the testing in the SRAT/SME supernate, the chloride and sulfate concentrations ((~5700 ppm (0.16M) and ~5600 ppm (0.058 M), respectively) were near the WAC limit [14], which is well above the measured concentrations in sludge batches for DWPF (see Table 4-2). Additionally, comparative tests in glycolic-free solutions or formic-based solutions were not performed.

In this follow-up testing, the hot-wall tests included only C276 in glycolate- and formate-containing solutions with sulfate and chloride concentrations (5571 and 100 ppm, respectively) that are considered maximums and nominal concentrations, respectively, in expected sludge compositions.

The C276 sample in the glycolic-based solution during the follow-up testing had similar results to the first data set, where small pits were observed. No significant deposits formed on the surface; deposits were generally limited to the gasket perimeter as seen in the post-test photographs in Figure 4-15 for the samples from both tests. Measured pit depths of the few located on the sample were slightly smaller than those measured for the first phase data set (3-5 µm versus 7-8 µm) but were of the same order of magnitude.
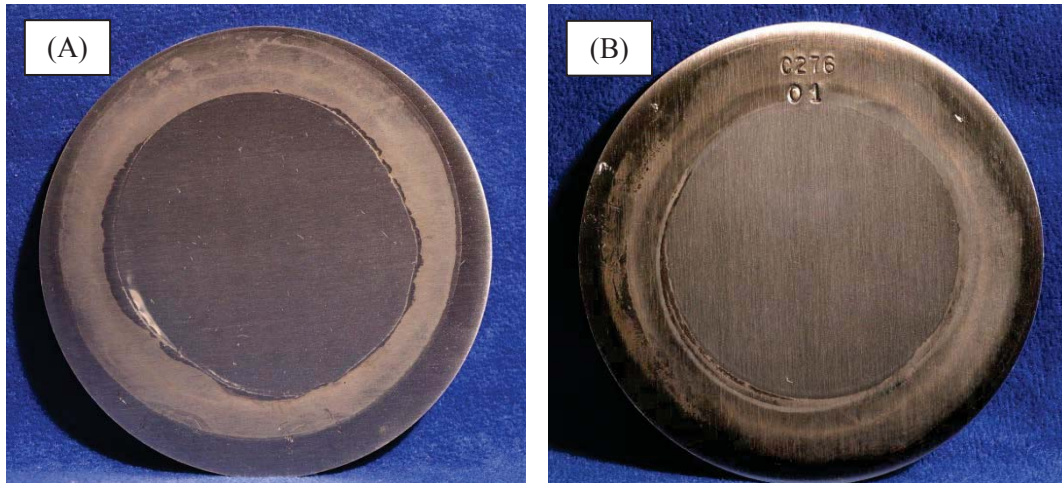
Figure 4-15. Post-test photographs of C276 hot-wall test samples after month exposure at boiling conditions in glycolate-based solutions: (A) follow-up test sample; and (B) first phase test sample

An untested C276 sample was also evaluated using the LCM to assess if any pit-like features were present in the as-received surface which had a final surface grinding with 600-grit silicon carbide paper. Figure 4-16 shows an as-received surface which had grooves up to 8 µm. Some pit-like features were located but appeared associated with the grinding process such as pushed up metal or irregular grinding. These features are identified by arrows in Figure 4-16A. The pits identified in the glycolic-based solutions from both phases of testing may have been original to the surface.
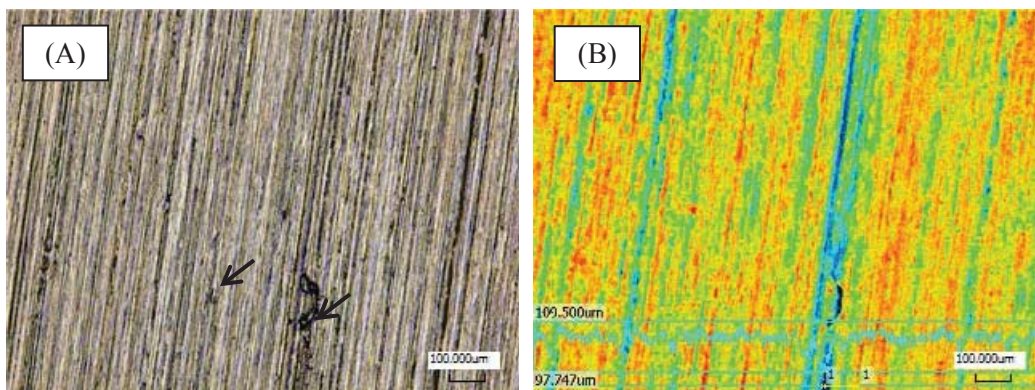
Figure 4-16. Photographs of as-received C276 hot-wall test sample (arrows identify pit-like features): (A) laser-optical image; and (B) height scan where red is highest point and dark blue is lowest

The C276 sample in the formic-based solution had a thick adherent coating that formed during the 29 days at boiling. The measured coating thickness ranged from 135 to 300 µm. A coating also formed

during electrochemical testing in the CPC simulant containing formate. This coating was much thinner (1.5-3 μm) and found to be manganese rich. The hot-wall coating could not be removed through chemical cleaning which included the use of both nitric acid and alkaline cleaning solutions. Mechanical cleaning measures were not used initially since the localized corrosion may have been removed. To obtain some indication of the presence of localized corrosion, the sample was sectioned with an electric discharge machine into a number of slices as shown in Figure 4-17.

After the pit depth analysis was completed, which is discussed below, the coating was evaluated using both x-ray fluorescence analysis and x-ray diffraction. Both techniques were performed with the coating on the test sample and x-ray fluoresce was also performed on coating ground off the test sample. The diffraction results showed the presence of some crystal structures, but the pattern could not be matched to any know compounds. For the x-ray fluorescence, slight differences were seen between the two scan. From both scans, identified elements were Mn, Ni, Fe, Hg, Zr, Al and Ca, which are all nitrate cations from the solution. Ni, Fe, and Mn are also present in the material, but the absence of chromium, a major constituent for C276 (Table 3-6), from the ground coating indicates that the solution is the more likely source. Cl, Si, and S peaks were also identified for the coating on the test sample. These elements could be from contamination or variation of the coating constituents.

Cross section of Slice #1 shown in Figure 4-18 (B)

Cross section of Slice #2 shown in Figure 4-18 (A)
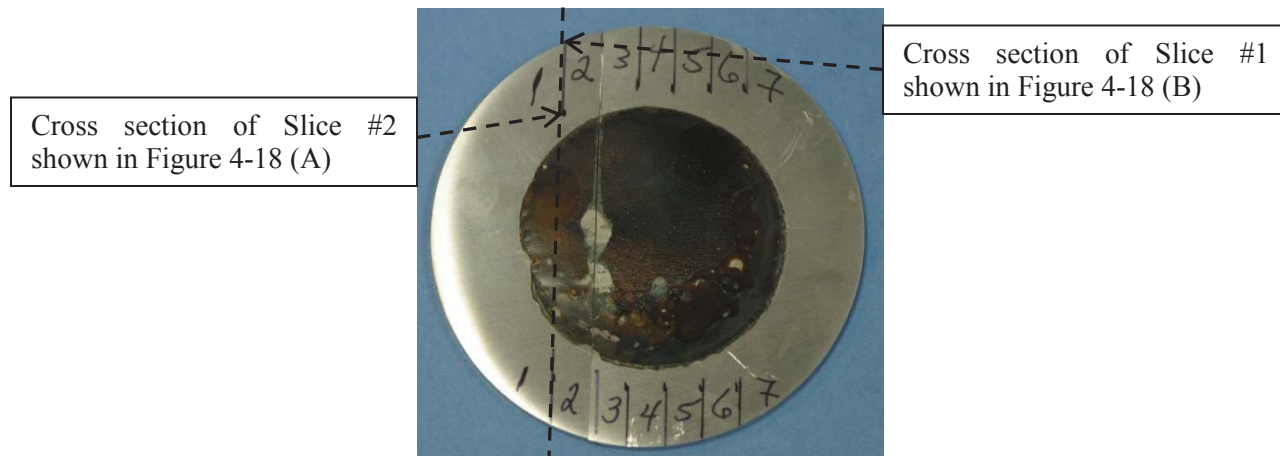
Figure 4-17. C276 hot-wall test sample after exposure to a formic-based solution showing sectioning prior to examination for localized corrosion (only one cut shown)

The cut edges of each slice were then examined in cross-section along the coating/metal interface for the presence of any pitting or crevice corrosion. In the initial analysis of these slices, the sample was thought not to have pitted. This result seemed inconsistent with electrochemical results discussed previously and the coupon immersion results discussed in Section 4.3. After a review of the analysis method for the LCM data and changes in the processing of the laser data from the LCM, pitting was identified on the slices. Two examples are shown in Figure 4-18 from Slices #1 and #2 (identified in Figure 4-17). In Figure 4-18 (A) a subsurface pit was identified (indicated by the arrow) on Slice #2, while in Figure 4-18 (B) a surface pit was identified on Slice #1.

In Figure 4-18 (A), the material above this pit is assumed to be some of the coating that has broken off. The line profile through the pit, shown in Figure 4-19 (A), shows a dip below the baseline indicating the pit. The rise above the profile baseline indicates the remnant piece of coating. The size of the pit in this plane is approximately 19 μm. In Figure 4-18 (B), the pit on the surface can be seen with the line profile through the pit shown in Figure 4-19 (B). The drop below the baseline for this pit is more difficult to decipher since the coating had separated from the sample, i. e. possible crevice. The pit depth was measured at approximately 11 μm.
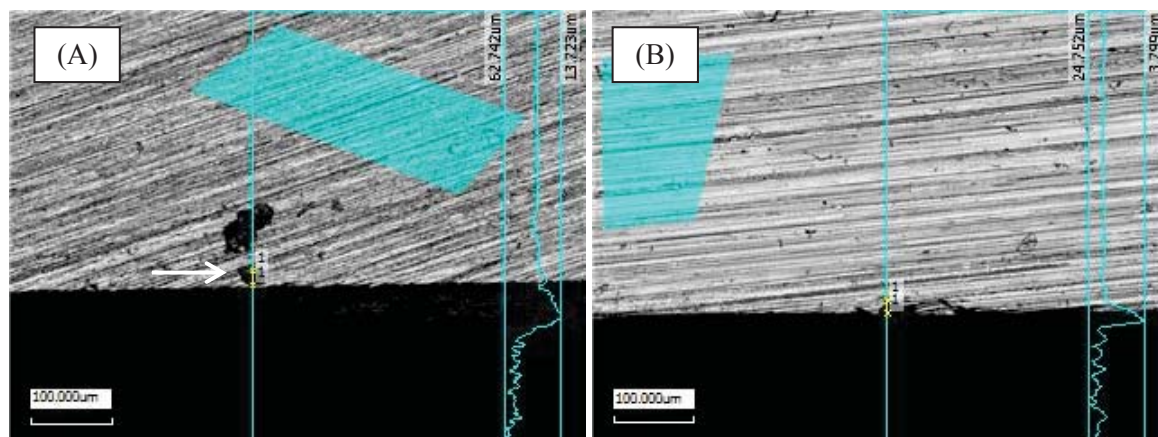
Figure 4-18. C276 hot-wall sample after testing in the formic-based SRAT/SME supernate: (A) cross-sectional view (400x) of Slice #2 showing sub-surface pit; (B) cross-sectional view (400x) from Slice #1 showing surface pit
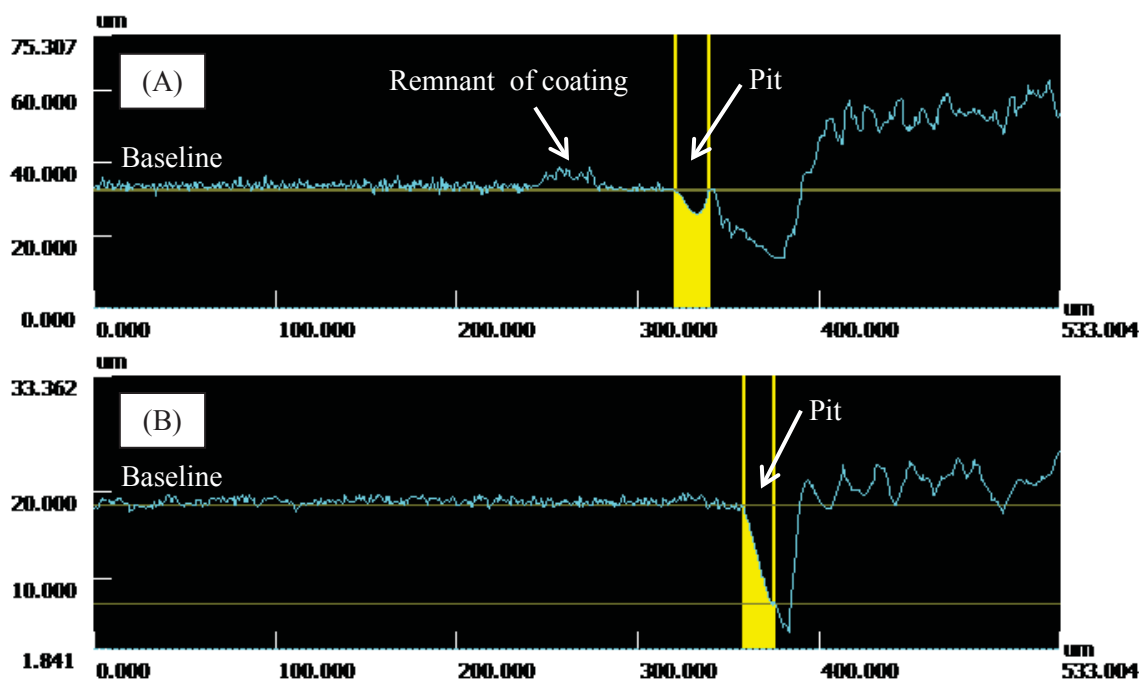
Figure 4-19. C276 hot-wall sample after testing in the formic-based CPC solution: (A) profile line shown in Figure 4-17(A) through sub-surface pits; and (B) profile line shown in Figure 4-17 (B) through surface pit

4.3 Coupon Immersion Test Results

The six-month coupon immersion test evaluated three chemistries of SRAT/SME supernates containing the glycolate anion and one with a formate-based supernate chemistry. All coupons were suspended vertically in the solutions. At the half way point in the testing, mercury was added to the three solutions, which were previously mercury free, to make the solutions more aggressive since significant pitting was not observed (significant pitting was taken as pit depths greater than 1 mil and pit density greater than 10). Only one solution with the highest sulfate and nitrate concentrations had mercury from the start of the test. Additionally, a set of coupons was placed in each of the respective solutions after the first set of coupons

was removed after one month. The solution compositions and coupon exposure and mercury addition times are summarized in Table 4-6. Over the course of the six-month test, solutions were changed five times.

Table 4-6. Coupon Exposure and Mercury Addition Times during Coupon Immersion Test*

Solution		Coupon Exposure Period (Month)				
Number	Chemistry	One	Three	Four	Five	Six
1	High sulfate and nitrate 100 ppm chloride	Hg - start C - start	Hg - start C - start	Hg - start C – 1 mo	No coupons	Hg - start C - start
2	Moderate sulfate High nitrate 100 ppm chloride	No Hg C - start	No Hg C - start	Hg – 3 mos C – 1 mo	No coupons	Hg – 3 mos C – start
3	Nominal sulfate and nitrate 50 ppm chloride	No Hg C - start	No Hg C - start	Hg – 3 mos C – 1 mo	Hg – 3 mos C – 1 mo	Hg – 3 mos C – start
4	Nominal sulfate and nitrate 50 ppm chloride	No Hg C - start	No Hg C - start	Hg – 3 mos C – 1 mo	Hg – 3 mos C – 1 mo	Hg – 3 mos C – start

* C indicates when coupons were placed into the test, either at the start of test or at 1 month (mo); Hg indicates when mercury additions were made to a solution, either from the start or beginning at 3 months (mos)

With increasing time in the test, coupons had an increasing buildup of deposits or a surface layer. Since both glycolate- and formate-based solutions had precipitates, the buildup could be deposits from solution. The formate-based solutions had so many precipitates that the coupons could not be seen during testing. The layers appeared similar for the glycolic-based solutions and differed from those formed in the formic-based solution. The coupons in the formic-based solution appeared to have the thickest layer, which was also the most difficult to remove during cleaning after the test. Layers formed in glycolic-based solutions were somewhat brittle and easily removed. These layers on the coupons were not analyzed. These features are shown in Figure 4-20 to Figure 4-22 for coupons prior to cleaning.

Figure 4-20 shows the buildup on C276 in Solution #1 over the six-month exposure, the other MoCs had similar increases in coverage. The layer was on both horizontal and vertical surfaces. Figure 4-21 shows welded C276 coupons from each solution (#1 through #4) at the end of the six-month exposure. The scratch on the welded C276 coupon exposed to Solution #1 was from tweezers and is an indication of the ease of removal of the layers. All six-month coupons from Solution #3, which was a glycolic-based solution, actually produced a darker coating not previously observed on coupons removed from Solution #3. The reason for the change is not known, but could be attributed to the mercury addition at the half way point in the test. The layer on the coupons exposed to Solution #3 was easily removed and came off during handling.

Visual examination (with the unaided eye) did not reveal any obvious evidence of corrosion on any of the coupons after they were initially removed from the immersion test. After the debris or layer was removed, grinding marks were still clear and there was minimal surface roughening. If the removed layers were a scale due to reaction of the material surface, they formed with minimal reactivity as based on the ease of removing the layers. Figure 4-23 shows the photographs of the cleaned coupons of those shown in Figure 4-21. The cleaned coupons clearly show the excellent condition of these coupons after six months. The location of weld can be seen in these post-test photographs. For comparison, an as-received C276 coupon is shown in Figure 4-24.

The corrosion rates measured from the weight changes during the test reflect a lack of significant general corrosion, similar to the visual observations. Table 4-7 shows the corrosion rates for the MoCs in these glycolic- and formic-based solutions during the six-month coupon immersion test. The complete listing of all the coupon weights and the calculated corrosion rates are given in Appendix D for all the different

time intervals that coupons were exposed. As shown in Table 4-7, the C276 corrosion rates for these longest exposure periods are all well below the estimates of the upper bound corrosion rates for the SRAT and SME tanks, i.e. 1 mpy [15]. These measured corrosion rates did not correlate to expected corrosivity of the glycolic-based solutions; i.e. decreasing rates progressing from Solution #1 to Solution #3.
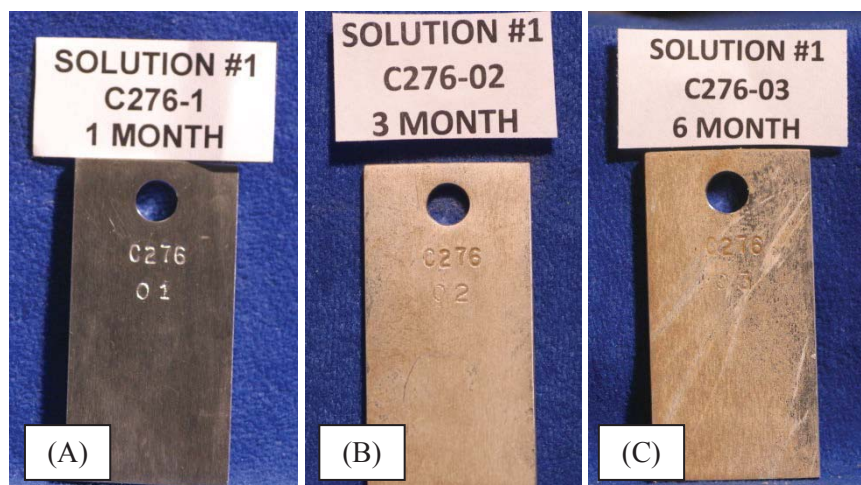
Figure 4-20. Photographs of uncleaned C276 coupons from the coupon immersion test after (A) 1 month, (B) 3 months, and (C) 6 months exposure in Solution #1
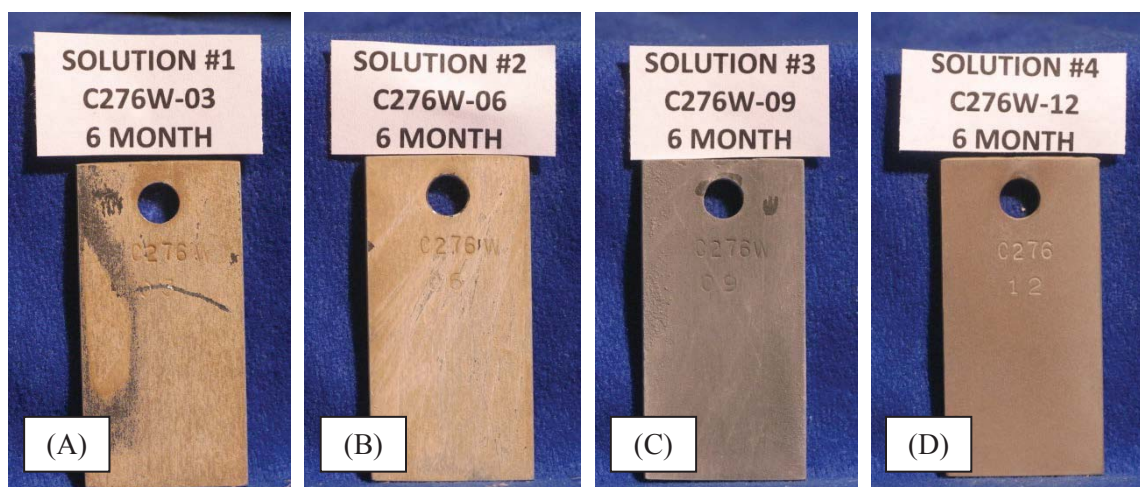
Figure 4-21. Photographs of uncleaned welded C276 coupons from the coupon immersion test after six-month exposure in (A) Solution #1, (B) Solution #2, (C) Solution #3, and (D) Solution #4
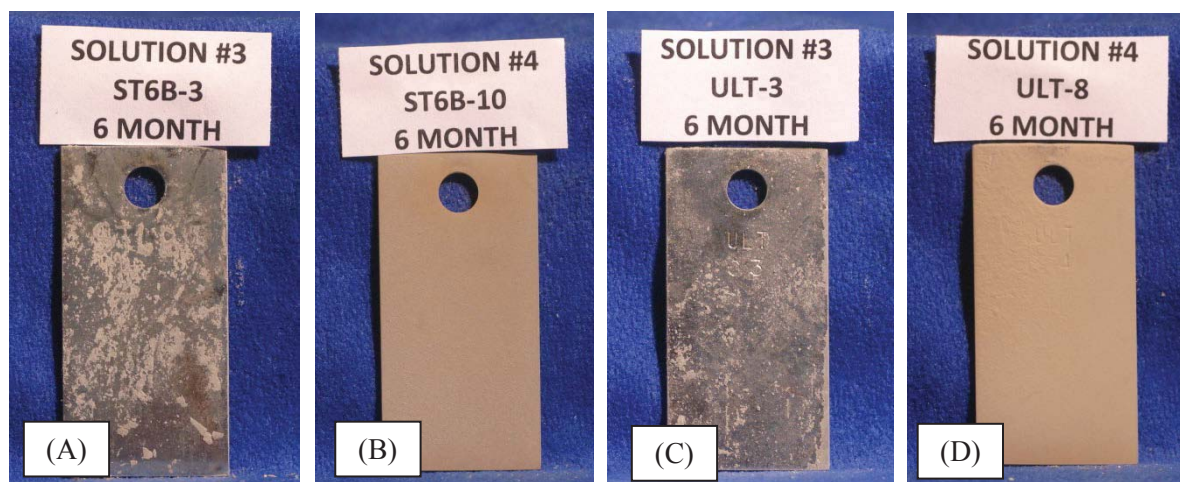
Figure 4-22. Photographs of uncleaned five-month exposure coupons: (A) Stellite 6B in Solution #3; (B) Stellite 6B in Solution #4; (C) Ultimet in Solution #3; and (D) Ultimet in Solution #4

Figure 4-23. Photographs of cleaned welded C276 coupons from the coupon immersion test after six-month exposure in (A) Solution #1, (B) Solution #2, (C) Solution #3, and (D) Solution #4

Figure 4-24. Photograph of as-received C276 coupon prior to testing

Table 4-7. Corrosion Rates for MoCs in Glycolic- and Formic-based CPC Solutions from the Six-month Coupon Immersion Test

Solution #	Solution Chemistry	Alloy	Duration (mos)	Corrosion Rate (mpy)
1	Glycolic-based, high sulfate and nitrate, 100 ppm chloride	C276	6	0.020
		C276W	6	0.027
		St6B	6	-0.008
		Ult	6	0.001
2	Glycolic-based, moderate sulfate, high nitrate ,100 ppm chloride	C276	6	0.011
		C276W	6	0.011
		St6B	6	-0.005
		Ult	6	-0.016
3	Glycolic-based, nominal sulfate and nitrate, 50 ppm chloride	C276	6	0.015
		C276W	6	0.018
		St6B	5	-0.005
		Ult	5	-0.004
4	Formic-based, nominal sulfate and nitrate, 50 ppm chloride	C276	6	-0.017
		C276W	6	-0.027
		St6B	5	-0.005
		Ult	5	-0.004

Negative corrosion rates were calculated generally for Stellite and Ultimet coupons in all test solutions and for all MoCs in the formic-based solution, which results from a greater weight after testing than before. This weight increase is attributed to an incomplete removal of the deposits or coatings that formed during the test. As previously stated above, the coatings that developed from the formic-based solutions were difficult to remove. A much smaller amount of residual deposits and coatings, if any, were found after cleaning coupons that were exposed to glycolic-based solutions. After most of the deposits or coatings were removed, more extensive cleaning for complete removal was not performed so as not to alter the surface morphology results from test solution exposure. Another contributing cause may have been surface oxidation although the coupon surfaces especially after glycolic-based solution exposure were fairly shiny (see Figure 4-23), which would not be expected for an oxidized surface.

These data clearly demonstrate that the general corrosion rates for the different MoCs during extended exposures to glycolic-based or formic-based DWPF simulants are acceptable, i.e. < 1mpy. The other aspect of this testing was to evaluate the occurrence of localized corrosion, especially pitting corrosion. Crevice or underdeposit corrosion was also evaluated due to the formation of deposits or coatings on the surface during the test. Table 4-8 summarizes the measured pit/crevice data showing pits depths for each MoC in each solution after one-, three-, and six-month exposures. Mercury was added to Solutions #2 - #4 after three months, whereas Solution #1 had mercury from the start.[11]

The measured pit counts and depths demonstrate that pitting and crevice corrosion is not a significant issue in these DWPF SRAT/SME supernate simulants. A progressive increase in pit count and depth from the one-month to the six-month coupon exposures was not observed. Three pits were measured at

---

[11] Similar to the electrochemical testing, the source of mercury used for Solution #1 during the first three months had absorbed moisture so that actual mercury concentrations were lower than planned.

greater than 1 mil (25.4 µm). Many small pits (< 10 µm) were observed, more similar to metastable pits that passivate and stop progressing [16]. Stellite and Ultimet may be showing a slightly greater tendency for localized corrosion in mercury bearing solutions. A comparison of the three- and six-month exposure results shows progressively more pitting with time (greater count or depth). Although some minimal non-progressing pitting was observed in this test, the MoCs did not show a greater susceptibility to localized corrosion in glycolic-based solutions than in formic-based solutions.

Table 4-8. Pit Count and Depth for DWPF MoC Samples from the Six-month Coupon Immersion Test

Solution #	Solution Chemistry	Alloy	Pit Count/Depths (#/µm)		
			One-Month	Three-Month	Six-Month*
1	Glycolic-based, high sulfate and nitrate, 100 ppm chloride	C276	3/4-21	4/5-16	1/9
		C276W	2/5-7	2/6-7	None
		Stellite	1/27	None	None
		Ultimet	4/2-4	None	12/7-43
2	Glycolic-based, moderate sulfate, high nitrate ,100 ppm chloride	C276	None	None	4/5-13
		C276W	None	3/7-10	None**
		Stellite	None	None	3/13-17
		Ultimet	1/6	1/6	5/7-12
3	Glycolic-based, nominal sulfate and nitrate, 50 ppm chloride	C276	None	None	9/13-17
		C276W	None	1/14	1/16
		Stellite	2/14-28	None	3/10-16
		Ultimet	No coupon	5/5-17	1/14
4	Formic-based, nominal sulfate and nitrate, 50 ppm chloride	C276	8/4-10	3/3-9	None**
		C276W	None	1/9	None**
		Stellite	None	None	5/5-11
		Ultimet	No coupon	3/3-9	9/6-34

* For Solutions #3 and #4, the Stellite and Ultimet samples were exposed for five months
** These coupons were re-evaluated to measure all marks on the surface using the LCM. A population (10-15) of marks measuring less than 5 um was identified and found to be as deep as the corrosion along grinding marks.

4.4 NDE – Large Scale Testing

When the large-scale 1/200th test was performed to assess scaling issues in the 1/200th test vessel and the heating coils were used as large-scale coupons to obtain a relative assessment of the process solution aggressiveness, i.e. corrosion and erosion, to the MoCs, which were 304L. UT wall measurements were made before and after the two-week test at key areas where erosion/corrosion might be an issue as based on past failures of actual DWPF SME coil assemblies. These locations included down the vessel wall at four orthogonal locations and along several ring lengths of the inner, outer and middle coils at four orthogonal locations [17-20]. In Figure 4-25 (A), the locations along the coils are shown by the green arrows, which also show the measurement locations relative to the agitator blades positions. Measurement accuracy at these thicknesses (~0.03-0.07 in) was +/- 0.001 inch. Measurements within this variability range were considered unchanged.

The largest wall loss was found on the inner and bottom surfaces of lowest ring of the heating coils and just below the bottom head to shell weld of the vessel. Figure 4-25 (B) shows the UT measurements

along the bottom surface of the lowest ring before (baseline) and after (final) the test. The ring wall losses were approximately 2-3 mils. No wall loss was measured for the coil lengths that were located between the agitator blades. The location of these losses was similar to those observed on the DWPF SME coil assemblies and where erosion is the primary degradation mode. Several circumferential welds for the coils also showed no wall loss. The loss of the vessel wall thickness below the weld was 2 mils. All the UT reports are in Appendix E.
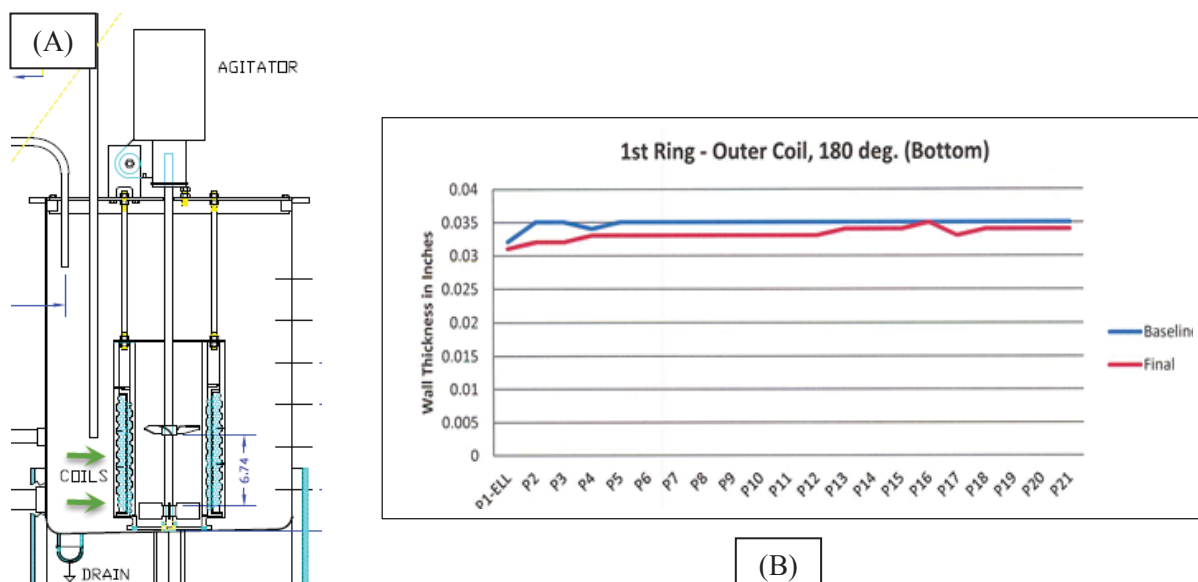
Figure 4-25. UT measurements of the 1/200th scale test vessel and coils: (A) vessel diagram with arrows showing coil measurement location; and (B) UT measurements for lowest (1st) ring of the outer coil welds along the bottom surface (180° position)

4.5 Discussion

This follow-up testing was conducted to address areas of concern that were identified from the first phase of testing. During the first phase of testing, the glycolate anion was found not to impact the corrosion of MoCs for most vessels and components within the DWPF and downstream facilities nor expected to impact service life. The vessels and components of concern at the end of the first phase of testing were those associated with the DWPF CPC and the heating components for the HLW Evaporators. Testing was also performed for the REDC which was not evaluated during the first phase testing.

The primary focus for this follow-up testing was on the DWPF CPC and understanding the different impacts on the MoCs of both formic and glycolic acids, the current and alternate DWPF reductants. The testing was not targeted at the rapidly changing conditions when the acidic reductant is added to the caustic sludge or the impact of erosion; so while DWPF processes are dynamic, laboratory tests simulated static operating conditions. The test solutions were based on chemistries from SME simulants determined during flowsheet development. The primary MoC is C276, which is the containment barrier for CPC vessels and components. Testing with Ultimet and Stellite, alloys used for erosion protection in the SRAT and SME, was limited to the coupon immersion test with only corrosion being evaluated.

The results in the formic-based solutions form a point of comparison between actual service history of the CPC vessels and components and the laboratory data for the glycolic-based solutions. The effect of formic acid on the MoCs using the current test scheme of electrochemical, hot-wall and coupon immersion had not previously been determined. The correspondence of these laboratory data to actual

service performance in the DWPF CPC is limited since regular or periodic inspection of the vessels and components in the CPC has not been performed.

For the formic-based solutions in both the hot-wall and coupon immersion tests, samples were covered with a tenacious layer. The measured pits found beneath these layers ranged between 10 and 20 μm for the hot-wall tests and < 20 μm for the coupon immersion test.[12] The smaller pits (< 5 μm) were of depths that were similar to corrosion along grinding marks so these pits may have also started from small surface imperfections and did not appear to be propagating. The larger pits (> 10 μm) may be indicative of some localized growth of a pit, although the progression of pit depth with time in the coupon immersion was not observed. Based on the coupon immersion test, pitting is not expected to grow under CPC conditions of boiling formic-based solutions although pits may initiate. Since heating coils have been removed from service in the SRAT, these coils provide an opportunity to validate the surface condition resulting from processing with formic acid as a reductant. A close visual inspection (adequate lighting, appropriate magnification, etc.) of the coil surface is recommended to determine actual material performance.

In the limited number of electrochemical test for the formic-based solutions, localized corrosion, i.e. pitting and possibly crevice corrosion, occurred with deposits. The deposits corresponded with bulk solution chemistries at either high chloride (247 ppm) or high sulfate (5571 ppm) conditions. The aggressive species concentrations below the deposits, however, may be considerably different than the bulk. If the sample did not pit in the high sulfate condition, the surface reacted with the solution since the sample had a bronze appearance. For the formic-based solutions, sufficient tests were not conducted to establish a cause and effect with either the deposits on or bronzing of the sample. Both solution chemistries where deposits and pitting were observed have not occurred in the DWPF as based on the sludge feed chemistries shown in Table 4-2. The electrochemical results for the solution chemistry used in the coupon immersion tests indicated no pitting.

In the glycolic-based solutions, the follow-up electrochemical testing for C276 showed that at a chloride concentration less than 100 ppm localized corrosion was not an issue unless the nitrate/glycolate concentration was low (~35,000/25,000 ppm), which resulted in deposits forming on the sample. For the Sludge Batch #8, nitrate concentrations with the current nitric-formic acid flowsheet are ~30,000 ppm which for a nitric-glycolic acid flowsheet would have an expected nitrate concentration of ~50,000 ppm [21]. Deposits would not be expected to form, but for future flowsheets the nitrate concentration will depend in part on the noble metal concentration since these metals catalyze the destruction of nitrate.

In the hot-wall tests in support of the nitric-glycolic flowsheet, pits associated with deposits were found on the C276 sample after one month at boiling conditions. The pit depths for the follow-up and first phase testing were less than 5 μm and 10 μm, respectively, after one-month of boiling. The chloride concentrations of these two tests also differed with 100 ppm for the follow-up testing and near the WAC limit (> 5000 ppm) for the first phase testing. The concentration of chlorides that remain soluble in both these tests is not known since deposits formed during both tests. These tests may indicate that the observed pitting is driven more by factors (surface imperfections, different heats of material, etc.) other than the chloride concentration.

The coupon immersion tests evaluated the corrosion over an extended time unlike the other two tests. Pitting was identified during this test in the glycolic-based solutions, although as shown by the data in Table 4-8, pit depths for C276 did not show a consistent trend of increasing depth with exposure time in any of the glycolic-based solutions. The largest measured pit depth was 17 μm, which was measured in the least corrosive solution (i.e., lowest sulfate and chloride concentrations). In the coupon immersion test, a debris or layer formed, which increased in coverage, on the test samples during the test as shown in

---

[12] Note that 25.4 μm is equivalent to 1 mil or 0.001 inch so a 5 μm pit is equivalent to 0.2 mil or 0.0002 inch.

Figure 4-20. Deposits, which may have contributed to pit formation, were observed also in both the electrochemical and hot-wall tests. The formation of these pits may be associated with surface imperfections and deposits.

In all the C276 tests with the glycolic-based solutions, pitting was observed. These data collectively show that localized corrosion can occur in glycolic-based solutions but may be independent of chloride concentrations. Both the hot-wall test results showing similar pit depths at different chloride concentrations and the coupon immersion test results where higher depths were found at the lowest chloride concentration support this statement and indicate other variables may be more important such as deposit formation, which was noted in all tests, or surface imperfections and inclusions. Although these pits form, the six-month coupon immersion test results indicate that pit growth would not be expected under similar conditions.

Since the tanks and components of the DWPF CPC cannot be inspected, analyses of components or tanks removed from the canyon are recommended to determine if localized corrosion is occurring with a nitric-glycolic flowsheet. This removal would most likely occur after a failure and a subsequent failure analysis would provide valuable data on the condition of these tanks or components, realizing that they also were exposed to the nitric-formic flowsheet. Without the data from periodic inspections within the CPC, a failure after the switch to the nitric-glycolic flowsheet will make a failure assessment difficult because of the uncharacterized degradation caused during the nitric-formic flowsheet.

The results for general corrosion for both the glycolic- and formic-based solutions show low corrosion rates. The coupon immersion test results after six months had rates << 1 mpy, while the electrochemical-measured corrosion rates were around 1 mpy for glycolic-based solutions and < 0.5 mpy for formic-based solutions. These measured rates are within the rates set forth in the DWPF Structural Integrity Progam [15].

Ultimet and Stellite are used in the SRAT and SME to provide wear resistance to agitator blades and the coil supports. The results from the coupon immersion test for these MoCs showed negligible general corrosion loss but a slight increase in localized corrosion susceptibility after six-month exposures versus the shorter times. Some depths are significant (1 mil) for Ultimet in both Solution #1 (glycolic-based, highest concentration of aggressive species) and #4 (formic-based). The coupon immersion test is a static test, whereas the Ultimet which is used for the SME agitator paddles and hydrofoil blades is in motion so should not readily form deposits. Deposits may be associated with the observed corrosion in the coupon immersion tests. Since the performance is similar between the formic- and glycolic-based solutions, these MoCs would be expected to perform as well with the nitric-glycolic acid flowsheet as they currently perform with the nitric-formic flowsheet in the DWPF.

Further investigation was also performed for 304L in 70 wt% glycolic acid at temperatures less than 50 °C. Both 316L and 304L are the MoCs for the formic acid feed tanks and components. In the first phase of testing, 316L performed well at 50 °C with no localized corrosion susceptibility, while 304L showed some tendency to pit. Testing at 35 °C and room temperature during the follow-up testing showed that 304L still showed some tendency for localized corrosion, especially in the presence of inclusions. No testing was performed to assess lower dilutions of glycolic acid. For the 304L components in the glycolic acid feed system, baseline and future inspections were recommended to determine if 304L is susceptible to pitting. DWPF identified a spool piece in the formic acid feed line which is accessible for inspections. A baseline inspection was performed showing pipe thickness within an acceptable range and no indication of localized corrosion [27]. After glycolic acid use is initiated, another inspection will be performed after six months of operation.

The testing in the decontamination solution (12.5 wt% nitric acid) for the REDC clearly showed that independent of the presence of the glycolate anion at a concentration of 10 g/L Alloy 20 showed passive corrosion behavior. The tests were performed at boiling since future plans include using a steam lance in the REDC soak tank if needed. Alloy 20 is expected to show no adverse effect from the presence of the glycolate anion even at high temperatures.

5.0 Results and Discussion – HLW Evaporators

Similar to the DWPF MoCs, the first phase results showed that pitting and crevice corrosion were the prevalent mechanisms in the presence of glycolic acid under heat transfer conditions for G30 and G-3. However, the test condition of low solution volume (~500 ml) lead to significant changes in the solution structure with deposits forming both in the solution and on the test sample and probable changes in the solution chemistry. Follow-up hot-wall tests were performed for the MoCs of the HLW evaporators. Similar results were obtained to the first phase testing in that G30 and G-3 degraded near the gasket and at deposits. The testing details and results are summarized in Table 5-1.

Table 5-1. Hot-Wall Test Results for the MoCs of the HLW Evaporators

Testing	Material	Solution	Duration (days)	Type	Location	Depth* (μm)
First Phase	G30	Basic Concentrated Recycle with Glycolate	22	Pitting	Deposits	18
	G-3	Dilute Waste with Glycolate	27	Crevice	Gasket	22
Follow-up	G30	Basic Concentrated Recycle with Glycolate	24	Crevice	Deposits	<13
		Basic Concentrated Recycle without Glycolate	29	Pitting/ Crevice	Deposits	3-24
	G-3	Dilute Waste with Glycolate	36	Pitting/ Crevice	Center/ Gasket	<10
		Dilute Waste without Glycolate	36	Crevice	Deposits	5-15

The G30 samples were tested in basic concentrated recycle solution to evaluate degradation for the 2H evaporator. In both follow-up tests (with and without the glycolate anion), a film formed on the sample. X-ray fluorescence results showed the film to be primarily composed of silicon. The silicon was likely from the glass test vessel, which was etched during the testing in these high pH solutions. Figure 5-1 shows the sample from the glycolate-containing solution before and after cleaning the sample.

As can be seen from the G30 data in Table 5-1, localized corrosion was associated with deposits on the surface in both the presence and absence of the glycolate anion. Measured pit depths were also similar between these two tests. The slight difference in depth may be associated with the difference in test duration. These results are similar to those from the first phase test data indicating the alloy is susceptible to underdeposit corrosion in these solutions.

The G-3 hot-wall samples tested in a dilute waste solution with and without the glycolate anion had a similar post-test appearance as well as pit characterization to the G30 hot-wall samples. Figure 5-2 shows the post-test photographs of the G-3 hot-wall samples. Their appearance was also similar to the G-3 sample tested in the first phase testing [2]. The spots in the center had pits in only some cases and only after exposure to the solution with the glycolate anion. Most of the pits were generally associated with deposits. The pit depths are shown in Table 5-1 for the first phase and follow-up tests with pit depths of the same order of magnitude and not considered different.
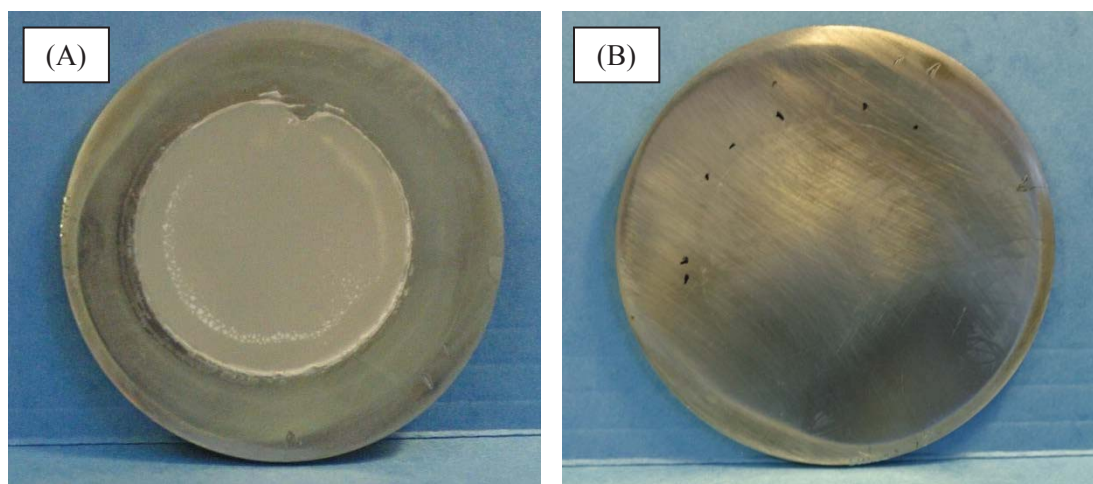
Figure 5-1. G30 hot-wall samples exposed to a boiling basic concentrated recycle solution: (A) post-test photograph showing silicon-rich film; and (B) post-cleaning photograph after removal of film (black spots showing locations of observed pitting
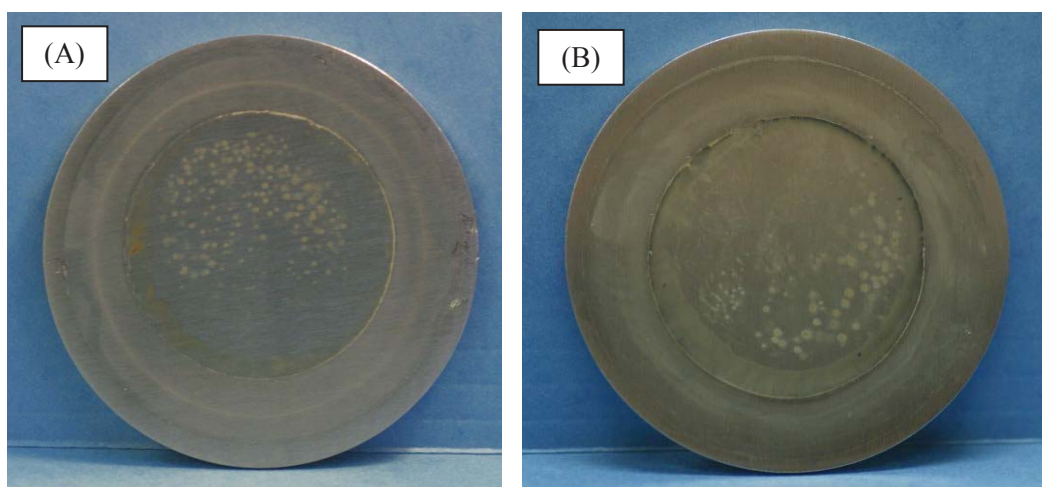
Figure 5-2. Post-test photographs of G-3 hot-wall sample exposed to a boiling dilute waste solution with (A) and without (B) the glycolate anion

For the G30 and G-3 samples, deposits on the samples appear to be a major contributor to the presence of localized corrosion but independent of the presence of the glycolate anion. The presence of the glycolate anion therefore is not expected to impact these MoCs in the HLW evaporators. The hot-wall tests do not replicate the facility conditions, that is, the operating conditions for the 2H Evaporator or the ETF heating coils. These tests were performed continuously without a cleaning step as is periodically performed in the evaporators which minimizes or eliminates the buildup of deposits on the heat-transfer surfaces.[13] These results indicate the importance of cleaning in maintaining these units in an operational condition which is necessary whether the glycolate anion is present or not.

---

[13] For the 2H Evaporator, the cleaning is performed based on an inspection evaluating deposit buildup. The DSA limits the buildup of deposits, specifically sodium aluminum silicate, to 200 gallons and the inspections provide an estimate of that quantity. Historically, a cleaning has been required every 3-5 years. The ETF does not clean but operates to minimize deposit formation including flushing and draining during extend outages.

Although 3H Evaporator conditions were not part of this testing, the current test results to evaluate the impact of glycolic acid along with the results of validation testing performed previously [5] for G-3 provide data that glycolate will not impact the corrosion resistance for the 3H Evaporator. The validation testing for G-3 was a series of hot-wall tests performed in high level waste simulants ranging between 3.8 and 45 wt% NaOH. The results showed that operating at up to 428 °F, G-3 showed either salt deposits with slight staining or no deposits (at 45 wt% NaOH only). Both G30 and G-3 in the current hot-wall testing also showed deposits both with and without glycolate present in the solution. For all the alloys tested in a range of waste compositions, the glycolate anion was not found to alter the corrosion behavior of the alloy. G-3 under high hydroxide concentrations in the presence of glycolate, therefore, is not expected to impact the corrosion resistance for the 3H Evaporator.

The recently operating evaporators, 2H, 3H, and ETF, have had extended service for 21, 16, and 28 years, respectively, which indicates that pits associated with deposits or crevices have not been an issue for G30 or G-3. The 2H Evaporator has been exposed to the formate anion (up to ~2000 ppm) in the waste over this period [25]. This lengthy performance is believed to be associated with the materials inherent corrosion resistance as well as the maintenance operations. Additionally, 2H and ETF Evaporators have cleaning/flushing procedures which minimize deposit buildup in the evaporators. The continued outstanding performance of the high level waste evaporators, therefore, is expected with a switch to glycolic acid as a reductant for the DWPF process.

6.0 Results and Discussion – Waste Tank Corrosion Control Program

Electrochemical tests were performed in eight simulated HLW chemistries over a range of temperatures (40-115 °C) to verify that the presence of glycolate or formate at a bounding concentration of 10,000 g/L did not impact the requirements of the CCP which are based on extensive testing dating back to the mid-1970s. The key parameters taken from the electrochemical data are the general corrosion rate, E_{corr}, i_{pass}, and the type of hysteresis. A negative hysteresis indicates a passive material not susceptible to localized corrosion. A positive hysteresis clearly indicates susceptibility to pitting, while a mixed or no hysteresis may indicate a borderline condition. A case of positive hysteresis did not occur during this testing. The other types were observed and are shown in Figure 6-1 to Figure 6-3.
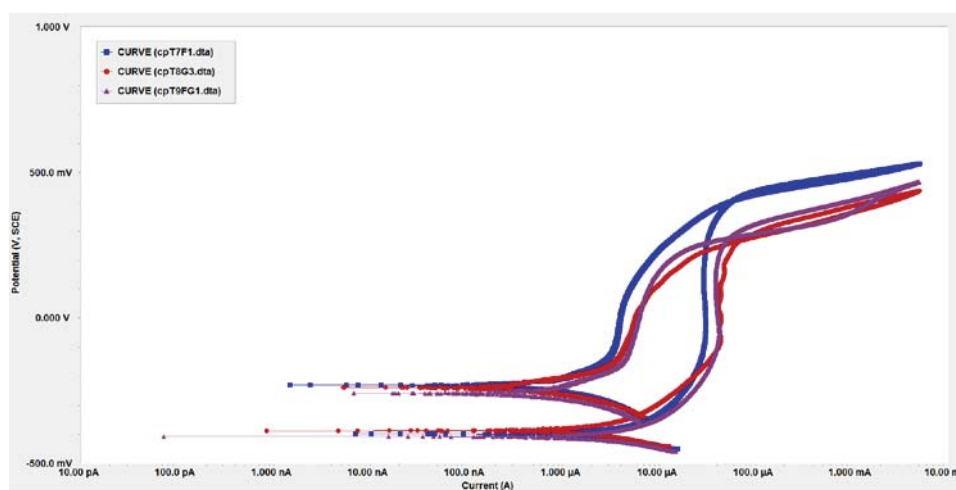
Figure 6-1. CPP scans for Tests #7-#9 showing negative hysteresis
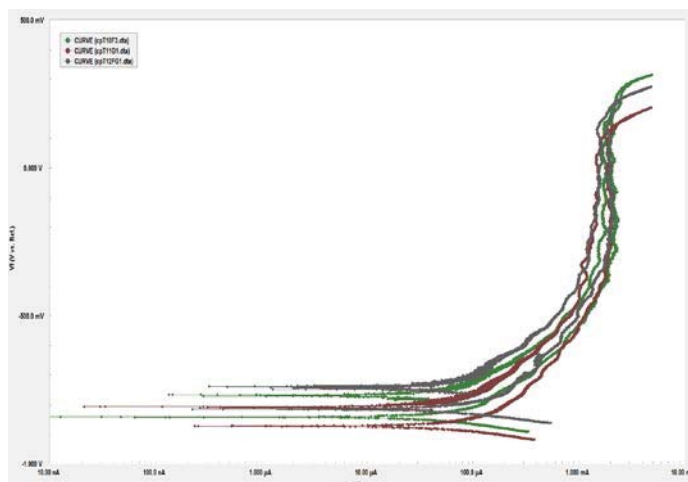
Figure 6-2. CPP scans for Tests #10-#12 showing no hysteresis
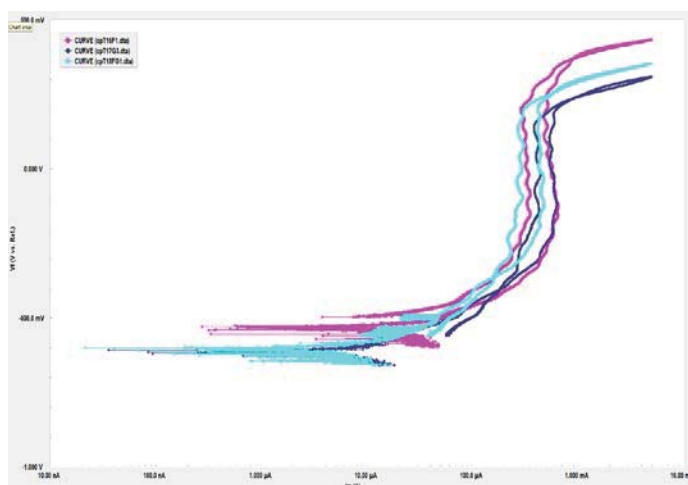
Figure 6-3. CPP scans for Tests #16-#18 showing mixed hysteresis

In Table 6-1 the average values for these parameters are shown for the eight simulated chemistries. The data in the table and figures demonstrate that the presence of either reductant produced similar electrochemical responses for carbon steel in the range of waste chemistries covered by the CCP. There was no consistent trend for any of the reductant conditions; i.e. the presence of formate did not always produce the lowest corrosion rate.

Two tests (Test #29 and #30) were performed in the concentrated chemistry without glycolate or formate in the solution. These had similar chemistries to Tests #4-#6 and Tests #19-#21, respectively. The results are shown in the table and in Figure 6-4 the data is plotted for Tests #4-#6 and Test #29. These data indicate a similar corrosion response for all test conditions. The concentrated chemistry of Tests #4-#6 (10M OH, 0.75M NO_3, and 1M NO_2) was chosen for assessing if the presence of the reductants changes carbon steel corrosion resistance from previous research without reductants used to establish the requirements of the CCP.

Table 6-1. Average Electrochemical Parameters for Waste Tank Chemistries in the Presence of Glycolate and Formate

Test	Solution/ Temp (°C)	Reductant	Corrosion Rate (mpy)	E_{corr} (V,SCE)	I_{pass} ($\mu A/cm^2$)	Hysteresis
1	OH≥8 T – 115 °C	Formate	51	-0.906	3950	Mixed
2		Glycolate	47	-0.905	4635	Mixed
3		Both	53	-0.904	4315	Mixed
4	NO_3<1 and OH>8 T – 75 °C	Formate	49	-0.903	2750	None
5		Glycolate	49	-0.901	2425	None
6		Both	52	-0.901	2635	None
29		None	47	-0.972	2391	Negative
7	5.5<NO_3≤8.5 T – 70 °C	Formate	0.5	-0.388	29	Negativex
8		Glycolate	0.4	-0.385	43	Negative
9		Both	0.6	-0.400	43	Negative
10	2.75<NO_3≤5.5 T – 112 °C	Formate	13	-0.842	2071	None
11		Glycolate	8	-0.868	1929	None
12		Both	9	-0.818	2000	None
13	2.75<NO_3≤5.5 T – 105 °C	Formate	0.2	-0.283	10	Negative
14		Glycolate	0.6	-0.348	37	Negative
15		Both	0.7	-0.366	37	Negative
16	1≤NO_3≤2.75 T – 105 °C	Formate	1.8	-0.559	506	None
17		Glycolate	0.9	-0.628	430	Mixed
18		Both	0.9	-0.624	479	Mixed
19	1≤NO_3≤2.75 T – 70 °C	Formate	0.6	-0.246	18	Negative
20		Glycolate	0.6	-0.310	36	Negative
21		Both	0.6	-0.355	40	Negative
30		None	0.5	-0.346	37	Negative
22	0.02<NO_3<1 and 1<OH≤8 T – 100 °C	Formate	3	-0.561	536	Negative
23		Glycolate	3	-0.535	628	Negative
24		Both	2	-0.543	708	Negative
25	NO_3≤0.02 and OH<1 T – 40 °C	Formate	0.3	-0.237	37	Negative
26		Glycolate	0.1	-0.257	14	Negative
27		Both	0.2	-0.289	19	Negative

Previously performed testing at high hydroxide (6-12M) chemistries determined inhibitor requirements with mid-range nitrate and low nitrite concentrations (1-3 M, 0.2-1 M, respectively) [24d]. This research supported the CCP requirements for hydroxide greater than >8M. The CPP scan from a 12 M OH, 3M NO_3 and 1M NO_2 solution is shown in Figure 6-5 [24]. The electrochemical response is typical for these high hydroxide solutions with a negative hysteresis and a stable i_{pass} indicating the presence of a stable oxide layer and no susceptibility to SCC. Similar results were obtained when formate and glycolate were present as shown in Figure 6-6
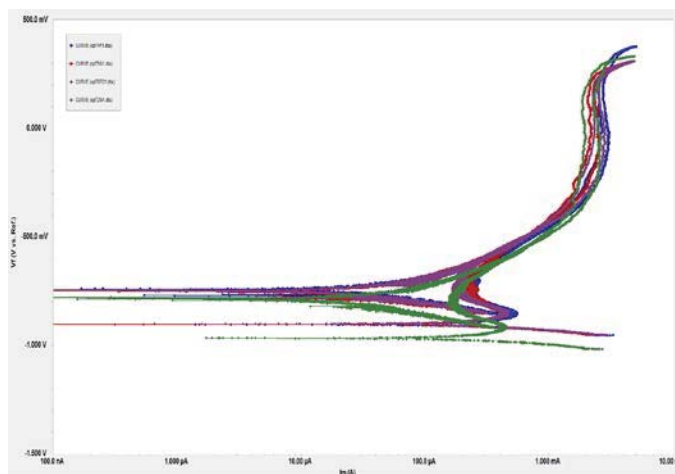
Figure 6-4. CPP Scans for Tests #4 - #6 which contain a reductant and Test #29 which has no reductant
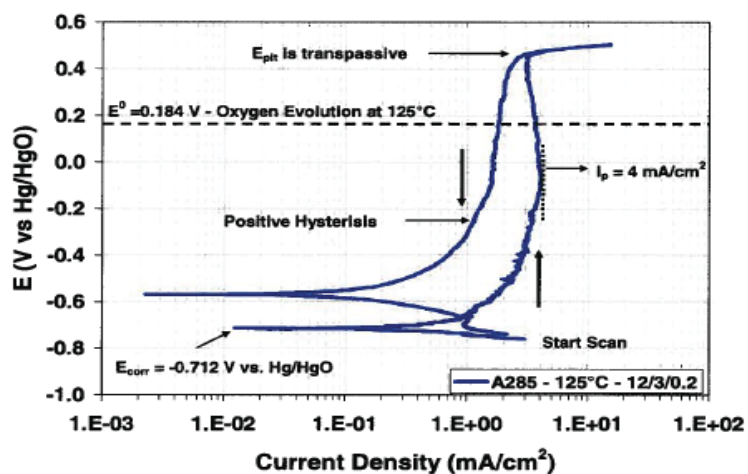
Figure 6-5. CPP scan for A285 carbon steel at 125 °C in a solution with 12M hydroxide, 3M nitrate, and 0.2M nitrite [24]
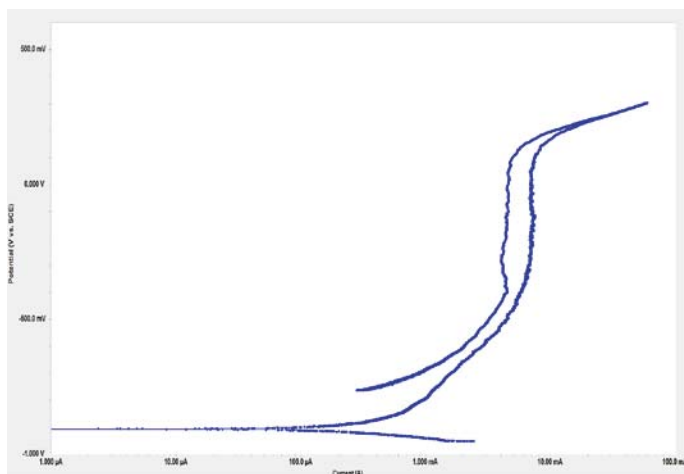
Figure 6-6. CPP scan for A537 carbon steel at 115 °C in a solution with 10M hydroxide, 0.75M nitrate, 1M nitrite, 0.07M formate, and 0.13M glycolate

Some pitting was observed on test samples from the more concentrated solutions. These pits were generally less than one mil and are attributed to the manganese sulfide inclusions in the sample material, which is vintage material from the time that the waste tanks were fabricated [27]. A photomicrograph of AARTC128 is shown in Figure 6-7, which shows the inclusions. The pits are a result of the inclusion being etched off the surface and not the propagation of a pit [27]. This hypothesis was further confirmed by performing a test with more recently produced A537 samples in a concentrated solution. A537 is the MoC for many Type III waste tanks. The sample was free of pits and appeared as if untested.

Figure 6-7. Photomicrograph of bullet-shaped test sample fabricated from AARTC128 carbon steel showing manganese sulfide inclusions (elongated black particles) [28]

7.0 Conclusions

To address the concerns with the use of glycolic acid identified during the first phase of testing, a follow-up testing was conducted to better identify temperature and waste chemistry conditions for acceptable performance of the MoCs, especially those susceptible to localized corrosion. The testing included a series of electrochemical and hot-wall tests, and a six-month coupon immersion test. The electrochemical tests were targeted towards the DWPF (glycolic acid feed tanks and piping, CPC components, and the REDC components) and the Tank Farm CCP. Hot-wall tests were conducted to further clarify the observed localized corrosion during the first phase of testing for the heat transfer surfaces in the CPC and the HLW evaporators. A six-month coupon immersion test was conducted to verify that the accelerated results of the electrochemical test are substantiated for an extended exposure in CPC simulated solution.

The results of the follow-up testing showed that for C276 under the CPC conditions localized corrosion was found to occur at chloride and sulfate concentrations as low as those processed in previous sludge batches. Deposits and coating occurred simultaneously and may be a contributing factor to the observed corrosion. These results occurred for both formic- and glycolic-based solutions with similar severity. The observed corrosion was not deep (less than 20 µm or approximately 0.001 inch) and did not progress with time up to six months. General corrosion rates in both glycolic- and formic-based solutions were found to be approximately 1 mil per year, which is given as acceptable performance in the DWPF Structural Integrity Program. Although the effect of mercury in these glycolic-based solutions was not studied extensively, mercury was found to impact the general corrosion rate but not the occurrence of localized corrosion.

For Ultimet and Stellite, the test results from the. six-month coupon immersion under CPC conditions from the follow-up testing were more limited. The corrosion of these materials in both glycolic- and formic-based solutions was similar. The localized corrosion, which again was associated with the

formation of deposits and coatings, showed a slight progression with time in the six-month coupon immersion test. This was a static test so the impact of the observed corrosion on the erosion characteristics of these wear resistant alloys was not studied. Performance of these materials during glycolic-based processing is expected to be similar to the performance during formic-based processing.

For other DWPF process areas, the glycolic acid feed tank and the REDC, the impact of the glycolate anion differed. For glycolic acid feed components, the MoC, 304L, was found to be susceptible to pitting in 70 wt% glycolic acid at temperatures from room temperature up to 50 °C. An inspection program for the 304L components that would handle the 70 wt% glycolic acid, was recommended to determine if this corrosion occurs. The DWPF will set these components up in their Structural Integrity Program. An initial inspection was performed to establish a baseline prior to the use of glycolic acid. Another option for assessing the impact of the glycolic acid here or in waste streams throughout waste processing facilities is to place corrosion coupons in the process stream, which would be removed at a set time after glycolic acid had been introduced. 316L is recommended as the MoC for any replacement components in the feed tank with 70 wt% glycolic acid. For the REDC, the presence of glycolate in the cleaning solution of the REDC did not impact MoC performance.

Localized corrosion was found to occur in this study in solutions with the glycolate anion, which simulated the conditions for CPC vessels at boiling. This corrosion was not severe and may not impact service life. However, if components are removed from service within the CPC or a failure occurs, a failure or metallurgical analysis is recommended of the failure area or probable areas of corrosion. These data could be used to substantiate laboratory results and assess if localized corrosion would cause a leak.

The results of both phases of testing showed that for the materials G30 and G-3, the MoCs for the HLW evaporators, localized corrosion was observed in the hot-wall tests regardless of the presence of the glycolate anion. Pit depths were found to be approximately 1 mil and associated with deposits whether the glycolate anion was present or not. The current operation of desalting or descaling in these facilities minimizes the formation of these deposits. Although the 3H Evaporator was not initially part of this testing, the current test results to evaluate the impact of glycolic acid along with the results of validation testing performed previously for G-3 provide data that glycolate will not impact the corrosion resistance for the 3H Evaporator. For all the alloys tested in a range of waste compositions, the glycolate anion was not found to alter the corrosion behavior of the alloy. G-3 under high hydroxide concentrations in the presence of glycolate, therefore, is not expected to impact the corrosion resistance for the 3H Evaporator. All HLW evaporators have had extended service from 16 to 28 years, which indicates that pits associated with deposits or crevices have not been an issue.

The electrochemical results in HLW simulants representative of the different chemistries covered within the Tank Farm CCP has shown that the presence of either formate, glycolate, or both together at a bounding concentration of 10,000 g/L does not alter the corrosion of carbon steel, the MoC of the waste tanks. Neither reductant impacted the corrosion requirements for maintaining the waste tanks in a safe operating regime. Data obtained with the reductants was similar to data gathered without reductant both within this current testing and the basis documents for the CCP.

8.0 References

1   T. L. Fellinger, "Impact of Nitric-Glycolic Acid Flowsheet – Material Evaluation for DWPF and Downstream Tank Farm Processes," HLW-DWPF-TTR-2013-0004, Revision 0, 2012

2   J. I. Mickalonis et al, "Corrosion Impact of Alternate Reductant on DWPF and Downstream Facilities," SRNL-STI-2014-00281, Revision 0, December 2014

3   J. I. Mickalonis and T. E. Skidmore, "Material Compatibility Evaluation for DWPF Nitric-Glycolic Acid – Literature Review," SRNL-STI-2013-00281, Revision 0, 2013

4   D.P. Lambert, M.E. Stone, J.D. Newell, D.R. Best, and J.R. Zamecnik, "Glycolic-Nitric Acid Flowsheet Demonstration of the DWPF Chemical Process Cell with Sludge and Supernate Simulants, SRNL-STI-2012-00018, Revision 1, 2012

5   G. T. Chandler, P. E. Zapp, and J. I. Mickalonis, "Hot-Wall Corrosion Testing Of Simulated High-Level Nuclear Waste," WSRC-MS-94-0367, CORROSION/95, Paper no. 431 (NACE International, Houston, TX), 1995

6   ASTM G5 – 13, "Standard Reference Test Method for Making Potentiodynamic Anodic Polarization Measurements," ASTM International, West Conshohocken, PA 2014

7   ASTM G59 – 97 (Reapproved 2009), "Standard Test Method for Conducting Potentiodynamic Polarization Resistance Measurements," ASTM International, West Conshohocken, PA 2014

8   ASTM G61 – 86 (Reapproved 2009), "Standard Test for Conducting Cyclic Potentiodynamic Polarization Measurements for Localized Corrosion Susceptibility of Iron-, Nickel-, or Cobalt-Based Alloys" ASTM International, West Conshohocken, PA 2014

9   ASTM G102 – 89 (Reapproved 2010), "Standard Practice for Calculation of Corrosion Rates and Related Information from Electrochemical Measurements," ASTM International, West Conshohocken, PA 2014

10 ASTM G31 – 72 (Reapproved 2004), "Standard Practice for Laboratory Immersion Corrosion Testing of Metals," ASTM International, West Conshohocken, PA 2014

11 "Ultrasonic Thickness Examination," Manual Y23 Procedure NDEP-7.1, SRS Procedure Manual for Nondestructive Examination Processess Revision 1, 2015

12 D.C. Silverman, "Practical Corrosion Prediction Using Electrochemical Techniques," R. W. Revie (ed), Uhlig's Corrosion Handbook, 2nd Ed, J. Wiley & Sons, 2000

13 Personal communications from T. L. Fellinger, February 2015

14 J. W. Ray, "Waste Acceptance Criteria for Sludge, ARU, and MCU Process Transfers to 512-S and DWPF," X-SD-G-00008, Revision 2, 2017

15 W. L. Daugherty, "Evaluation of Potential for Materials Degradation of DWPF Safety Class and Safety Significant Components," WSRC-TR-95-0385, Revision 0, 1995

16 M.H. Moayed and R.C. Newman, "Evolution of Current Transients and Morphology of Metastable and Stable Pitting on Stainless Steel near the Critical Pitting Temperature," *Corrosion Science*, Vol 48 (4), pp 1004-1018, 2006

17 W. R. Hinz, "Nondestructive Examination Condition Report," Job#A20140207, February 18, 2014

18 W. R. Hinz, "Nondestructive Examination Condition Report," Job#A20140469, July 28, 2014

19 W. R. Hinz, "Nondestructive Examination Condition Report," Job#A20150085, November 20, 2014

20 W. R. Hinz, "Nondestructive Examination Condition Report," Job#A20150084, November 20, 2014

21 Personal communications with D. P. Lambert, November 16, 2015

22 E. W. Holtzscheiter, "Evaluation of Glycolate Impact to Tank Farm and Radiolytic Hydrogen Generation," X-TTR-S-00060, Revision 0, 2017

23 M. S. Willams et al, "Corrosion Testing of Monofrax™ K-3 Refractory in Defense Waste Processing Facility (DWPF) Alternate Reductant Feeds," SRNL-STI-2016-00030, 2016

24 B. Garcia-Diaz, "Mechanistic Understanding of Caustic Cracking of Carbon Steels," SRNL-STI-2009-00596, 2010

25 R. Fuentes et al, "Hanford Double Shell Waste Tank Corrosion Studies – Final Report 2014," SRNL-STI-2014-00616, Rev 0, 2014

26 K. Martin, "CSTF Corrosion Control Program Description Document," WSRC-TR-2002-00327, Revision 9, 2015

27 R. Wyrwas, "SRNL Report for the Tank Waste Disposition Integrated Flowsheet: Corrosion Testing," SRNL-STI-2015-00506, Revision 0, 2015

28 NDE Condition Report, Job # S20170341, 2017

29 R. E. Fuentes, B. J. Wiersma, and K. D. Boomer, "Laboratory Simulation of Vapor Space Corrosion in Radioactive Waste Storage Tanks," Corrosion2015, Paper # 5572, NACE International, 2015

Appendix A.   Resolution of Corrosion Issues Identified during First Phase Material Evaluation Testing for DWPF Nitric-Glycolic Acid Flowsheet

Row	Alloy/Exposure Conditions	First Phase Testing Results	Follow-up Testing/Data Resolution
1	304L, 70wt wt% glycolic acid at 50 °C	Pitting observed on electrochemical test samples; general corrosion rate ≤6 mil per year (mpy).	Electrochemical testing at room temperature and 35 °C, more typical of operating conditions.
2	C276, SRAT/SME simulant at boiling	<u>Electrochemical</u>: Mixed results for pitting (≤15 μm) in glycolate-containing and glycolate-free solutions; general corrosion rate ≤12 mpy. <u>Hot-wall</u>: Pitting (≤8 μm) was associated with gasket and possibly inclusions; general corrosion rate ≤10 mpy. <u>CPC Coupon</u>: No pitting or weight loss observed after 170-hour exposure.	Electrochemical and hot wall tests with simulant chemistries chosen to bracket bounding values for past and expected DWPF sludge batches. Formic acid based simulants, prototypical of current process, included for comparison. 6-month coupon immersion was included as part of testing.
3	Ultimet, SRAT/SME simulant at boiling	<u>Electrochemical</u>: Similar to C276 with pit depths ≤ 50 μm; general corrosion rate ≤10 mpy. <u>Hot-wall</u>: Pitting (≤42 μm) including near gasket.	Coupon immersion in same simulants used for C276.
4	Stellite, SRAT/SME simulant at boiling	<u>Electrochemical</u>: Similar C276 with pit depths ≤10 μm; general corrosion rate ≤10 mpy.	Coupon immersion in same simulants used for C276.

A-1

Row	Alloy/Exposure Conditions	First Phase Testing Results	Follow-up Testing/Data Resolution
5	AllCorr, SMECT simulant, neutral and acidic pH at 100 °C	Electrochemical: Pitting (≤1 µm) observed at neutral pH (8.1), but not acidic pH (<2); general corrosion rate ≤0.4 mpy.	The pit protection potential measured for pH 8.1 solutions was greater than 200 mV from open circuit potential, which is a corrosion industry value used to indicate pitting not expected in service. [Ref: Uhlig's Corrosion Handbook, 2nd Ed, R. Winston Revie (ed), John Wiley & Sons, 2000, p 1186] AllCorr is used only in the quencher of the offgas system where condensate is acidic.
6	304L, SMECT simulant, neutral and acidic pH at ≤50 °C	Electrochemical: Pit like features (not measureable) observed with neutral pH (7.7) at 50 °C, but not acidic pH (1.5) at 30 °C; general corrosion rates <0.1 mpy.	The pit protection potential measured for pH 7.7 solutions was greater than 200 mV from open circuit potential, which is a corrosion industry value used to indicate pitting not expected in service. [Ref: ibid.]
7	G-3, Dilute waste simulant at boiling	Electrochemical: Pitting observed on samples; general corrosion rate typically <0.1mpy. Hot-wall: Pitting (≤22 µm) observed near gasket.	Hot-wall testing in glycolic- and formic-based simulants
8	G30 at tank farm evaporation conditions (basic recycle)	Electrochemical: No pitting; general corrosion rate typically <0.1mpy. Hot-wall: Pitting (≤18 µm) observed near deposits, but not associated with gasket.	Hot-wall testing in glycolic- and formic-based simulants
9	A537 in dilute waste	Electrochemical: Pitting for pH of neutral (5.5) and alkaline (~12) at 30 and 95 °C. Samples were heavily corroded and pitted (deepest pit 10 µm) in solution chemistries free of nitrite	Electrochemical testing in glycolic- and formic-based simulants to verify the SRS Tank Farm Corrosion Control Program

Row	Alloy/Exposure Conditions	First Phase Testing Results	Follow-up Testing/Data Resolution
10	A537 in basic recycle	Electrochemical: Scans at 100 °C for solutions with and without glycolate indicated pitting, but no pitting noted on samples. No pitting indications observed at 30 °C. General corrosion rates <0.6 mpy.	Electrochemical testing in glycolic- and formic-based simulants within the SRS Tank Farm Corrosion Control Program
11	Astralloy in salt processing	Electrochemical: For glycolate-free solution, one scan indicated pitting with no pits observed on sample; the other scan did not indicate pitting. For glycolate-containing solution, scans did not indicate pitting with no pits found on sample. General corrosion rates < 1 mpy.	None

Appendix B Test Solution Compositions

Table B-1 CPC Simulants – Analyzed Chemistries*.

Element/Compound	Analysis	Glycolic-based	Formic-based
Ag	ICPES	<1.00	ND
Al		137	94
B		53.0	23.8
Ba		0.652	0.383
Ca		1930	1885
Cd		ND	4.736
Cr		0.712	0.359
Cu		14.0	233.8
Fe		89.4	ND
K		418	1345
La		ND	6.443
Li		298	164
Mg		575	360
Mn		13700	6820
Na		37500	57850
Ni		1320	82
P		<1.00	<1.00
Pb		ND	<1.00
Pd		<1.00	<1.00
Rh		26.6	1.8
Ru		164	752
S		953	ND
Si		93.8	59.2
Sn		8.35	ND
Ti		<1.00	<1.00
Zn		18.2	2.5
Zr		<1.00	<1.00
F	IC Anion	<100	<500
Cl		874	247
NO2		<100	<250
NO3		92700	27500
SO4		2635	2550
C2O4		1220	3340
C2H3O3		62950	N/A
HCO2		230	75200
PO4		<100	<500
	pH	5.75	5.17

* ND – no data

Table B-2 Baseline CPC Simulant for Electrochemical, Hot-Wall and Coupon Immersion Testing

Component	Added Mass (g)	Anion Concentration (ppm)
Aluminum Nitrate ($Al(NO_3)_3 \cdot 9H_2O$)	3.0100	1,493
Calcium Nitrate ($Ca(NO_3)_2 \cdot 4H_2O$)	0.6423	337
Iron Nitrate ($Fe(NO_3)_3 \cdot 9H_2O$)	1.0164	468
Potassium Nitrate (KNO_3)	0.8288	508
Magnesium Nitrate ($Mg(NO_3)_2 \cdot 6H_2O$)	2.1416	1,036
Manganese Nitrate (50 wt % $Mn(NO_3)2 + 5$ wt % HNO_3)	17.3892	6,881
Nickel Nitrate ($Ni(NO_3)_2 \cdot 6H_2O$)	0.4955	211
$RuCl_3$ (41.74wt% Ru)	0.0217	0
Rhodium Nitrate (4.933 wt % solution)	0.5285	47
Zirconium Nitrate ($ZrO(NO_3)_2 \cdot 6H_2O$)	0.0840	31
Sodium Nitrate ($NaNO_3$)	63.6692	46,450
Sodium Glycolate ($NaC_2H_3O_3$)	63.4888	48,600
Sodium Oxalate ($Na_2C_2O_4$)	5.7851	3,800
Sodium Sulfate (Na_2SO_4)	3.8960	2,635
Sodium Chloride ($NaCl$)	1.3532	821
Mercury Nitrate ($(HgNO_3)_2 \cdot H_2O$)	0	0

Table B-3. Dilute Waste Solution.

Recipe	1L Solution Mass, g
Sodium Carbonate (Na2CO3)	0
Calcium Nitrate (Ca(NO3)2.4H2O)	0.0061
Iron Nitrate (Fe(NO3)3.9H2O)	0.0024
Potassium Nitrate (KNO3)	0.0015
Magnesium Nitrate (Mg(NO3)2.6H2O)	0.001
Ammonium Nitrate (NH4NO3)	0.0051
Mercury Nitrate (Hg(NO3)2.H2O	0.0064
Sodium Nitrate (NaNO3)	0.0165
Sodium Glycolate (NaC2H3O3)	0.033
Sodium Sulfate (Na2SO4)	0.0503
Sodium Chloride (NaCl)	0.0272

Table B-4. Basic Recycle Solution

Recipe	1L Solution Mass, g
Sodium Hydroxide (NaOH)	0.4
Sodium Carbonate (Na2CO3)	48.02
Sodium Sulfate (Na2SO4)	2.66
Sodium Phosphate (Na3PO4·12H2O)	1.6
Sodium Formate (NaCHO2)	2.4
Sodium Glycolate (NaC2H3O3)	13.06
Sodium Oxalate (Na2C2O4)	0.26
Sodium Nitrate (NaNO3)	90.1
Sodium Nitrite (NaNO2)	113.62

Appendix C Corrosion Control Program Experimental Gaps in Demonstrating Impact of Glycolate

| | Corrosion Control Program | | | | Supporting Literature Data[1] | | | |
| | | | | | With Glycolate | | Without Glycolate | |
Chemistry[10]	Corrosion[11]	Inhibitor Requirements	Max T (°C)	Waste Type/Tanks	Reference	Condition	Reference	Condition
$OH \geq 8$	OH-SCC	$NO_2 \geq 0.3$, $T \leq 10^9$	115	Aluminum dissolution, Salt Receipt				
$NO_3 \leq 0.02$ and $1 < OH \leq 8$	OH-SCC	$OH > 1$	60^8	Not seen in SRS Tank Farm[2]				
$NO_3 < 1$ and $OH > 8$	OH-SCC	$OH > 1$	60^8	Aluminum dissolution, Tanks 30&37				
$5.5 < NO_3 \leq 8.5$	NO_3-SCC	$OH \geq 0.6$, $NO_2 + OH \geq 1.1$	$70\ (R<2)$	Salt dissolution				
$2.75 < NO_3 \leq 5.5$	NO_3-SCC	$OH \geq 0.3$, $NO_2 + OH \geq 1.1$	$112\ (R>2)$ $105\ (R<2)$	Salt receipt	Fuentes 2014[3] Fuentes 2016[4] Brossia 2006[6]	$30\text{-}50\ ^\circ C$, $OH < 0.3$, $NO_2 + OH \geq 1.5$; $50\ ^\circ C\ (R<2)$, $OH < 0.1[NO_3]$, $NO_2 + OH \geq 1.1$	Fuentes 2016[5]	$40\ ^\circ C$, $OH < 0.3$, $NO_2 + OH \geq 1.5$
$1 \leq NO_3 \leq 2.75$	NO_3-SCC	$OH \geq 0.1[NO_3]$, $NO_2 + OH \geq 0.4[NO_3]$	$105\ (R>2)$ $70\ (R \leq 2)$	Canyon receipt; Concentrated salt receipt	Fuentes 2014[3] Fuentes 2016[4] Brossia 2006[6]	$30\text{-}50\ ^\circ C$, $OH < 0.3$, $NO_2 + OH \geq 1.5$; $50\ ^\circ C\ (R<2)$, $OH < 0.1[NO_3]$, $NO_2 + OH \geq 0.4[NO_3]$	Fuentes 2016[5]	$40\ ^\circ C$, $OH < 0.3$, $NO_2 + OH \geq 1.5$
$0.02 < NO_3 < 1$ and $OH < 1$	Pitting	$pH > 10.3$, $[NO_2] = f\{NO_3, Cl, and\ SO_4\}$	40	DWPF Recycle, Tank 51	Mickalonis 2014[7]	$50\ ^\circ C$	Mickalonis 2014	$50\ ^\circ C$
$0.02 < NO_3 < 1$ and $1 < OH \leq 8$	Pitting	$OH > 1$	100	Aluminum dissolution				
$NO_3 \leq 0.02$ and $OH < 1$	Pitting	$pH > 10.3$, $[NO_2] = f\{NO_3, Cl, and\ SO_4\}$	40	DWPF Recycle				

[1] The "without Glycolate" category focuses on test comparative to those with glycolate. Most, if not all the testing used to support the corrosion control program is based on simulants made without glycolate or formate. The "with Glycolate" category shows any tests in which glycolate was used and there is no detrimental effect. In many cases a positive or inhibitive effect is noted. In the review, no cases were identified in which glycolate had a negative effect on the corrosion resistance of carbon steel which is the primary material of construction used in the SRS Tank Farm.

[2] Not seen in the SRS Tank Farm; inhibitors limits for this category were established for waste chemistries anticipated from aluminum dissolution.

[3] R. E. Fuentes et al, Hanford Double Shell Waste Tank Corrosion Studies – Final Report FY2014, SRNL-STI-2014-00616, Rev 0, Dec 2014 (conditions covered in testing - [OH] 0.032-0.262 M, [NO$_2$] 1-2.24 M, [NO$_3$] 3-3.7 M, [Gly] 0.161 or 8,600 mg/L, [For] 0.233 or 11,300 mg/L).

[4] R. E. Fuentes et al, HANFORD DOUBLE SHELL WASTE TANK CORROSION STUDIES – FINAL REPORT FY2015, SRNL-STI-2016-00117, Rev 0, May 2016 (conditions covered in testing -[OH] 0.01-0.05 M, [NO$_2$] 0.5-1.5 M, [NO$_3$] 1.1-5.5 M, [Gly] 0.161 or 8,600 mg/L, [For] 0.233 or 11,300 mg/L).

[5] R. E. Fuentes et al, HANFORD DOUBLE SHELL WASTE TANK CORROSION STUDIES – FINAL REPORT FY2016, SRNL-STI-2016-00721, Rev Draft (conditions covered in testing - [OH] 0.01-0.05 M, [NO$_2$] 0.5-1.0 M, [NO$_3$] 1.1-5 M, [Gly] 0, [For] 0, T=40 °C).

[6] C. S. Brossia et al, "Hanford Tanks 241-AN-107 and 241-AN-102;", Final Report 805602, September 8, 2006 (conditions covered in testing - [OH] 10 or 11 M; [NO$_2$] 2.3 or 3.7M; [NO$_3$] 2.4 or 1.2 M; [Gly] ~13500 mg/L, [For] ~11000 mg/L).

[7] J. I. Mickalonis et al, "Corrosion Impact of Alternate Reductant on DWPF and Downstream Facilities," SRNL-STI-2014-00281, Revision 0, December 2014 (conditions covered in testing - [OH] 0.08 M; [NO$_2$] 0.09 M; [NO$_3$] 0.076 M, [Gly] 10000 mg/L, [For] 562 mg/L).

[8] During waste removal operations, mixing pumps are needed to combined the added inhibited water or dilute supernate into the tank waste. The temperature of the supernate will rise with pump operation. The temperature limit for the bulk supernate during slurry pump operation shall be 75 °C for supernate.

[9] R = {[NO$_2$] + [OH]}/ [NO$_3$], T = [OH] / {[NO$_3$] + [NO$_2$]}, concentrations are in units of M.

[10] The chemistry shown is the dominant species concentrations that impact the corrosion. Concentrations are in units of M.

[11] The primary form of corrosion that is being controlled for each chemistry include caustic stress corrosion cracking (OH-SCC), nitrate stress corrosion cracking (NO$_3$-SCC), and pitting.

Appendix D Coupon Immersion Test Results - Weight Losses and Calculated Corrosion Rates*

Solution #	Coupon ID		Duration		Average Weights (g)		Corrosion
	Alloy	Number	(Mos)	(Days)	Initial	Final	Rate (mpy)**
1	C276	1	1	30	34.7366	34.7351	0.025
		2	3	87	34.1443	34.1404	0.023
		13	4	112	34.5592	34.5538	0.025
		3	6	183	34.6072	34.6000	0.020
	C276W	1	1	30	31.6650	31.6632	0.030
		2	3	87	30.6471	30.6423	0.029
		13	4	112	32.4063	32.4057	0.003
		3	6	183	31.1502	31.1409	0.027
	St6B	1	1	30	15.4433	15.4431	0.004
		2	3	87	16.0153	16.0164	-0.008
		1'	4	100		15.4698	0.001
		3	6	183	15.9195	15.9218	-0.008
	Ult	1	1	30	7.8617	7.8596	0.079
		2	3	87	7.9518	7.9541	-0.030
		1	4	100	14.8689	14.8688	0.001
		3	6	183	8.0344	8.0343	0.001
2	C276	4	1	30	34.2534	34.2525	0.015
		5	3	87	33.9067	33.9054	0.008
		14	4	112	33.9586	33.9557	0.013
		6	6	183	34.5488	34.5448	0.011
	C276W	4	1	30	30.7130	30.7125	0.009
		5	3	87	29.8705	29.8694	0.007
		14	4	112	31.5526	31.5489	0.017
		6	6	183	31.6351	31.6312	0.011
	St6B	4	1	30	16.0413	16.0413	-0.001
		5	3	87	16.1606	16.1618	-0.008
		2	4	100	15.4959	15.4957	0.001
		6	6	183	16.0347	16.0363	-0.005

Solution #	Coupon ID		Duration		Average Weights (g)		Corrosion Rate (mpy)**
	Alloy	Number	(Mos)	(Days)	Initial	Final	
	Ult	4	1	30	7.8495	7.8471	0.089
		5	3	87	7.7434	7.7430	0.006
		2	4	100	15.1973	15.1974	-0.001
		6	6	183	7.8890	7.8915	-0.016
3	C276	7	1	30	34.3034	34.3026	0.013
		8	3	87	34.3993	34.3975	0.011
		15	4	112	34.4942	34.4895	0.021
		9	6	183	34.8625	34.8571	0.015
	C276W	7	1	30	31.5743	31.5744	-0.002
		8	3	87	31.5225	31.5200	0.015
		15	4	112	31.7389	31.7342	0.022
		9	6	183	31.5921	31.5858	0.018
	St6B	7	1	30	15.8586	15.8587	-0.003
		8	3	87	15.9217	15.9236	-0.013
		3	5	141	16.0033	16.0045	-0.005
	Ult	7	3	87	8.0379	8.0401	-0.029
		3	5	141	14.9532	14.9541	-0.004
4	C276	10	1	30	34.5718	34.5747	-0.051
		11	3	87	34.3583	34.3628	-0.027
		16	4	112	34.1133	34.1178	-0.021
		12	6	183	35.1012	35.1071	-0.017
	C276W	10	3	87	31.2478	31.2509	-0.019
		11	1	30	30.8441	30.8436	0.009
		16	4	112	31.5866	31.5880	-0.007
		12	6	183	32.1752	32.1846	-0.027
	St6B	9	1	30	15.8251	15.8272	-0.042
		10	3	87	15.8135	15.8154	-0.013
		4	5	141	15.7326	15.7338	-0.005
	Ult	8	3	87	8.0514	8.0552	-0.050
		4	5	141	15.3377	15.3387	-0.004

* The table is color coded for the materials of construction for ease of comparison among the different solutions.
** A negative corrosion rate indicates a weight gain which may be associated with the incomplete removal of deposits and coating or of base metal oxidation.

Appendix E Non-Destructive Examination Reports

A	1/03	**Nondestructive Examination** **Condition Report**	Job #: A 20140207
			Work Request #: N/A
			Keywords: Coils

Distribution:

B.N. Price, SRNL R&EP, 773-A
J.I. Mickalonis, SRNL MS&T, 773-A
S.A. Martin, SRNL QA, 773-41A

N. C. Iyer, SRNL, 773-41A
R. L. Bickford, MNDE&C, 730-A
730-A NDE Files *

Page: 1 of 1   Date: 2/18/2014

Reported by: W. R. Hinz	Inspectors/Level: W.R. Hinz, UT Level III
Equipment Examined: SME Coil Mockup	
Location: 723-A	Component Identification # IDP# N/A Component SME Coil Mockup
Date(s) of Examination: 2/5-6/14	CLI# N/A
Service Condition: New Assembly	Materials of Construction: 300 Grade Stainless Steel
NCR Number (if applicable): None	
Inspection Procedure (Number and Title): NDEP 7.1, Ultrasonic Thickness Examination	
Acceptance Criteria (Source): Information Only, Baseline Inspection	

Inspection Summary:

MNDE&C completed ultrasonic baseline measurement of the miniature SME Coil mockup (also known as the "Steeper" Coil). These measurements establish the basis for future comparison after the unit has been subjected to a certain level of service to determine the erosion rate. These measurements can also be used for determining the initial structural integrity of the coil assembly.

The bulk of the measurements were obtained in those areas expected to erode most rapidly based on experience with several past failures of actual DWPF SME Coil assemblies. 249 individual measurements were made on the coil base material with the thinnest area being 0.030", typical coil measurements were 0.033" at the outer radius of coil bends and 0.035" at the inner radius. Thickness values at 7 coil circumferential welds were also obtained and ranged from 0.022" to 0.035".

For more information see report #2013-IR-11-0164 or contact W.R. Hinz at 5-4896.

7.05 5/09

SRS
SAVANNAH RIVER SITE

ULTRASONIC THICKNESS REPORT

JOB #	A 20140207
REPORT #	2014-IR-11-0164
CLI#	N/A

AREA / SYSTEM	PROCEDURE	REV	SEE COVER SHEET FOR ACCEPTANCE CRITERIA
723-A	NDEP 7.1	0	

WELD / COMPONENT I.D.	INSPECTION PLAN#	IDP#	WORK REQUEST #
SME Coil Mockup	N/A	N/A	N/A

DRAWING	REV.	MATERIAL TYPE	SURFACE CONDITION	NORMAL DIA/SCH OR THK.	MINIMUM ALLOWABLE THK.
N/A	N/A	300 Grade Stainless	As Fabricated	.033"	Not Established

EQUIPMENT

INSTRUMENT	MANUFACTURER	MODEL	UT M&TE #	CAL DUE DATE
☐ DTG ☒ CRT	Krautkramer Branson	USN-60	4-2094	4/14/2014

TRANSDUCER	MANUFACTURER	MODEL	S/N	SIZE	FREQ
☒ SGL ☐ DUAL	Panametrics	V260 Sonopen	4-1637	0.080"	15 Mhz

CABLE LENGTH	COUPLANT	BATCH	CAL STANDARD M&TE#	CALIBRATION POINTS
6'	Pana. SWC	11654	4-1545	0.029", 0.058"

EXAMINATION RESULTS

Location	0°	90°	180°	270°	SKETCH - IDENTIFY AREAS/CONTROL POINTS EXAMINED
see Pgs. 2-7		N A			

☒ ACC. ☐ REJ. ☐ N/A

MINIMUM READING OBTAINED
.030" (coil), .022" (circ. weld)

REMARKS - Provide details concerning nature of reduction in wall thickness. List all other M&TE used, M&TE#, and due dates.
See pages 2-7 for details. Note that portions of welds are less than full penetration (prior internal video inspection), this explains the lower thickness value in the weld joint.

PAGE
1 OF 7

2014-IR-II-0164 Page 2 of 7

UT Locations, Small Scale SME Mockup

A20140207

Inlet/Outlet
Lines (5)

.25"
1.0"
(typ.)

0
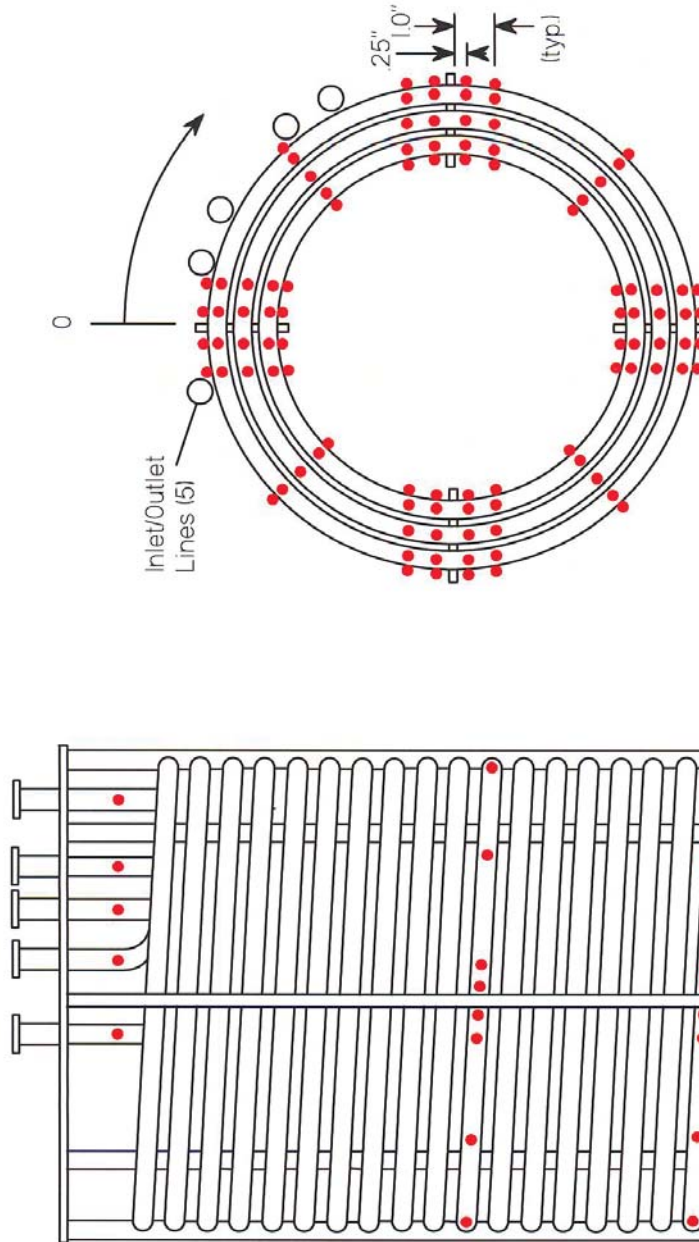
Progression – start at bottom ring elbows
(locations on inlet/outlet line elbows and radial
weld locations are not shown)

P1-P26 for each ring along pipe axis
0/90/180/270 radial location, 0 @ top, 90 @ interior
O – outer coil, C – center coil, I – inner coil

A20140207   2014-IR-11-0164 Page 3 of 7

1st Ring

	O-0	O-90	O-180	O-270	C-0	C-90	C-180	C-270	I-0	I-90	I-180	I-270
P1-ELL	0.036		0.032	0.034		0.033	0.032	0.033		0.03	0.032	
P2			0.035	0.033			0.035	0.033		0.032	0.033	0.033
P3			0.035	0.032			0.035			0.034	0.035	0.033
P4			0.034	0.032			0.035			0.034	0.034	0.033
P5			0.035	0.033			0.035			0.034	0.034	0.033
P6			0.035	0.033			0.035			0.034	0.034	0.033
P7			0.035	0.033			0.034			0.034	0.034	0.033
P8			0.035	0.033			0.035			0.034	0.035	0.033
P9			0.035	0.033			0.035			0.034	0.034	0.033
P10			0.035	0.033			0.035			0.034	0.034	0.033
P11			0.035	0.033			0.034			0.034	0.035	0.033
P12			0.035	0.033			0.035			0.035	0.035	0.033
P13			0.035	0.033			0.034			0.035	0.035	0.033
P14			0.035	0.033			0.034			0.035	0.035	0.033
P15			0.035	0.033			0.035			0.035	0.035	0.033
P16			0.035	0.033			0.035			0.034	0.035	0.033
P17			0.035	0.033			0.035			0.035	0.035	0.033
P18			0.035	0.033			0.035			0.035	0.035	0.033
P19			0.035	0.033			0.035			0.034	0.035	0.033
P20			0.035	0.033			0.034			0.034	0.035	0.033
P21			0.035	0.033			0.034			0.035	0.035	0.033

2nd Ring

	O-0	O-90	O-180	O-270	C-0	C-90	C-180	C-270	I-0	I-90	I-180	I-270
P1-ELL												
P2				0.033						0.035		
P3				0.032						0.035		
P4				0.032						0.035		
P5				0.033						0.035		
P6				0.033						0.035		
P7				0.033						0.035		
P8				0.033						0.035		
P9				0.033						0.035		
P10				0.033						0.035		
P11				0.033						0.035		
P12				0.033						0.035		
P13				0.033						0.035		
P14				0.033						0.035		
P15				0.033						0.035		
P16				0.033						0.035		
P17				0.033						0.035		
P18				0.033						0.035		
P19				0.033						0.035		
P20				0.033						0.035		
P21				0.033						0.035		

1st Ring (Bottom) Outer, Center and Inner Coils

2nd Ring Outer, Center and Inner Coils

3rd Ring

	O-0	O-90	O-180	O-270	C-0	C-90	C-180	C-270	I-0	I-90	I-180	I-270
P1-ELL												
P2				0.033						0.035		
P3				0.033						0.035		
P4				0.033						0.035		
P5				0.033						0.035		
P6				0.033						0.035		
P7				0.033						0.035		
P8				0.033						0.035		
P9				0.033						0.035		
P10				0.033						0.035		
P11				0.033						0.035		
P12				0.033						0.035		
P13				0.033						0.035		
P14				0.033						0.035		
P15				0.033						0.035		
P16				0.033						0.035		
P17				0.033						0.035		
P18				0.033						0.035		
P19				0.033						0.035		
P20				0.033						0.035		
P21				0.033						0.035		

Midpoint - 10th Ring

	O-0	O-90	O-180	O-270	C-0	C-90	C-180	C-270	I-0	I-90	I-180	I-270
P1-ELL												
P2				0.033						0.035		
P3				0.033						0.035		
P4				0.033						0.035		
P5				0.033						0.035		
P6				0.033						0.035		
P7				0.033						0.035		
P8				0.033						0.035		
P9				0.033						0.035		
P10				0.033						0.035		
P11				0.033						0.035		
P12				0.033						0.035		
P13				0.033						0.035		
P14				0.033						0.035		
P15				0.033						0.035		
P16				0.033						0.035		
P17				0.033						0.035		
P18				0.033						0.035		
P19				0.033						0.035		
P20				0.033						0.035		
P21				0.033						0.035		

3rd Ring Outer, Center and Inner Coils

Midpoint, 10th Ring Outer and Inner Coils

A20140207   2014-IR-11-0164 Page 7 of 7

Various Tubing Weld Circ. Seams

	O-0	O-90	O-180	O-270	C-0	C-90	C-180	C-270	I-0	I-90	I-180	I-270
W1	0.035			0.026								
W2	0.027			0.022								
W3			0.033	0.03								
W4							0.032	0.033				
W5							0.031	0.024				
W6										0.022	0.035	
W7											0.031	0.026

Thickness at Various Tubing Weld Circ. Seams

A	1/03	**Nondestructive Examination** **Condition Report**	Job #:	A 20140469
			Work Request #:	N/A

Keywords: Tank

Distribution:

J.D. Newell, SRNL E&CPT/RP, 999-W
J.I. Mickalonis, SRNL MS&T, 773-A
S.A. Martin, SRNL QA, 773-41A

N. C. Iyer, SRNL, 773-41A
R. L. Bickford, MNDE&C, 730-A
730-A NDE Files *

Page: 1 of 1

Date: 7/28/2014

Reported by: W. R. Hinz	Inspectors/Level: W.R. Hinz, UT Level III
Equipment Examined: SME/SRAT Tank Mockup	
Location: 723-A	Component Identification # IDP# N/A Component SME/SRAT Tank Mockup
Date(s) of Examination: 7/24/2014	CLI# N/A
Service Condition: New Assembly	Materials of Construction: Stainless Steel
NCR Number (if applicable): None	

Inspection Procedure (Number and Title):
NDEP 7.1, Ultrasonic Thickness Examination

Acceptance Criteria (Source):
Information Only, Baseline Inspection

Inspection Summary:

MNDE&C completed ultrasonic baseline or preservice measurement of the miniature SME/SRAT Tank mockup (a scaled down coil bundle will be placed internally). These measurements establish the basis for future comparison after the unit has been subjected to a certain level of service to determine the erosion rate.

The measurements were obtained in those areas expected to erode most rapidly based on experience with several past failures of actual DWPF SME Coil assemblies. 24 individual measurements were made on the tank base material with the thinnest area being 0.049" at the bottom head, just below the head to shell weld.

For more information see report #2014-IR-11-0444 or contact W.R. Hinz at 5-4896.

SRS	7.05 5/09		JOB # A 20140469
SAVANNAH RIVER SITE		**ULTRASONIC THICKNESS REPORT**	REPORT # 2014-IR-11-0444
			CLI# N/A

AREA / SYSTEM 999-W		PROCEDURE NDEP 7.1		REV 0	SEE COVER SHEET FOR ACCEPTANCE CRITERIA	
WELD / COMPONENT I.D. SME/SRAT Tank Mockup		INSPECTION PLAN# N/A		IDP# N/A	WORK REQUEST # N/A	

DRAWING N/A	REV. N/A	MATERIAL TYPE Stainless Steel	SURFACE CONDITION As Fabricated	NORMAL DIA/SCH OR THK. Unknown	MINIMUM ALLOWABLE THK. Not Established

EQUIPMENT

INSTRUMENT ☐ DTG ☒ CRT	MANUFACTURER Krautkramer Branson		MODEL USN-60		UT M&TE # 4-2045	CAL DUE DATE 10/14/2014
TRANSDUCER ☒ SGL ☐ DUAL	MANUFACTURER GEIT		MODEL ALPHA	S/N 4-3025	SIZE 0.250"	FREQ 10 Mhz
CABLE LENGTH 6'	COUPLANT Ultragel II	BATCH 11654	CAL STANDARD M&TE# 4-1543		CALIBRATION POINTS .029" - .103"	

EXAMINATION RESULTS

Location	0°	90°	180°	270°	SKETCH - IDENTIFY AREAS/CONTROL POINTS EXAMINED
see page 2					
				N A	

☐ ACC. ☐ REJ. ☒ N/A	MINIMUM READING OBTAINED .049" (bottom head)

REMARKS - Provide details concerning nature of reduction in wall thickness. List all other M&TE used, M&TE#, and due dates.
See page 2 for details.

PAGE 1 OF 2

2014-IR-II-0444 Page 2 of 2

W20140469

SCALED DOWN SME/SRAT VESSEL – PRESERVICE UT MEASUREMENTS
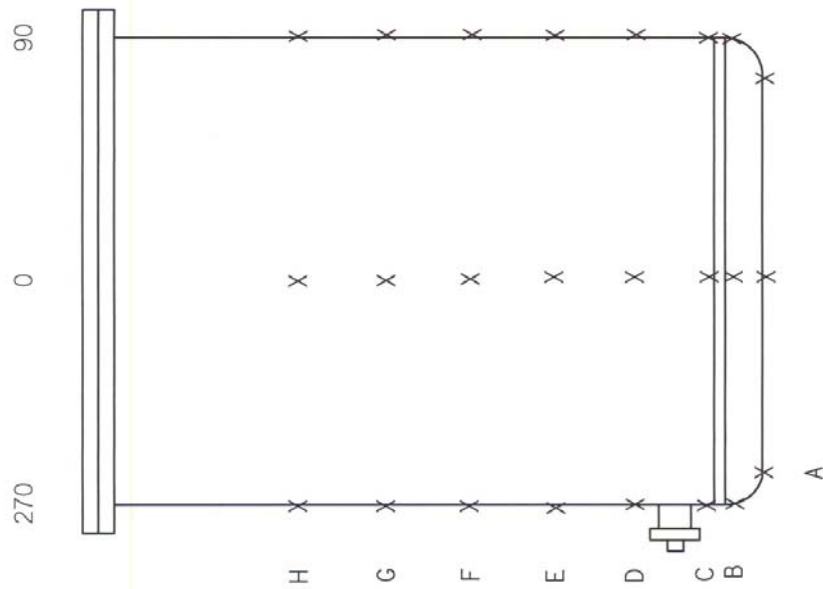
	0	90	270
A	0.055	0.055	0.055
B	0.049	0.049	0.049
C	0.073	0.073	0.072
D	0.072	0.072	0.072
E	0.072	0.072	0.072
F	0.072	0.072	0.072
G	0.071	0.072	0.072
H	0.072	0.071	0.072

Viewed from front of hood

E-11

| A | 1/03 | Nondestructive Examination **Condition Report** | Job #: | A 20150084 |
| | | | Work Request #: | N/A |

Keywords: Coils

Distribution:

J.D. Newell, SRNL E&CPT/RP, 999-W
J.I. Mickalonis, SRNL MS&T, 773-A
S.A. Martin, SRNL QA, 773-41A
J.E. Ziska, SRNL MS&T, 730-A

N. C. Iyer, SRNL, 773-41A
R. L. Bickford, MNDE&C, 730-A
730-A NDE Files *

Page: 1 of 1   Date: 11/20/2014

Reported by:	Inspectors/Level:
W. R. Hinz	W.R. Hinz, UT Level III, J.E. Ziska, UT-T
Equipment Examined:	
SME Coil Mockup	Component Identification # IDP# N/A
Location:	Component
723-A	SME Coil Mockup
Date(s) of Examination:	CLI#
11/12/2014	N/A
Service Condition:	Materials of Construction:
New Assembly	300 Grade Stainless Steel

NCR Number (if applicable):
None

Inspection Procedure (Number and Title):
NDEP 7.1,Ultrasonic Thickness Examination

Acceptance Criteria (Source):
Information Only, Final Inspection

Inspection Summary:

MNDE&C completed final ultrasonic measurement of the miniature SME Coil mockup following the baseline measurements and after two weeks of run time. The measurements are being compared to determine if there is any evidence of process induced erosion and for the prediction of erosion rates, where erosion has occurred.

Original preservice selection of the locations for the bulk of these measurements targeted those areas expected to erode most rapidly based on experience with several past failures of actual DWPF SME Coil assemblies. 249 individual measurements were made on the coil base material in the same locations as the baseline measurements.

Measurement accuracy in this thickness range is +/- 0.001". Measurements within +/- 0.001" are considered to be unchanged and within the "noise" level. Measurements beyond this range are indicative of some level of erosion. Predictably, in the same pattern of the real SME coil bundles, inner and bottom surfaces of the lowest, or "1st" ring showed the greatest reductions in thickness (0.002" to 0.003"). These areas would be the most exposed to the outflow from the agitator blades when in operation. Visual appearance of the surfaces at these locations indicate a burnished surface. Measurements of the higher elevations fell in the "noise" level of +/- 0.001" and do not indicate erosion is taking place at these locations.

Thickness values at 7 coil circumferential welds were also compared with baseline measurements and also fall within the +/- 0.001" range. For more information see report #2014-IR-11-0718 or contact W.R. Hinz at 5-4896.

7.05 5/09

JOB #	A 20150084
REPORT #	2014-IR-11-0718
CLI#	N/A

SRS
SAVANNAH RIVER SITE

ULTRASONIC THICKNESS REPORT

AREA / SYSTEM				PROCEDURE			REV		SEE COVER SHEET FOR
999-W				NDEP 7.1			0		ACCEPTANCE CRITERIA

WELD / COMPONENT I.D.	INSPECTION PLAN#	IDP#	WORK REQUEST #
SME Coil Mockup	N/A	N/A	N/A

DRAWING	REV.	MATERIAL TYPE	SURFACE CONDITION	NORMAL DIA/SCH OR THK.	MINIMUM ALLOWABLE THK.
N/A	N/A	300 Grade Stainless	As Fabricated	.033"	Not Established

EQUIPMENT

INSTRUMENT	MANUFACTURER	MODEL	UT M&TE #	CAL DUE DATE
☐ DTG ☒ CRT	Krautkramer Branson	USN-60	4-2094	1/13/2015

TRANSDUCER	MANUFACTURER	MODEL	S/N	SIZE	FREQ	
☒ SGL ☐ DUAL	Panametrics	V260 Sonopen	4-1637	0.080"	15	Mhz

CABLE LENGTH	COUPLANT	BATCH	CAL STANDARD M&TE#	CALIBRATION POINTS
6'	Pana. SWC	11654	4-1545	0.029", 0.058"

EXAMINATION RESULTS

Location	0°	90°	180°	270°	SKETCH - IDENTIFY AREAS/CONTROL POINTS EXAMINED
see pg. 2-10					

N/A

☒ ACC. ☐ REJ. ☐ N/A   MINIMUM READING OBTAINED
.030" (coil), .022" (circ. weld)

REMARKS - Provide details concerning nature of reduction in wall thickness. List all other M&TE used, M&TE#, and due dates.
See pages 2-10 for details. Note that portions of welds are less than full penetration (prior internal video inspection), this explains the lower thickness value in the weld joint.

PAGE
1 OF 10

2014-IR-II-0718 Page 2 of 10

Inlet/Outlet Lines (5)

.25" 1.0"

0
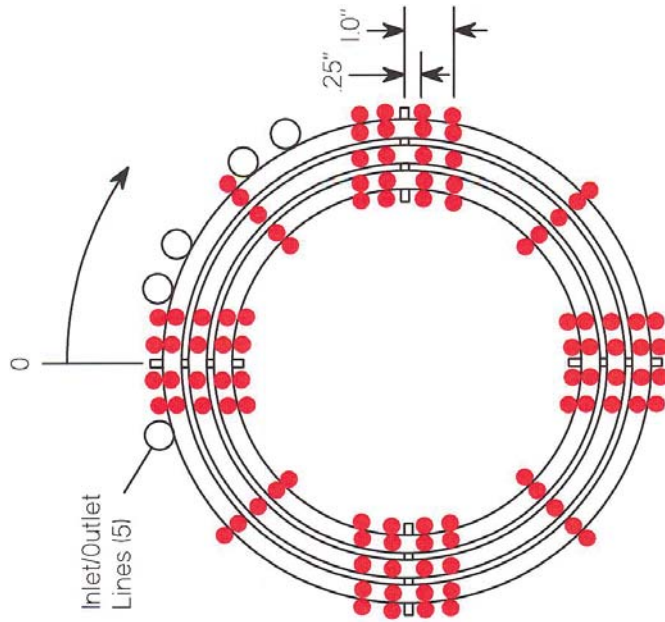
Progression - start at bottom ring elbows (location on inlet/outlet line elbows and radial weld locations are not shown)

P1-P26 for each ring along pipe axis 0/90/180/270 radial location, 0 @ top, 90 @ interior, 180 @ bottom, 270 @ exterior. O – outer coil, C – center coil, I – inner coil

A20150084

A20150084

2014-IR-11-0718 Page 3 of 10
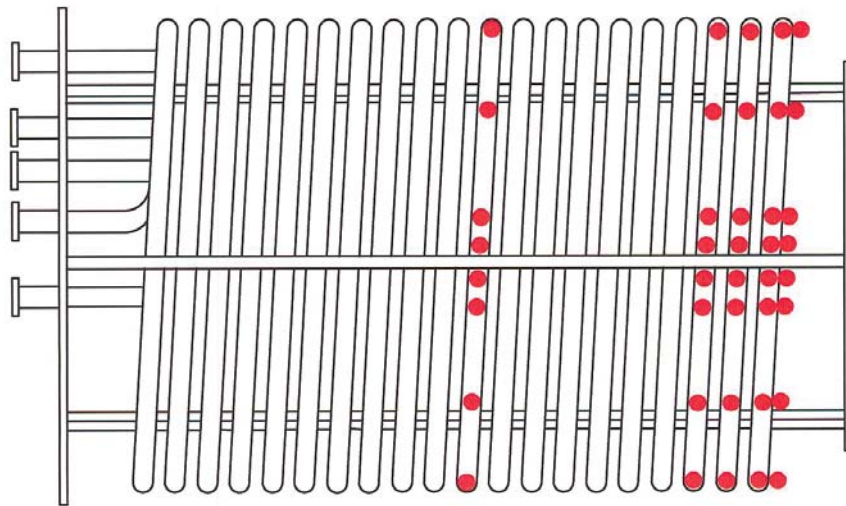
1st Ring - Outer Coil, 0 deg. (Top)

	Baseline	Final
P1-ELL	0.036	0.036

(not shown)

1st Ring - Outer Coil, 180 deg. (Bottom)

	Baseline	Final
P1-ELL	0.032	0.031
P2	0.035	0.032
P3	0.035	0.032
P4	0.034	0.033
P5	0.035	0.033
P6	0.035	0.033
P7	0.035	0.033
P8	0.035	0.033
P9	0.035	0.033
P10	0.035	0.033
P11	0.035	0.033
P12	0.035	0.033
P13	0.035	0.034
P14	0.035	0.034
P15	0.035	0.034
P16	0.035	0.035
P17	0.035	0.033
P18	0.035	0.034
P19	0.035	0.034
P20	0.035	0.034
P21	0.035	0.034

1st Ring - Outer Coil, 270 deg. (Side, Outer)

	Baseline	Final
P1-ELL	0.034	0.033
P2	0.033	0.032
P3	0.032	0.032
P4	0.032	0.032
P5	0.033	0.033
P6	0.033	0.033
P7	0.033	0.033
P8	0.033	0.033
P9	0.033	0.033
P10	0.033	0.033
P11	0.033	0.033
P12	0.033	0.033
P13	0.033	0.033
P14	0.033	0.033
P15	0.033	0.033
P16	0.033	0.033
P17	0.033	0.033
P18	0.033	0.033
P19	0.033	0.033
P20	0.033	0.033
P21	0.033	0.033

1st Ring - Center Coil, 90 deg. (Side, Inner)

	Baseline	Final
P1-ELL	0.033	0.031

(not shown)

1st Ring - Center Coil, 180 deg. (Bottom)

	Baseline	Final
P1-ELL	0.032	0.03
P2	0.035	0.034
P3	0.035	0.033
P4	0.035	0.033
P5	0.035	0.033
P6	0.035	0.033
P7	0.034	0.033
P8	0.035	0.034
P9	0.035	0.033
P10	0.035	0.034
P11	0.034	0.034
P12	0.035	0.033
P13	0.034	0.033
P14	0.034	0.034
P15	0.035	0.034
P16	0.035	0.033
P17	0.035	0.033
P18	0.035	0.033
P19	0.035	0.034
P20	0.034	0.033
P21	0.034	0.033

1st Ring - Center Coil, 270 deg. (Side, Outer)

	Baseline	Final
P1-ELL	0.033	0.034
P2	0.033	0.032

(not shown)

E-15

A20150084

1st Ring - Inner Coil, 90 deg. (Side, Inner)

	Baseline	Final
P1-ELL	0.03	0.03
P2	0.032	0.032
P3	0.034	0.035
P4	0.034	0.034
P5	0.034	0.034
P6	0.034	0.033
P7	0.034	0.033
P8	0.034	0.035
P9	0.034	0.034
P10	0.034	0.034
P11	0.034	0.033
P12	0.035	0.032
P13	0.035	0.033
P14	0.035	0.034
P15	0.035	0.035
P16	0.034	0.033
P17	0.035	0.034
P18	0.035	0.034
P19	0.034	0.035
P20	0.034	0.034
P21	0.035	0.034

1st Ring - Inner Coil, 180 deg. (Bottom)

	Baseline	Final
P1-ELL	0.032	0.032
P2	0.033	0.034
P3	0.035	0.035
P4	0.034	0.031
P5	0.034	0.033
P6	0.034	0.034
P7	0.034	0.034
P8	0.035	0.035
P9	0.034	0.035
P10	0.034	0.034
P11	0.035	0.034
P12	0.035	0.034
P13	0.035	0.035
P14	0.035	0.034
P15	0.035	0.035
P16	0.035	0.035
P17	0.035	0.034
P18	0.035	0.033
P19	0.035	0.034
P20	0.035	0.034
P21	0.035	0.034

1st Ring - Inner Coil, 270 deg. (Side, Outer)

	Baseline	Final
P1-ELL		
P2	0.033	0.033
P3	0.033	0.033
P4	0.033	0.032
P5	0.033	0.033
P6	0.033	0.032
P7	0.033	0.033
P8	0.033	0.033
P9	0.033	0.034
P10	0.033	0.034
P11	0.033	0.034
P12	0.033	0.034
P13	0.033	0.033
P14	0.033	0.033
P15	0.033	0.033
P16	0.033	0.033
P17	0.033	0.033
P18	0.033	0.033
P19	0.033	0.032
P20	0.033	0.032
P21	0.033	0.033

2nd Ring - Outer Coil, 270 deg. (Side, Outer)

	Baseline	Final
P1-ELL		
P2	0.033	0.033
P3	0.032	0.033
P4	0.032	0.033
P5	0.033	0.033
P6	0.033	0.033
P7	0.033	0.033
P8	0.033	0.033
P9	0.033	0.032
P10	0.033	0.032
P11	0.033	0.032
P12	0.033	0.033
P13	0.033	0.033
P14	0.033	0.033
P15	0.033	0.033
P16	0.033	0.033
P17	0.033	0.033
P18	0.033	0.032
P19	0.033	0.033
P20	0.033	0.033
P21	0.033	0.032

2nd Ring - Inner Coil, 90 deg. (Side, Inner)

	Baseline	Final
P1-ELL		
P2	0.035	0.033
P3	0.035	0.034
P4	0.035	0.034
P5	0.035	0.034
P6	0.035	0.034
P7	0.035	0.035
P8	0.035	0.035
P9	0.035	0.034
P10	0.035	0.035
P11	0.035	0.035
P12	0.035	0.035
P13	0.035	0.035
P14	0.035	0.035
P15	0.035	0.035
P16	0.035	0.035
P17	0.035	0.035
P18	0.035	0.035
P19	0.035	0.035
P20	0.035	0.035
P21	0.035	0.035

A20150084

3rd Ring - Outer Coil, 270 deg. (Side, Outer)

	Baseline	Final
P1-ELL		
P2	0.033	0.033
P3	0.033	0.033
P4	0.033	0.032
P5	0.033	0.032
P6	0.033	0.033
P7	0.033	0.033
P8	0.033	0.033
P9	0.033	0.033
P10	0.033	0.033
P11	0.033	0.033
P12	0.033	0.033
P13	0.033	0.033
P14	0.033	0.033
P15	0.033	0.033
P16	0.033	0.033
P17	0.033	0.033
P18	0.033	0.033
P19	0.033	0.033
P20	0.033	0.033
P21	0.033	0.033

3rd Ring - Inner Coil, 90 deg. (Side, Inner)

	Baseline	Final
P1-ELL		
P2	0.035	0.035
P3	0.035	0.034
P4	0.035	0.035
P5	0.035	0.035
P6	0.035	0.035
P7	0.035	0.035
P8	0.035	0.035
P9	0.035	0.035
P10	0.035	0.035
P11	0.035	0.035
P12	0.035	0.035
P13	0.035	0.035
P14	0.035	0.035
P15	0.035	0.035
P16	0.035	0.035
P17	0.035	0.035
P18	0.035	0.035
P19	0.035	0.035
P20	0.035	0.035
P21	0.035	0.035

Midpoint - 10th Ring - Outer Coil. 270 deg. (Side, Outer)

	Baseline	Final
P1-ELL		
P2	0.033	0.033
P3	0.033	0.033
P4	0.033	0.033
P5	0.033	0.033
P6	0.033	0.033
P7	0.033	0.033
P8	0.033	0.033
P9	0.033	0.033
P10	0.033	0.033
P11	0.033	0.033
P12	0.033	0.033
P13	0.033	0.033
P14	0.033	0.033
P15	0.033	0.032
P16	0.033	0.033
P17	0.033	0.033
P18	0.033	0.033
P19	0.033	0.033
P20	0.033	0.032
P21	0.033	0.033

Midpoint - 10th Ring - Inner Coil. 90 deg. (Side, Inner)

	Baseline	Final
P1-ELL		
P2	0.035	0.035
P3	0.035	0.035
P4	0.035	0.035
P5	0.035	0.035
P6	0.035	0.035
P7	0.035	0.035
P8	0.035	0.035
P9	0.035	0.035
P10	0.035	0.035
P11	0.035	0.035
P12	0.035	0.035
P13	0.035	0.035
P14	0.035	0.035
P15	0.035	0.035
P16	0.035	0.035
P17	0.035	0.035
P18	0.035	0.035
P19	0.035	0.035
P20	0.035	0.035
P21	0.035	0.035

A20150084

Various Tubing Weld Circ. Seams

	Baseline	Final
W1-O-0 deg.	0.035	0.036
W1-O-270 deg.	0.026	0.027
W2-O-0 deg.	0.027	0.028
W2-O-270 deg.	0.022	0.022
W3-O-180 deg.	0.033	0.032
W3-O-270 deg.	0.03	0.031
W4-C-180 deg.	0.032	0.032
W4-C-270 deg.	0.033	0.033
W5-C-180 deg.	0.031	0.032
W5-C-270 deg.	0.024	0.025
W6-I-90 deg.	0.022	0.023
W6-I-180 deg.	0.035	0.035
W7-I-180 deg.	0.031	0.03
W7-I-270 deg.	0.026	0.027

Various Tubing Weld Circ. Seams

1st Ring - Outer Coil, 180 deg. (Bottom)

1st Ring - Outer Coil, 270 deg. (Side, Outer)

1st Ring - Center Coil, 180 deg. (Bottom)

1st Ring - Inner Coil, 90 deg. (Side, Inner)

1st Ring - Inner Coil, 180 deg. (Bottom)

1st Ring - Inner Coil, 270 deg. (Side, Outer)

2nd Ring - Outer Coil, 270 deg. (Side, Outer)

2nd Ring - Inner Coil, 90 deg. (Side, Inner)

3rd Ring - Outer Coil, 270 deg. (Side, Outer)

3rd Ring - Inner Coil, 90 deg. (Side, Inner)

Midpoint - 10th Ring - Outer Coil, 270 deg. (Side, Outer)

Midpoint - 10th Ring - Inner Coil, 90 deg. (Side, Inner)

A	1/03	Nondestructive Examination Condition Report	Job #:	A 20150085

Work Request #: N/A

Keywords: Tank

Distribution:

J.D. Newell, SRNL E&CPT/RP, 999-W
J.I. Mickalonis, SRNL MS&T, 773-A
S.A. Martin, SRNL QA, 773-41A
J.E. Ziska, SRNL MS&T, 730-A

N. C. Iyer, SRNL, 773-41A
R. L. Bickford, MNDE&C, 730-A
730-A NDE Files *

Page: 1 of 1

Date: 11/20/2014

Reported by: W. R. Hinz	Inspectors/Level: W.R. Hinz, UT Level III, J.E. Ziska, UT-T
Equipment Examined: SME/SRAT Tank Mockup	
	Component Identification # IDP# N/A
Location: 999-W	Component SME/SRAT Tank Mockup
Date(s) of Examination: 11/12/14	CLI# N/A
Service Condition: Standby, after 2 weeks run time	Materials of Construction: Stainless Steel

NCR Number (if applicable):
None

Inspection Procedure (Number and Title):
NDEP 7.1,Ultrasonic Thickness Examination

Acceptance Criteria (Source):
Information Only, Final inspection after 2 week run time

Inspection Summary:

MNDE&C completed final ultrasonic measurement of the miniature SME/SRAT Tank mockup after 2 weeks of run time with an abrasive mixture and the SME coil assembly in place. Baseline measurements had been acquired at the same locations prior to the tank being put in service.

Comparison with the baseline values indicate a very slight wall thickness reduction at row "B", the area just below the bottom head to shell weld. This is in a region just below the coils where the coil mass would not provide sheilding or protection from the flow of material stirred by the agitator under operating conditions.

The accuracy of these measurements in this thickness range is +/- 0.001". The final measurements at row "B" are 0.002" less than the baseline measurements, just beyond the "noise" level. Since all other locations were within 0.001" of the baseline measurements there is no clear evidence that any wall loss is occuring elsewhere in the tank.

For more information see report #2014-IR-11-0719 or contact W.R. Hinz at 5-4896.

	7.05 5/09		JOB # A 20150085
SRS SAVANNAH RIVER SITE		**ULTRASONIC THICKNESS** **REPORT**	REPORT # 2014-IR-11-0719 CLI# N/A

AREA / SYSTEM 999-W				PROCEDURE NDEP 7.1		REV 0		SEE COVER SHEET FOR ACCEPTANCE CRITERIA
WELD / COMPONENT I.D. SME/SRAT Tank Mockup				INSPECTION PLAN# N/A		IDP# N/A		WORK REQUEST # N/A
DRAWING N/A	REV. N/A	MATERIAL TYPE Stainless Steel		SURFACE CONDITION As Fabricated	NORMAL DIA/SCH OR THK. Unknown			MINIMUM ALLOWABLE THK. Not Established

EQUIPMENT

INSTRUMENT ☐ DTG ☒ CRT	MANUFACTURER Krautkramer Branson		MODEL USN-60		UT M&TE # 4-2045		CAL DUE DATE 1/13/2015
TRANSDUCER ☒ SGL ☐ DUAL	MANUFACTURER GEIT		MODEL ALPHA	S/N 4-3025	SIZE 0.250"	FREQ 10	Mhz
CABLE LENGTH 6'	COUPLANT Ultragel II	BATCH 11654		CAL STANDARD M&TE# 4-1543	CALIBRATION POINTS .029" - .103"		

EXAMINATION RESULTS

Location	0°	90°	180°	270°	SKETCH - IDENTIFY AREAS/CONTROL POINTS EXAMINED
see page 2					

N/A

☐ ACC. ☐ REJ. ☒ N/A	MINIMUM READING OBTAINED .047" (bottom head)

REMARKS - Provide details concerning nature of reduction in wall thickness. List all other M&TE used, M&TE#, and due dates.
These are followup or "final" measurements after 2 weeks run time. See Page 2 for comparison with baseline measurements.
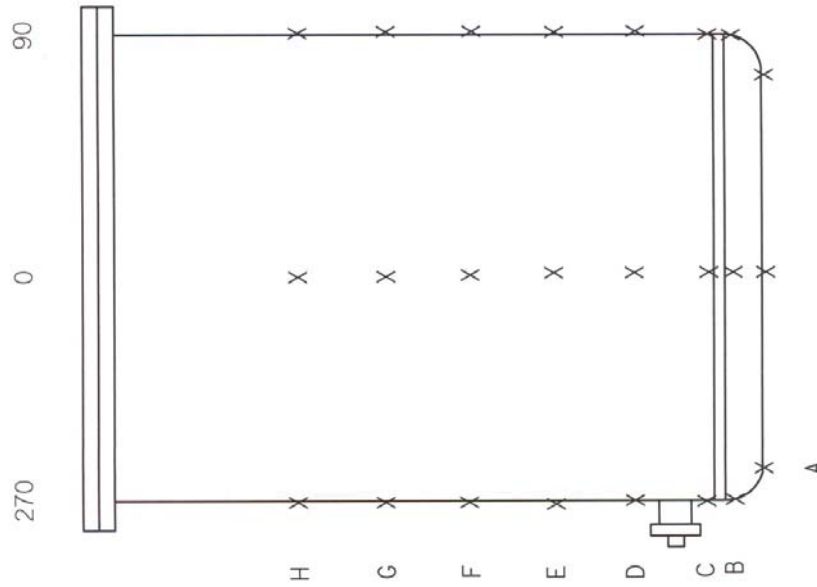
	PAGE 1 OF 2

A20150085

2014-IR-II-0719 Page 2 of 2

MINI SME/SRAT VESSEL – BASELINE AND FINAL (2 wk. run) UT MEASUREMENTS

	Baseline	Final
A-0	0.055	0.055
A-90	0.055	0.056
A-270	0.055	0.054
B-0	0.049	0.047
B-90	0.049	0.047
B-270	0.049	0.047
C-0	0.073	0.072
C-90	0.073	0.072
C-270	0.072	0.072
D-0	0.072	0.072
D-90	0.072	0.072
D-270	0.072	0.072

	Baseline	Final
E-0	0.072	0.072
E-90	0.072	0.071
E-270	0.072	0.072
F-0	0.072	0.072
F-90	0.072	0.072
F-270	0.072	0.072
G-0	0.071	0.072
G-90	0.072	0.072
G-270	0.072	0.072
H-0	0.072	0.072
H-90	0.071	0.072
H-270	0.072	0.072
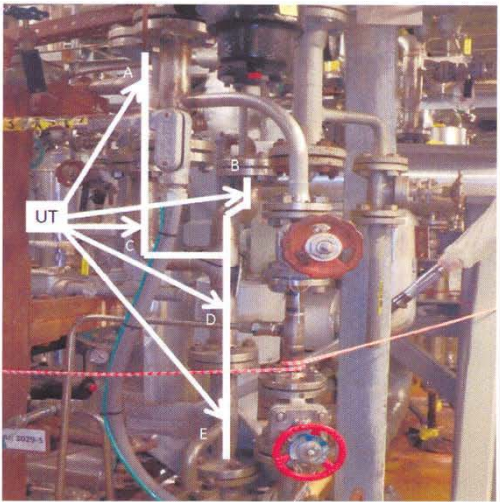
Viewed from front of hood

S	1/13	Nondestructive Examination **Condition Report**	Job #:	S20170341
			Work Request #:	1558884

Keywords: Pipe

Distribution:

P. Woodward, Mech. Eng., 704-24S
R. Arrington, QA, 704-71S
M. Brown, DWPF Eng., 704-25S
S. Askew, ME, 742-13G

R. L. Bickford, MS&T/ME, 730-A
730-A NDE Files *

Page: 1 of 1

Date: 4/24/2017

Reported by:	Inspectors/Level:
C.C. Hamm	P. R. Smock / L-II UT C. C. Hamm / L-II UT

Equipment Examined:	
Formic spool to sprat FAK15-P212-1/2 piping	Component Identification # IDP# N/A

Location:	Component
221-S	FAK15-P212-1/2

Date(s) of Examination:	CLI#
4/19/2017	WD-221000-S-FAK-L-FAK15-P212-1/2

Service Condition:	Materials of Construction:
Inservice	Stainless Steel

NCR Number (if applicable):
None

Inspection Procedure (Number and Title):
NDEP 7.1,Ultrasonic Thickness Examination

Acceptance Criteria (Source):
Information Only

Inspection Summary:

An ultrasonic thickness examination (2017-IR-11-0351) was conducted on the Formic spool to sprat FAK15-P212-1/2 piping. The following information was obtained:

Readings taken in areas identified by engineering. Thickness readings obtained around circumference of pipe and provided in a range.

Lowest thickness reading obtained: 0.129"

Attachments documenting these inspections have been sent to the appropriate personnel.

If additional information or inspection is required, please contact C. Hamm @ 5-3413, pager 15694

7.05A 1/13		JOB #	S20170341

SRS
SAVANNAH RIVER SITE

ULTRASONIC THICKNESS REPORT

REPORT # 2017-IR-11-0351

CLI# WD-221000-S-FAK-L-FAK15-P212-1/2

AREA / SYSTEM	PROCEDURE	REV	
221-S	NDEP 7.1	1	SEE COVER SHEET FOR ACCEPTANCE CRITERIA

WELD / COMPONENT I.D.	INSPECTION PLAN#	IDP#	WORK REQUEST #
FAK15-P212-1/2	N/A	N/A	1558884

DRAWING	REV.	MATERIAL TYPE	SURFACE CONDITION	NORMAL DIA/SCH OR THK.	MINIMUM ALLOWABLE THK.
N/A	N/A	Stainless Steel	As Welded	0.145" (1-1/2" Sch. Std./40)	N/A

EQUIPMENT

INSTRUMENT	MANUFACTURER	MODEL	UT M&TE #	CAL DUE DATE
☒ A SCAN ☐ ARRAY	Krautkramer Branson	USN-52L	4-1439	6/27/2017

TRANSDUCER	MANUFACTURER	MODEL	S/N	SIZE	FREQ
☒ SGL ☐ DUAL / ARRAY	GE/IT	ALPHA	4-3020	0.250"	10 Mhz

CABLE LENGTH	COUPLANT	BATCH	CAL STANDARD M&TE#	UT CALIBRATION POINTS
6'	Ultragel II	14H073	4-0110	0.1" - 0.3"

EXAMINATION RESULTS

Location/Thickness

Location	Range
A	0.143"-0.152"
B	0.129"-0.133"
C	0.143"-0.133"
D	0.146"-0.150"
E	0.137"-0.143"

SKETCH - IDENTIFY AREAS/CONTROL POINTS EXAMINED

☐ ACC.	☐ REJ.	☒ N/A	MINIMUM READING OBTAINED 0.129"

REMARKS - Provide details concerning nature of reduction in wall thickness. List all other M&TE used, M&TE#, and Due Dates.

Readings taken in areas identified by engineering in picture above. Thickness readings obtained around circumference of pipe and provided above in a range.

PAGE	1 OF 1

Distribution:

D. E. Dooley
C. C. Herman
F. M. Pennebaker
H. P. Boyd
J. M. Bricker
T. H. Huff
T. L. Fellinger
E. J. Freed
J. M. Gillam
B. A. Hamm
E. W. Holtzscheiter
J. F. Iaukea
V. Jain
C. J. Martino
J. W. Ray
P. J. Ryan
M. A. Rios-Armstrong
K. M. Brotherton
T. E. Colleran
V. M. Kmiec
C. Ridgeway
H. B. Shah
D. C. Sherburne
K. B. Martin
S. T. Isom
K. E. Zeigler
B. J. Wiersma
K. I. Imrich